THE EFFECT OF MOLECULAR WEIGHT ON THE ABSORPTION ENHANCING PROPERTIES OF *n*-TRIMETHYL CHITOSAN CHLORIDE

Bruno Alexander Rebolo

B.Eng. (North-West University, Potchefstroom Campus)

This dissertation is presented in fulfillment of the requirements for the degree Masters of Science (Engineering) in the School of Chemical and Minerals engineering at the North-West University, Potchefstroom Campus.

Supervisor: Prof. H.W.J.P. Neomagus

ACKNOWLEDGEMENTS

I would like to take the opportunity to thank the following persons for their contributions:

Prof Neomagus – For all your help, time, effort and guidance.

Prof Everson - For your time, effort and guidance.

Prof. Kotze – For your guidance, time and effort. It is appreciated.

Dewald, Marisa and Chrizelle – For all you assistance with experiments and scientific information.

Mrs Anriette Pretorius – For your help with literature survey.

Candice and Natalie Blewitt – Thank you for all your motivation.

Ivo and Fatima Rebolo – For all your sacrifices so that I could get an education.

Chris and Marthie van Wyk – Thank you for your encouragement and support.

Prof James E Rollings (1950 – 2001) – "If I knew what I was doing, I wouldn't be doing research"

Carmen – This is for you, my girl.

Marina – Thank you for sticking with me through this Masters. I love you.

My Lord – For making our universe so interesting – "Lord of all of creation, of water, earth and sky… the universe declares Your Majesty…"

DECLARATION

Hereby I, Bruno Alexander Rebolo, declare that the dissertation with title THE EFFECT OF MOLECULAR WEIGHT ON THE ABSORPTION ENHANCING PROPERTIES OF *n*-TRIMETHYL CHITOSAN CHLORIDE in fulfillment of the requirements for the M.Sc. (Engineering) degree, is my work and has not been submitted at any other university either in whole or in part.

Signed at Secunda.

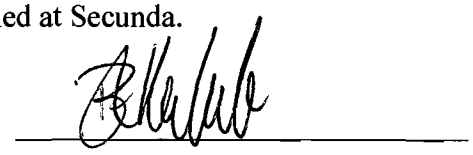

Bruno Rebolo

26/08/2008

Date

ABSTRACT

Delivery problems have limited the uptake of many promising new peptides drugs. The co-administration of absorption enhancing agents such as *n*-Trimethyl chitosan chloride (TMC), a chitosan derivative, has been proven. The aim of this study is to determine the influence of molecular weight on the absorption enhancement properties of TMC.

Three different molecular weights of TMC were synthesized, with molecular weight varying between 2.03 x 10^5 g/mol (low molecular weight TMC) to 3.28 x 10^5 g/mol (high molecular weight TMC). Intrinsic viscosity of the different molecular weights was determined and ranged from 3.4 ml/g (low molecular weight TMC) to 9.2 ml/g (high molecular weight TMC). The results showed that the intrinsic viscosity increased with an increase in molecular weight. ^{1}H-NMR spectra analyses were done on the different molecular weights of TMC and the degree of quaternization (DQ) were calculated with the ranges of 33.7 % (low molecular weight TMC) to 37.7 % (high molecular weight TMC).

From the mucoadhesion data obtained, an increase in molecular weight had an increase in mucoadhesive strength as well as surface tension and the high molecular weight TMC exhibited the best mucoadhesive properties, which means that the high molecular weight TMC will bond best to epithelial surfaces and have a longer contact period, thus improving its absorption enhancing effect.

The effects of molecular weight on transepithelial electrical resistance (TEER) and transport experiments were studied at different TMC concentrations (0.1 % and 0.5 % w/v). All different molecular weights of TMC caused immediate and pronounce reduction in TEER values as well as an increase in transport rate. At lower concentrations (0.1 %) the high molecular weight TMC had the biggest increase in transport rate while at higher TMC concentrations the low molecular weight TMC had the biggest increase. A possible conclusion for the highest effect on the TEER and transport rate by the low molecular weight at higher concentrations (0.5% w/v), is the short chain length and low viscosity of low molecular weight TMC. The compound could "move" closer to the tight junctions and have the largest influence on the tight junction. Another reason could be that at higher concentrations (0.5% w/v) the high molecular weight TMC could be

clogging the tight junctions. Because of the high molecular weight TMC's high mucoadhesive property and contact sites (due to large chain), at lower concentrations the high molecular weight TMC has a bigger effect than the low molecular weight TMC.

The discrepancy in TEER and transport results of the medium molecular weight can possibly be attributed to the degree of quaternization (DQ). Because DQ is a relationship of the amount of tri-methyl amino groups present on the TMC molecule, the medium molecular weight TMC with highest DQ and thus most tri-methyl amino groups, might also be clogging the tight junction openings and restricting the transport of [^{14}C]-mannitol despite causing the tight junction to open up as seen by drop in TEER values.

A transport model was derived that described the paracellular transport of [^{14}C]-mannitol across an epithelial membrane and the effect of using an absorption enhancer. With this model, the diffusion coefficient through the membrane could be obtained, and it was found that there was an increase in the diffusion coefficient with the administration of TMC. An initial penetration period was also observed and this influenced the calculation of the diffusion coefficients, whereby experimental data after 120 minutes only could be used.

INDEX

LIST OF FIGURES

LIST OF TABLES

NOMENCLATURE

A	**Area of membrane (m^2)**
c	**Concentration of the solution (g/ml)**
C	**Concentration (mol/m^3)**
C_A	**Concentration in donor side (Chamber A) (mol/m^3)**
C_B	**Concentration in receiver side (Chamber B) (mol/m^3)**
C_0	**Initial concentration in the donor side (mol/cm^3)**
$\frac{dC}{dt}$	**Change in transport drug in receiver side ($mol/cm^3.s$)**
cpm	**Counts per minute**
D	**Diffusion coefficient (m^2/s)**
DA	**Degree of acetylation**
DDA	**Degree of deacetylation**
DQ	**Degree of quaternization**
I_{AC}	**Peak intensity for acetyl group of N-acetyl-D-glucosamine**
I_{H1}	**Peak intensity for H-1 of N-acetyl-D-glucosamine**
$I_{H1'}$	**Peak intensity for H-1 of D-glucosamine**
I_{H2}	**Peak intensity for H-2 of D-glucosamine**
J	**Flux (rate of transfer) ($mol/m^2.s$)**
M	**Molecular weight (g/mol)**
MW	**Molecular weight (g/mol)**
P_{aq}	**Permeability of the aqueous boundary layer (m/s)**
P_{eff}	**Effective permeability (cm/s)**
R(t)	**Electrical resistance measured at time t (ohm)**
$R_{t=0}$	**Electrical resistance before incubation of absorption enhancer (TMC) (ohm)**
R_R	**Tight junction pore radius (m)**
t	**Time (s)**
t_o	**Efflux time of the solvent (seconds)**
t_s	**Efflux time of the solution (seconds)**
t_δ	**Penetration time (s)**
TEER	**Transepithelial electrical resistance**

%TEER	**Percentage reduction from maximum TEER value**
V	**Volume in chamber (m^3)**
V_A	**Volume in donor side (Chamber A) (m^3)**
V_B	**Volume in receiver side (Chamber B) (m^3)**
δ	**Thickness of membrane (m)**
δ_i	**Penetration depth (m)**
η	**Viscosity of liquid medium (poise)**
η_{inh}	**Inherent viscosity (dimensionless)**
η_o	**Viscosity of the solvent (dl/g)**
η_r	**Relative viscosity (dimensionless)**
η_s	**Viscosity of the solution (dl/g)**
ρ	**Density of molecule (kg/m^3)**

CHAPTER 1

Drug transport: Introduction and aim of study

Successful drug development requires the optimisation of specific and potent pharmacological activity and the efficient delivery to target sites. Many promising new peptides drugs with novel therapeutic potential for the treatment of AIDS, cardiovascular diseases and other numerous disorders have been identified in recent years; yet their clinical utility have been limited by delivery problems (Burton *et al.*, 1996). The transport of most drugs (hydrophobic and hydrophilic) across the intestinal epithelium involves two distinct pathways as shown schematically in figure 1.1.

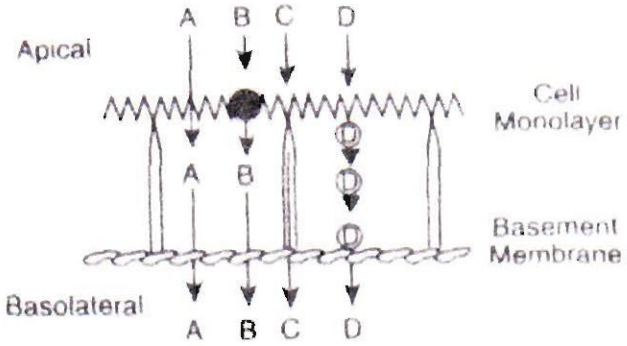

Figure 1.1: Pathways by which a drug may cross a cellular barrier (Burton *et al.*, 1996)

(A): Transcellular passive diffusion through the plasma membranes and cytoplasmic compartment.

(B): Carrier-mediated uptake and passive diffusion.

(C): Paracellular passive diffusion through the intercellular space.

(D): Receptor-mediated or adsorptive transcytosis.

The transcellular pathway requires movement of the solute across or / and through the cell membrane. It can be active or passive transport. For such an active process to occur, the solute must interact with some component of the cell membrane. In the case of a polarized epithelial cell, the apical membrane consists of an array of peripherally and integrally associated proteins within an organized lipid matrix. For some solutes, these proteins serve as specific transporters

or receptors for the uptake into the cell. However, for the vast majority of drug molecules, no such specific mechanism exists and transport is mediated by the passive diffusion of the drug through the apical membrane to move across the cell (Burton *et al.*, 1996)

The transcellular route is mainly restricted to small hydrophobic compounds capable of passing through the lipophilic cell membrane. The paracellular route, which involves a small part of the epithelium, comprises only the transport of some hydrophilic compounds (such as peptides) (Schipper et al., 1996). Among other factors, lipophilicity and the size of molecules are probably the most important factors for epithelial transport. Most drugs are small molecules and lipophilic in nature; therefore, they permeate readily across the cell membranes in sufficient amounts to obtain the necessary therapeutic response. Large molecules are generally excluded from the transcellular pathway due to their size. Furthermore, compounds such as peptide and protein drugs are highly hydrophilic in nature and they do not partition into the cell membranes; therefore, administration of these classes of drugs mostly results in inadequate absorption and very poor systemic availability if any. Larger molecules are also excluded from the paracellular pathway, which is effectively sealed by the tight junctions (Kotzé, *et al.*, 1998).

The epithelial membrane is not a continuous layer and divisions between the cells are referred to as cell junctions. Tight junctions are a type of cell junction and are formed when specific proteins in two interacting plasma membranes make direct contact across the intercellular space (figure 1.2) (Wilson *et al.*, 1989).

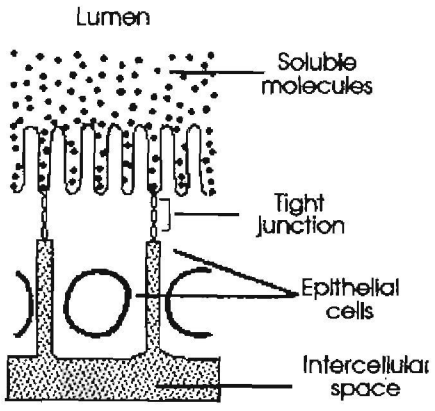

Figure 1.2: Tight junctions hold cells together at their apical end.

Tight junctions play a crucial part in maintaining the selective barrier function of cell sheets. For example, the epithelial cells lining the small intestine must keep most of the gut contents in the lumen; simultaneously, the cells must pump selected nutrients across the cell sheet into the extracellular fluid on the other side, from which they are absorbed into the blood (Wilson *et al.*, 1989). Tight junction performs its duties in two different ways (Wilson *et al.*, 1989):

a) Act as diffusion barriers within the lipid bilayer of the plasma membrane, thus preventing the transport proteins in the apical membrane from diffusing into the basolateral membrane, and vice versa.

b) Seal neighbouring cells together to create a continuous sheet of cells between which even small molecules are unable to pass.

Many efforts have been made to improve the uptake of poorly absorbed drugs. One approach to overcome the restriction of paracellular transport is the co-administration of absorption enhancing agents, which regulate the integrity of the tight junctions. Two general classes of enhancers investigated were calcium chelators such as EDTA and surfactants such as bile salts and palmitoylcarnitine. However, the toxicity of these compounds excluded them from pharmaceutical use (Kotzé *et al.*, 1998).

Recently, chitosan has been studied as a potential enhancer of musocal drug absorption at low pH values (Schipper *et al.*, 1996). Chitosan is a linear polysaccharide made by N-deacetylation of chitin. Chitin is an abundant biopolymer found in crustacean's shells (Schipper *et al.*, 1997). As a natural product, chitosan and its derivatives are biodegradable, non toxic and useful as a drug adjuvant (Borchard *et al.*, 1996). But at high pH, chitosan was ineffective as an absorption enhancer, limiting its use in the more basic environment of the intestine and colon (Kotzé *et al.*, 1998).

n-Trimethyl chitosan chloride (TMC), a chitosan derivative that is synthesised by the reductive methylation of chitosan (Sieval *et al.*, 1998), has been proven to be useful as an absorption enhancer in neutral and basic environments. TMC is a water-soluble, positively charged polymer (Kotzé *et al.*, 1998).

TMC caused a pronounced and immediate reduction in the transepithelial electrical resistance (TEER) and an increase in the transport of the hydrophilic model compound [^{14}C]-mannitol across human intestinal epithelial cell membranes (Caco-2) (Kotzé *et al.*, 1997 and Van der Merwe *et al.*, 2004). TEER is a measurement of the potential difference over the cells and an indication of integrity of the cell monolayer (Artursson, 1990).

Schipper *et al.* (1996) investigated the influence of molecular weight and degree of acetylation (DA) of chitosan on drug transport across intestinal epithelial cells (Caco-2). They concluded that at low degrees of acetylation (1 %) (or high degree of deacetylation – 99 %) the low molecular weight chitosan (31 x 10^3 Dalton) caused a higher permeability for [^{14}C]-mannitol across the monolayer than the high molecular weight chitosan (170 x 10^3 Dalton). At a 15 % degree of acetylation (85 % degree of deacetylation of chitosan) the situation changed. The high molecular weight chitosan (190 x 10^3 Dalton) caused a higher permeability for [^{14}C]-mannitol across the monolayer than the low molecular weight chitosan (4.7 x 10^3 Dalton). The effect of high molecular weight chitosan on the permeability of [^{14}C]-mannitol increased with an increase in the degree of acetylation (with a decrease in the degree of deacetylation). They also concluded that the structural properties of chitosan were very important for the absorption enhancement of hydrophilic drugs across mucosal tissues (Schipper *et al.*, 1996).

The aim of this study is to determine the effect of the molecular weight of TMC on its absorption enhancing properties. This will be done by:

- Characterise different chitosans by determining their molecular weight, viscosity and degree of acetylation and deacetylation.
- Synthesise three different molecular weights of TMC from three different molecular weights of chitosan.
- Characterise the TMC polymers by determining their molecular weight, viscosity and degree of quaternization.
- Determine the effect of the molecular weight of TMC on its mucoadhesive properties by tensile separation testing and surface tension analysis.

- Determine the effect of the molecular weight of TMC on its absorption enhancing properties by measurement of the transepithelial electrical resistance of Caco-2 cell monolayer and by permeability studies on Caco-2 cell monolayers.
- Describe mathematically the transport of [^{14}C]-mannitol in the presence of TMC polymers.

CHAPTER 2

Synthesis and Characterization of *n*-Trimethyl Chitosan Chloride (TMC): An absorption enhancing agent

2.1 INTRODUCTION

The passive absorption of drugs across mucosal membranes can involve either trans- or paracellular diffusion. Small hydrophobic compounds are able to move across an epithelial membrane (transcellular route) due to their ability to diffuse through the lipophilic cell membrane. Large hydrophilic compounds are transported across the epithelial membrane through the intercellular spaces (paracellular transport). However this transport is limited by tight junctions that seal epithelial cells at their apical surfaces. The tight junctions restrict especially the transport of orally administered hydrophilic drugs, such as peptides and proteins (Schipper *et al.*, 1996). One approach to overcome the restriction to paracellular transport is the co-administration of absorption enhancing agents which regulate the integrity of the tight junctions (Kotzé *et al.*, 1998).

In this chapter the synthesis of *n*-trimethyl chitosan chloride with different molecular weights as well as the characterization of these polymers by means of size exclusion chromatography (SEC) connected to a multi-angle laser light scattering apparatus, NMR and viscosity analysis is discussed.

2.2 THEORETICAL BACKGROUND

2.2.1 Drug absorption enhancers

Many efforts have been made to improve the uptake of hydrophilic drugs. Numerous classes of compounds that enhance the intestinal uptake of hydrophilic drugs have been described (Schipper *et al.*, 1996). These absorption enhancers can be divided into different classes according to their different chemical structures and characteristics, mechanism of action and routes of transport enhancement. In table 2.1 a general classification of absorption enhancing agents is rendered with

examples, applicable transport routes and the mechanism of action (Junginger *et al.*, 1999, Lee *et al.*, 1991, Van Hoogdalem *et al.*, 1989 & Hamman, 2000).

Table 2.1: Classes of absorption enhancers

Class	Route of transport	Mechanism of action	Examples
Non-steroidal anti-inflammatory drugs (NSAID)	Transcellular	Reduction of membranes fluidity	Sodium salicylate, indomethacin and diclofenac
Surfactants	Transcellular and paracellular	Phospholipid acyl chain perturbation	Sodium lauryl sulfate, bile salts: sodium deoxycholate, sodium glycocholate, sodium taurodihydro-fusidate
Fatty acids and derivates	Transcellular and paracellular	Phospholipid acyl chain perturbation	Oleic acid, caprylic acid, capric acid, acylcarnitines, acylcholines, mono- and diglycerides
Cyclodextrins	Transcellular and paracellular	Inclusion of membrane compounds	α-, β-, γ- cyclodextrin, methylated β-cyclodextrin
Chelating agents (Ca^{2+} - binding agents)	Transcellular and paracellular	Complexation of Ca^{2+}	EDTA, citric acid, N-acyl derivatives of collagen and N-amino acyl derivatives of B-diketones (enamines)
	Paracellular		Polyacrylates
Cationic polymers	Paracellular	Ionic interaction with groups of glycocalyx	Chitosan and *n*-trimethyl chitosan chloride

However, in most cases, drug absorption enhancement is accompanied by mucosal damage induced by the enhancer (Schipper *et al.*, 1996). Nevertheless, a few compounds, including the fatty acid sodium caprate and long chain acylcarnitines, have been shown to improve absorption without obvious harmful effects to the intestinal mucosa (Schipper *et al.*, 1996).

Recently, chitosan has been studied as a potential enhancer of musocal drug absorption (Schipper *et al.*, 1996). Chitosan is a linear polysaccharide made by N-deacetylation of chitin (figure 2.1). Chitin is an abundant biopolymer found in, for example, crab and shrimp shells (Schipper *et al.*, 1997).

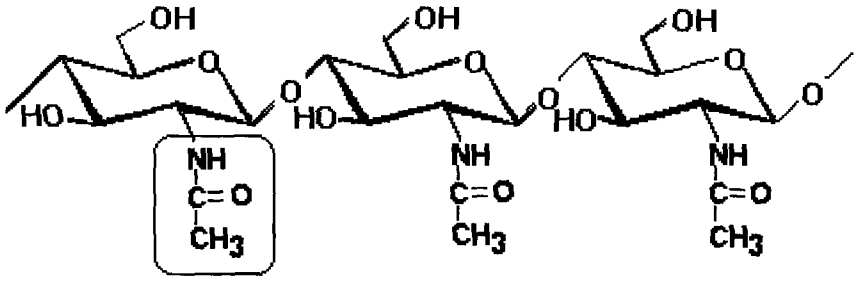

Figure 2.1: Chemical structure of chitin

2.2.2 Chitosan

Chitosan (figure 2.2) is a linear polysaccharide made by N-deacetylation of (1:4-linked 2-acetamide-2-deoxy-β-D-glucopyranose (GlcNAc)), resulting in a copolymer of GlcNAc and 2-amino-β-D-glucopyranose (GlcN). Chitosan is a polycation at acidic pH values, with an intrinsic pK_a value independent of degree of acetylation (DA) of approximately 5.6 - 6.5 (Schipper *et al.*, 1996).

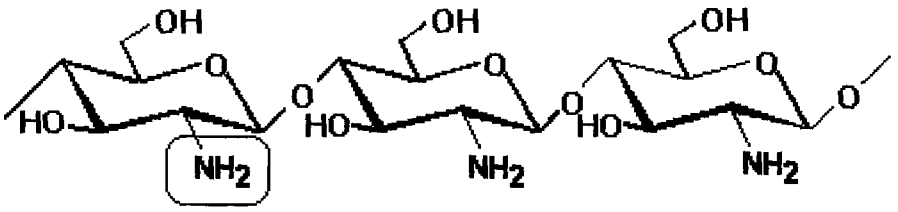

Figure 2.2: Chemical structure of chitosan

Chitosan is non-toxic (Borchard *et al.*, 1996) while other cationic polymers such as poly-L-lysine displayed pronounced toxicity in a variety of studies. This due to chitosan large molecular size and the fact that chitosan is not absorbed into the epithelial cells. Chitosan has mucoadhesive properties which are mediated through ionic interactions between positively charged amino groups in chitosan and negatively charged sialic acid residues in mucus or on cell surfaces. The mucoadhesive properties will be discussed in detail in chapter three. Studies employing chitosan as an absorption enhancer showed that the transport of insulin and a decapeptide across nasal and intestinal mucosa could be increased significantly (Schipper *et al.*, 1996).

In a study by Schipper *et al.*, 1996, chitosan increased the transport of a hydrophilic marker molecule across monolayers of a cultured human intestinal epithelial cell line (Caco-2). The increase in epithelial permeability was dependent on the pH of the chitosan solutions. The influence of chitosan on the transport of the marker molecule was the strongest when the pH was well below the pK_a of 6.5. This suggests that charge density may be important for the enhancement of musocal absorption. Varying the degree of acetylation (DA) also influences the charge density of chitosan, since only the 2-amino-β-D-glucopyranose (GlcN) is positively charged (Schipper *et al.*, 1996).

It has been proven that the interior of the tight junction channels (or pores) is highly hydrated and contains fixed negative charges. The conclusion was made that cationic macromolecules (like chitosan) are able to displace cations from these electronegative sites on the membrane, which

require coordination with the cations for dimensional stability. Thus, a relatively modest alteration in the relative concentration of specific species of ions within the volume of the pore could result in substantial alterations in tight junction resistance leading to loosening or opening of the pore (Artursson *et al.*, 1994). Another possibility for the absorption enhancing effect, is attributed to the interaction of chitosan with the cell membrane and this results in a structural reorganization of tight junction-associated proteins (cytoskeletal F-actin) (Schipper *et al.*, 1997).

Further, the interaction between the apical membrane of the epithelial cell and chitosan appear to be specific and saturable, as opposes to the non-specific and non-saturable effects seen for surfactants and bile salts (Artursson *et al.*, 1994). This effect makes chitosan a good contender for usage in novel drug delivery systems for hydrophilic drugs

2.2.3 Chitosan derivates

Kotzé *et al.* (1998) studied the effects of two chitosan salts, namely chitosan hydrochloride and chitosan glutamate, on the transepithelial electrical resistance (TEER) and permeability of Caco-2 cells. They conclude from their results that these salts are potent absorption enhancers in acidic environments (Kotzé *et al.*, 1998).

However, increased transport was only obtained in acidic conditions, where the pH was less or in order of the pK_a value (6.0 to 6.5) of chitosan. Chitosan is a weak base and requires a certain amount of acid to transform the glucosamine units into the positively charged water-soluble form, and in neutral and basic environments the chitosan molecules will loose its charge and precipitate from solution. At these conditions chitosan will be ineffective as an adsorption enhancer, limiting its use in the more basic environment of the large intestine and colon (Kotzé *et al.*, 1998). It was concluded that there is a need for chitosan derivatives with increased solubility at neutral and basic pH values (Kotzé *et al.*, 1998). Derivatives with quaternary amino groups such as *n*-trimethyl chitosan chloride have been proven to be useful as absorption enhancers in neutral and basic environments since they are well water-soluble and positively charged over a wide pH range (Kotzé *et al.*, 1999). TMC also does not damage the cell membrane and therefore do not alter the viability of the intestinal epithelial cells (Thanou *et al.*, 2001).

2.2.4 *n*-Trimethyl chitosan chloride (TMC)

The synthesis of TMC (figure 2.3) is done by the reductive methylation of chitosan with methyliodide. The counterion (I^-) was exchanged to Cl^- by dissolving the quaternized polymer in a small quantity of water, followed by the addition of HCl in methanol (Kotzé *et al.*, 1999).

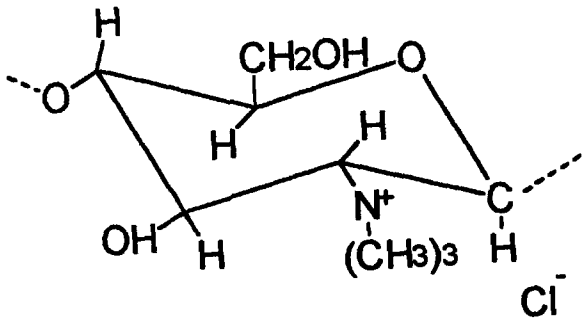

Figure 2.3: Chemical structure of *n*-Trimethyl chitosan chloride

A pronounced decrease in the intrinsic viscosity of TMC, compared with the starting material, was observed and this correlated well with the degradative reaction conditions in alkaline medium. A slight increase in pK_a from 5.5 to 6.0 was also found. The increase in solubility and basicity could be attributed to the replacement of the primary amino group on the C-2 position of chitosan with quaternary amino groups. Complete quaternization of chitosan will probably be difficult due to the presence of some acetyl groups (from chitin) and possible steric effects of the attached methyl groups on adjacent quaternary amino groups. TMC, as a partially quaternized derivative of chitosan, shows superior solubility, compared with other chitosan salts (Kotzé *et al.*, 1999).

Already at very low degrees of quaternization TMC is soluble at every pH and an increase in basicity has been found. Kotzé *et al.* (1999) looked at the effect of different degrees of quaternization had on the transport. TMC with a degree of quaternization of 61.2 % was more effective to promote the transport of hydrophilic compounds than TMC with a degree of quaternization of 12.3 %. However, in a study by Hamman *et al.* (2003), it was shown that for range of DQ of between 12% and 59%, the transport of hydrophilic and macromolecular model

compounds reached a maximum for TMC with DQ of 48%. The reversibility of the effect of TMC has also been proven as well as the fact that TMC does not cause any permanent damage to the Caco-2 cell monolayers (Kotzé *et al.*, 1999). TMC's potential has been proven as absorption enhancer.

2.3 EXPERIMENTAL SYNTHESIS OF TMC

2.3.1 Synthesis of TMC

2.3.1.1 Experimental apparatus

The synthesis of TMC was done in an Erlenmeyer flask (250 ml) coupled to a Liebig's condenser. The reaction mixture was heated to 60 °C in a water bath for 45 minutes and the following steps as per the experimental procedure (2.3.1.2) were performed.

2.3.1.2 Experimental procedure

The synthesis of TMC was performed based on the method of Sieval *et al.* (1998). A two-step methylation process with an extra procedure was used to obtain a polymer with a 42 % degree of quaternization. The whole synthesis process was repeated with three different molecular weight chitosans (Sigma Aldrich, South Africa) to ensure that TMC with three different molecular weights was obtained, e.g. low molecular weight chitosan is used to synthesis low molecular weight TMC. The reaction procedure is summarized below.

Step 1:

A mixture of 2 g chitosan, 4.8 g of sodium iodide, 11 ml of a 15 % aqueous NaOH solution and 11.5 ml of methyl iodide in 80 ml of N-methylpyrrolidone was stirred on a water bath at a temperature of 60 °C for 45 minutes. The methyl iodide was kept in the reaction by using a Liebig's condenser. The product was precipitated with ethanol and diethyl ether, and isolated by centrifugation.

Step 2:

The product obtained in step 1, was dissolved in 80 ml N-methylpyrrolidone and 4.8 g of sodium iodide, 11 ml of a 15 % aqueous NaOH solution and 7 ml of methyl iodide were added. The mixture was stirred on a water bath at a temperature of 60 °C for 30 minutes.

Step 3:

An additional 2 ml methyl iodide and 0.6 g NaOH pellets were added while stirring was continued for another 30 minutes at a temperature of 60 °C. The product was precipitated with ethanol and isolated by centrifugation. After washing with ethanol and diethyl ether the product was dissolved in 40 ml of a 5 % aqueous NaCl solution to exchange the iodide-ion with a chloride-ion. The polymer was precipitated using ethanol and diethyl ether, and isolated by centrifugation. The product was again dissolved in 40 ml water and precipitated with ethanol and diethyl ether to remove the remaining NaCl from the material. The product was dried in a vacuum oven at 40 °C for 24 hours.

2.3.2 Characterization of Chitosan and TMC

2.3.2.1 Introduction

The following analytical techniques were used to ensure that TMC with three different molecular weights were synthesised while maintaining a constant degree of quaternization. The TMC polymers were characterized by measurement of their molecular weight with size exclusion chromatography (SEC) connected to a multi-angle laser light scattering apparatus (MALLS). Both the degree of deacetylation of chitosan and the degree of quaternization of TMC was determined with nuclear magnetic resonance (NMR). The intrinsic viscosity of chitosan and TMC were also determined.

2.3.2.2 Methods

2.3.2.2.1 Measurement of molecular weight by SEC / MALLS

The measurement of the molecular weight of chitosan and TMC was done using a size exclusion chromatograph (Hewlett Packard 1100) connected to a laser photometer (DAWN DSP) and refracting index detector (ERC 7515A).

The chitosan and TMC polymers were prepared in solutions of 5 mg/ml samples for the different molecular weights and 1.8 ml of theses samples were collected in chromatographic sample vials. The mobile phase consisted of 0.2 M ammonium acetate and the pH was adjusted to 4.5 with acetic acid. The size exclusion chromatograph (SEC) system consists of a HP 1100 vacuum degasser, isocratic pump, an auto sampler with a TSK-guard PWH (Toso Haas) inline column and two size exclusion columns connected in serie: a TSK G6000 PW (Toso Haas) (with inside diameter = 7.5 mm, length = 30 cm, particle size = 17 μm, pore size > 1000 Å) and TSK G5000 PW (Toso Haas) (with inside diameter = 7.5 mm, length = 30 cm, particle size = 17 μm, pore size = 1000 Å). Samples of 100 μl were injected at a flow rate of 0.8 ml/min and was analysed with a laser photometer (DAWN DSP) (with a He/Ne laser, λ = 633 nm) and refracting index detector. The molecular weight was calculated with Astra for Windows (Version 4.72.03, Wyatt Technology Corp).

2.3.2.2.2 Determination of intrinsic viscosity

In polymer science it is not the absolute viscosity of a solvent or a solution that is of particular interest, but the increase in viscosity attributed to the dissolved polymer. Therefore, in the viscometry of polymer solutions it is some expression of the relative viscosity that is useful (Anon, 1965). The relative viscosity (η_r) is defined as the quotient of the viscosity of the solution, η_s, and the viscosity of the solvent, η_o,

$$\eta_r = \frac{\eta_S}{\eta_0} \qquad (2.1)$$

or

$$\eta_r = \frac{t_S}{t_0} \qquad (2.2)$$

Where t_s is the efflux for the solution and t_o is the efflux time for the solvent (Collins *et al.*, 1973).

An additional quantity useful in viscometry is the inherent viscosity (η_{inh}), defined as $\ln\frac{\eta_r}{c}$ (c is the concentration of the solution):

$$\eta_{inh} = \ln\frac{\eta_r}{c} \qquad (2.3)$$

The relative viscosity value is the limiting viscosity when $\ln\frac{\eta_r}{c}$ or η_{inh} is extrapolated to zero concentration (Anon, 1965). This quantity is termed the intrinsic viscosity or the limiting viscosity number, [η]. Since relative viscosity is dimensionless, the units for [η] are those of reciprocal concentration, dl/g or ml/g.

A capillary viscometer (specifically a Cannon-Fenske Viscometer) was used to determine viscosity of chitosan and TMC. A size 100 Cannon-Fenske viscometer was used for the TMC and size 200 Cannon-Fenske viscometer for the chitosan.

A glass syringe (20 ml) with a polypropylene filter holder in which a 45μm cellulose acetate filter is housed, was used to filter all solutions carefully as they are introduced into the viscometer. This was done due to the fact that capillary viscometers are easily clogged by small particles. Solutions of the chitosan polymers and TMC polymers were prepared in 0.2 % v/v acetic acid in concentrations of 0.05, 0.1, 0.15, 0.2 and 0.25 % w/v. The solutions are then drawn through the capillary until the reservoir above is filled. After this, the pressure is released and the fluid is allowed to flow freely. The efflux time is measured from the instant the meniscus passes the upper mark on the bulb to the time it passes the lower mark (Tuijman *et al.*, 1957). The viscometer was thoroughly rinsed with 0.2 % v/v acetic acid solution after each experiment. The viscometer was placed rigidly and reproducibly vertical in a constant-temperature bath, for which the thermostat was maintained at 25 °C ± 0.1 °C. A manually triggered timing device (Casio stop watch) was used which was readable to at least 0.1 second (Gramain *et al.*, 1970). Each experiment was done in triplicate.

2.3.2.2.3 Nuclear magnetic resonance spectrometry (NMR)

Nuclear magnetic resonance spectroscopy is based upon the measurement of absorption of electromagnetic radiation (absorption process which involves nuclei of atoms) in the radio-frequency region of roughly 4 to 600 MHz. The analyte is placed in an intense magnetic field in order to cause nuclei to develop the energy states required for absorption to occur (Skoog *et al.*, 1992).

The ^{1}H-NMR analysis was performed at the Leiden/Amsterdam Center for Drug Research in the Netherlands and the method previously reported by Sieval *et al.* (1998) was used. In short, 10 mg of polymer was dissolved in D_2O in a NMR tube and the solution is measured in a 600 MHz DMX Brucker apparatus. This was repeated for all three different molecular weights of chitosan and TMC.

2.3.2.2.4 Calculation of the degree of deacetylation of chitosan

By using the NMR data obtained and the following equation, the degree of acetylation (DA) for chitosan was determined:

$$DA(\%) = \frac{I_{H1'} + \frac{I_{AC}}{3}}{I_{H1} + I_{H2} + I_{H1'} + \frac{I_{AC}}{3}} \times 100 \qquad (2.4)$$

where I_{H1}, I_{H1}, I_{H2} and I_{AC} are peak intensities for H-1 or D-glucosamine (GlcN) unit at 4.60 ppm, for H-1 of N-acetyl-D-glucosamine (GlcNAc) units at 4.86 – 4.88 ppm, for H-2 of GlcN at 3.17 ppm and for the acetyl group of the GlcNAc units at 2.05 ppm, respectively. The dividing factor of 3 for I_{AC} is associated with the proton number for the acetyl group (Sato *et al.*, 1998). The degree of deacetylation (DDA) can then be determined as follows:

$$DDA(\%) = 100 - DA(\%) \qquad (2.5)$$

2.3.2.2.5 Calculation of the degree of quaternization of TMC

The degree of quaternization (DQ) of TMC was determined by using the following equation (Thanou *et al.*, 2000):

$$DQ(\%) = \frac{\int peak\ at\ 3.4\ ppm}{\left(\int peak\ at\ 4.7\ ppm + \int peak\ at\ 5.4\ ppm\right)} \times \frac{1}{9} \times 100 \qquad (2.6)$$

where

$\int$ peak at 3.4 ppm = integral of the tri-methyl amino group peak at 3.4 ppm

$\int$ peak at 4.7 ppm and $\int$ peak at 5.4 ppm = integral of the ^{1}H peaks at 4.7 and 5.4 ppm

2.4 RESULTS

2.4.1 Molecular weight and intrinsic viscosity of chitosan and TMC

The mean molecular weights of the chitosan and TMC polymers as determined by the size exclusion chromatography and multi-angle laser light scattering apparatus (SEC/MALLS) are listed in table 2.2.

Table 2.2: Mean molecular weight (g/mole) of the chitosan and TMC polymers

Polymer	Molecular Weight (x 10^5 g/mole)
Chitosan	
Low MW Chitosan	0.49
Medium MW Chitosan	1.10
High MW Chitosan	1.63
TMC	
Low MW TMC	2.03
Medium MW TMC	2.65
High MW TMC	3.28

The results show that TMC with three different molecular weights were synthesized from chitosan with three different molecular weights. The molecular weight of the TMC polymers is higher than that of the starting polymer (chitosan) and this is due to the methylation of the amino groups on the subunits of chitosan during the synthesis of TMC (this is confirmed in section 2.5.2).

In table 2.3 the intrinsic viscosity of the chitosan and the TMC polymer are given. These values were calculated as explained by figure 2.4. For the low molecular weight TMC the inherent viscosity is plotted against concentration. A straight light fit is used to determine the intrinsic viscosity at zero concentration.

Table 2.3: Intrinsic viscosity of chitosan and TMC polymers

Polymer	Intrinsic Viscosity (ml/g)
Chitosan	
Low MW Chitosan	13.5
Medium MW Chitosan	23.7
High MW Chitosan	31.5
TMC	
Low MW TMC	3.4
Medium MW TMC	6.6
High MW TMC	9.2

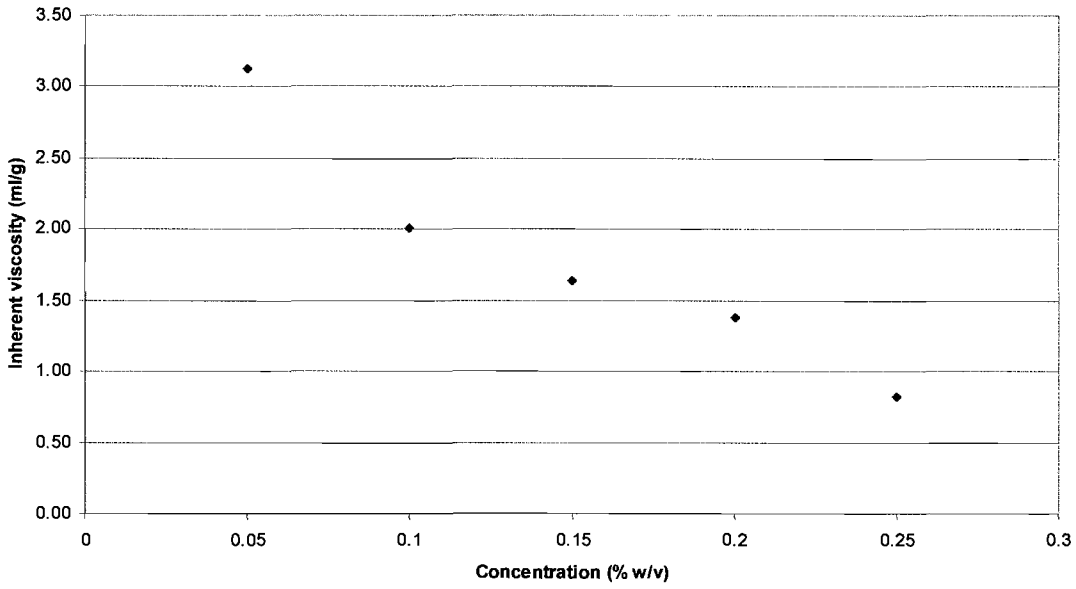

Figure 2.4: Inherent viscosity versus concentration for low molecular weight TMC

For low molecular weight TMC the straight line fit through the data points gave the following fit: $y = -10.44x + 3.36$ (see Appendix A), where the intrinsic viscosity is the intercept of the line. The intrinsic viscosity of the low molecular weight TMC was calculated as $[\eta] = 3.36$ ml/g. These calculations were repeated for all the different molecular weight chitosan and TMC polymers (Appendix A).

2.4.2 NMR and the calculation of degree of deacetylation and quaternization

In figures 2.5 to 2.7 the ^{1}H-NMR spectra of the different chitosan polymers are presented. Figures 2.8 to 2.10 show the ^{1}H-NMR spectra of different molecular weight TMC polymers. For chitosan Sato *et al.*, (1998) assigned the peak at 4.60 ppm to the ^{1}H-proton of the D-glucosamine (GlcN) unit and the peak at 3.17 ppm to the ^{2}H-proton of the D-glucosamine (GlcN) unit. The peak between 4.86 – 4.88 ppm was assigned to the ^{1}H-proton of the N-acetyl-D-glucosamine (GlcNAc) unit and the peak at 2.05 ppm for the acetyl group of the N-acetyl-D-glucosamine (GlcNAc) unit (figures 2.5 to 2.7).

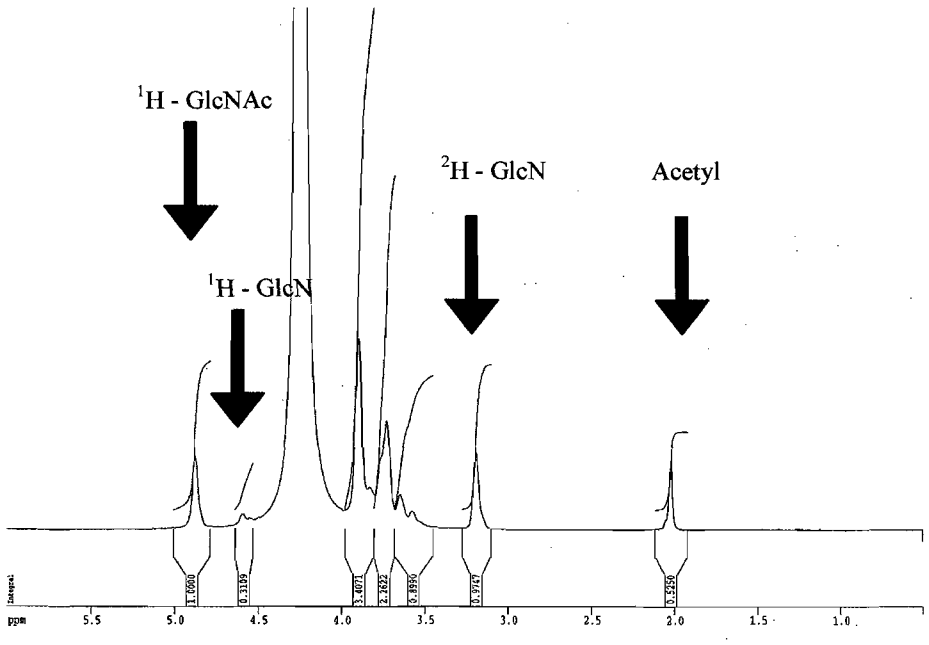

Figure 2.5: ^{1}H-NMR spectrum of low molecular weight chitosan.

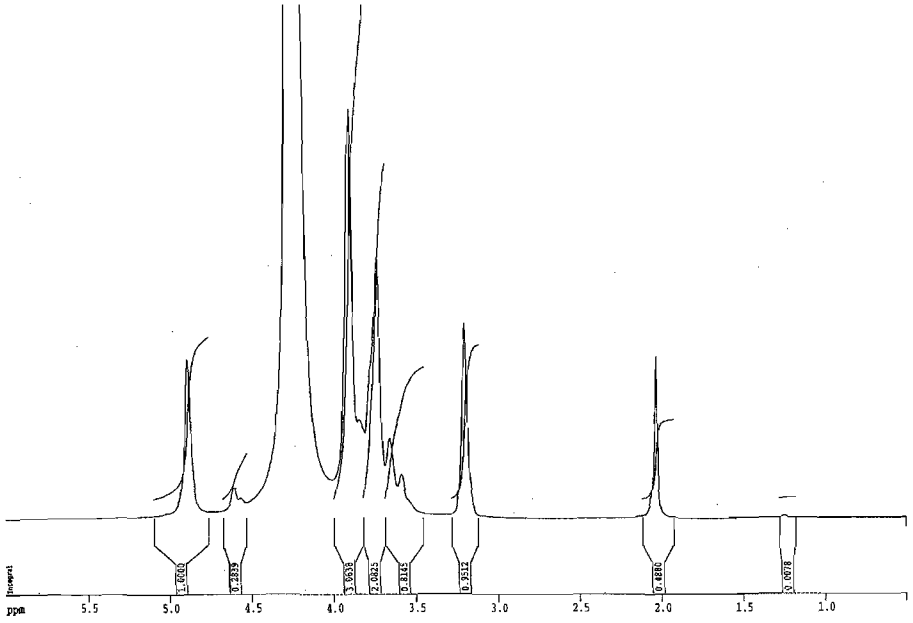

Figure 2.6: ^{1}H-NMR spectrum of medium molecular weight chitosan.

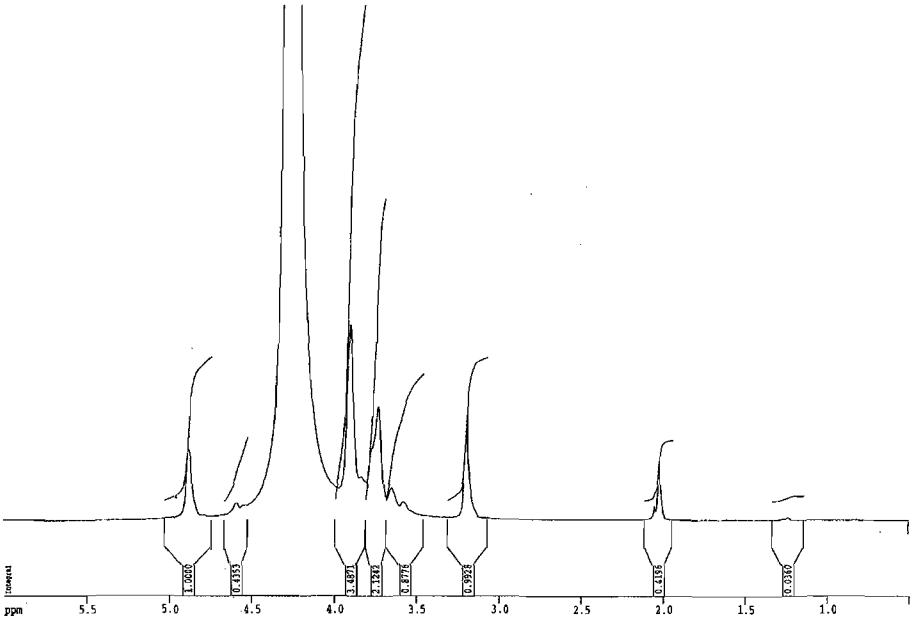

Figure 2.7: ^{1}H-NMR spectrum of high molecular weight chitosan.

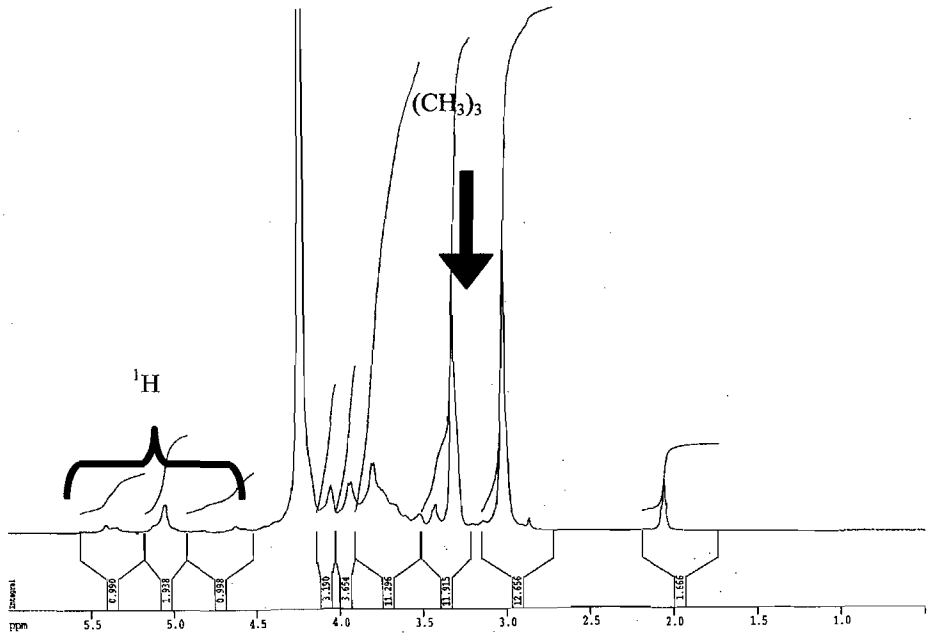

Figure 2.8: ^{1}H-NMR spectrum of low molecular weight TMC.

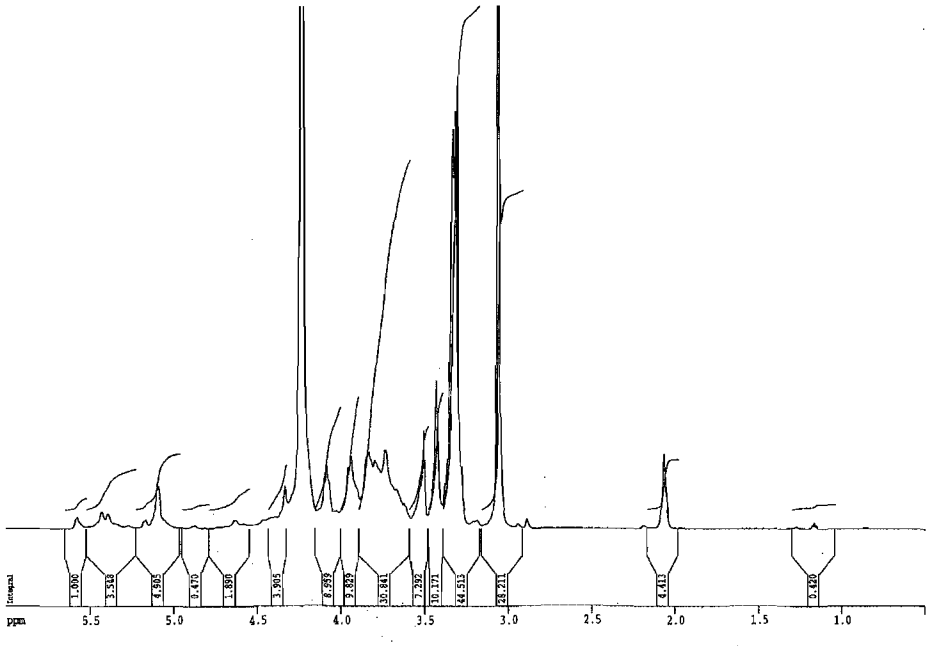

Figure 2.9: ^{1}H-NMR spectrum of medium molecular weight TMC.

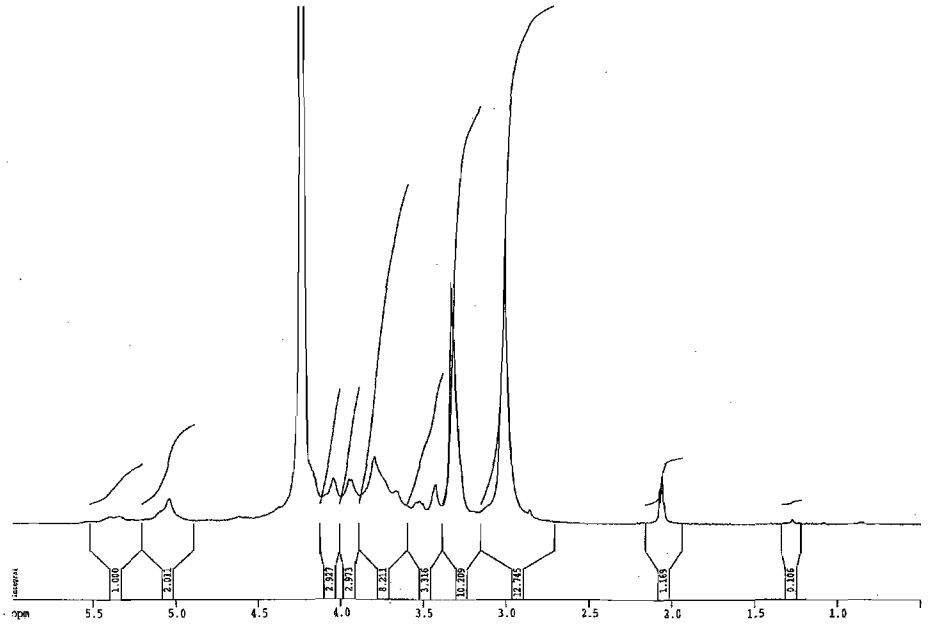

Figure 2.10: ^{1}H-NMR spectrum of high molecular weight TMC.

On the spectra of TMC, Sieval *et al.* 1998, has assigned the peak at 3.4 ppm to trimethyl amino groups and the peaks between 4.7 and 5.4 ppm to the ^{1}H-protons (figures 2.8 to 2.10).

With the NMR data of chitosan, equation 2.4 and equation 2.5, the degree of acetylation (DA) and degree of deacetylation (DDA) were calculated for all three chitosan polymers. These values are presented in table 2.4. There was an increase in the degree of acetylation of the chitosan polymer with an increase in the molecular weight.

Table 2.4: Degree of acetylation and deacetylation of chitosan

Chitosan	DA (%)	DDA (%)
Low MW	19.7	80.3
Medium MW	18.6	81.4
High MW	22.4	77.6

With the NMR data of TMC and equation 2.6 the degree of quaternization (DQ) of each TMC polymer were calculated. These values are presented in table 2.5.

Table 2.5: Degree of quaternization of TMC

TMC polymer	DQ (%)
Low MW	33.7
Medium MW	41.9
High MW	37.7

No conclusive pattern was obtained with degree of quaternization versus molecular weight.

2.5 CONCLUSION

Table 2.6 gives a summary of the characteristics of the chitosan and TMC polymers.

Table 2.6: Characteristics of chitosan and TMC

Polymer	MW ($x10^5$ g/mole)	Intrinsic Viscosity (ml/g)	DA (%)	DDA (%)
Chitosan				
Low MW	0.49	13.5	19.7	80.3
Medium MW	1.10	23.7	18.6	81.4
High MW	1.63	31.5	22.4	77.6
TMC	**MW ($x10^5$ g/mole)**	**Intrinsic Viscosity (ml/g)**	**DQ (%)**	
Low MW	2.03	3.4	33.7	
Medium MW	2.65	6.6	41.9	
High MW	3.28	9.2	37.7	

From the data in table 2.6, it can be concluded that three different molecular weights chitosan was used to synthesis TMC and that the degree of acetylation and degree of deacetylation of the chitosan are relative constant. From the SEC/MALLS data it was established that three different molecular weights of TMC were synthesized. The degree of quaternization for the medium (41.9 %) and high (37.7 %) molecular weight TMC were relatively close to each other. The lower degree of quaternization of the low molecular weight TMC could be caused by the low value of

the molecular weight (0.49 x 10^5 g/mole) of the chitosan polymer that was used to synthesis TMC. A lower molecular weight points to smaller molecular chain. This smaller chain means that the methyl groups that had bonded to the chain during the reductive methylation process will hinder other methyl groups from binding even if there are sites available to bind. The increase in degree of quaternization with the increase in molecular weight is also noted in literature (Van der Merwe *et al.*, 2004).

The intrinsic viscosity increased with an increase in molecular weight, which corresponds with literature (Snyman *et al.*, 2002). There was also a pronounce decrease in the intrinsic viscosity of TMC, compared with the original chitosan, and this is consistent with what is found in literature (Kotzé *et al.*, 1999).

CHAPTER 3

The effect of molecular weight on the mucoadhesive properties of *n*-Trimethyl chitosan chloride

3.1 INTRODUCTION

Junginger (1990) stated that to maximise the effect on absorption, the absorption enhancers should be able to come in close contact with the absorbing surface. The inclusion of a mucoadhesive polymer in a formulation to optimise the effects of an absorption enhancing agent may be an important contribution in the development of novel drug delivery systems. The superiority of chitosan as mucoadhesive substance has been described by Lehr *et al.* (1992) and Park (1989). This is due to the fact that chitosan is cationic polymer (Schipper *et al.*, 1996). Its applicability as a mucoadhesive substance and absorption enhancer in the small and large intestine is severely limited because chitosan is insoluble in neutral and basic solutions (Kotze *et al.*, 1998). Snyman (2000) showed in his studies the positive mucoadhesive influence of TMC as shown in the following table (table 3.1):

Table 3.1: Positive mucoadhesive influence of TMC

	Degree of quaternization	Molecular weight g/mol x 10^5	Intrinsic mucoadhesivity	% Relative to Pectin
Clean plate reference	-	-	0.0959	-
Pectin	-	-	0.1242	100
TMC 1	22.1	2.47	0.1440	169.96
TMC 2	38.1	1.70	0.1401	156.18
TMC 3	42.8	2.11	0.1341	134.98
TMC 4	48.8	1.94	0.1257	105.30

In this chapter the influence of the molecular weight on the mucoadhesive properties of TMC will be studied.

3.2 THEORETICAL BACKGROUND

Bioadhesion is defined as the attachment of synthetic or biological macromolecules to a biological surface (Peppas *et al.*, 1985 & Snyman, 2000). Mucoadhesion is when a bioadhesive polymer adheres primarily to the mucus layer of the mucosal epithelium (Junginger, 1990 & Snyman, 2000). In mucoadhesion, one of the adhering surfaces is a mucus membrane. Mucus membranes line the walls of various body cavities such as the gastrointestinal and respiratory tracts.

There are several epithelial cell types:

a) Simple squamous epithelium, which forms a thin layer in blood vessels.
b) Simple columnar epithelium, which is found in areas such as the stomach and small intestine.
c) Stratified epithelial membranes, which are found in areas such as the inside of the mouth and esophagus (Wilson *et al.*, 1989).

The squamous and columnar epithelium contain goblet cells that secrete mucus directly onto the epithelial surfaces, while the stratified epithelial membrane contain or are adjacent to tissues containing specialized glands such as salivary glands that secrete mucus onto the epithelial surface (Smart, 1999 & Snyman, 2000). The thickness of the mucus layer varies on different mucosal surfaces; from 50 to 450 μm in the stomach to 0.7 μm in the oral cavity.

The importance of mucus is in its protective, barrier, adhesion and lubrication properties. The protective role results from its hydrophobicity to protecting the mucosa of the stomach from hydrochloric acid. Mucus also constitutes a diffusion barrier for molecules and its influence is determined by physicochemical properties of the molecules such as molecular charge, hydration radius, ability to form hydrogen bonds and molecular weight. Mucus has strong adhesional properties and firmly binds to the epithelial cell surface as a continuous gel layer. Mucus also helps to keep the mucosal membrane moist. Continuous secretion of mucus from the goblet cells is necessary to compensate for the removal of the mucus layer due to digestion, bacterial degradation and solubilisation of mucus molecules (Ahuja *et al.*, 1997 & Snyman, 2000).

The molecular building blocks of native mucus of the intestine and other organs are large glycopeptides (monomers) that vary in size (molecular weight ranging from 2.5×10^5 to 2×10^6 Dalton) and in the composition of their oligosaccharide side chains. The protein content tends to be low (20 % by weight) and individual peptides consist of at least two regions: the major region (70 % – 80 %) is heavily glycosylated and the minor region is poorly glycosylated and is susceptible to proteolytic degradation (Neutra *et al.*, 1987 & Snyman, 2000). In general mucus consists of 95% water, 0.5% to 5% glycoproteins and lipids, 1% mineral salts and 0.5% to 1% free proteins (Ahuja *et al.*, 1997 & Snyman, 2000).

The mucus glycoproteins are the most important component of the mucus gel, resulting in its characteristic gel-like, cohesive and adhesive properties (Duchene *et al.*, 1988; Gu *et al.*, 1988; Snyman, 2000). Based on the structure of mucus, there are four characteristics of the mucus layer that relate to mucoadhesion (Junginger, 1990 & Snyman, 2000). The mucus layer is a network of linear, flexible and random coil mucus molecules. It is negatively charged due to the presence of sialic acid, which has a pK_a of 2.6, and sulphate residues on the mucus molecule. The mucus is a cross-linked network because of disulphide bonds and physical entanglement between mucus molecules. It is also highly hydrated.

3.2.1 Mechanisms of mucoadhesion

The mechanisms responsible for the formation of bioadhesive bonds are not completely clear. The process involved in the formation of a bioadhesive bond between polymer and soft tissue includes wetting and swelling of the polymer to permit intimate contact with a biological tissue, the interpenetration of bioadhesive polymer chains and entanglement of the polymer and mucus chains, and the formation of weak chemical bonds between entangled chains (Duchene *et al.*, 1988; Chickering *et al.*, 1999; Snyman, 2000).

To obtained adhesion there must be sufficient quantities of hydrogen-bonding chemical groups (–OH and –COOH) available on polymer and it must have anionic surface charges, with high molecular weight and high chain flexibility as well as surface tensions that will induce spreading

on the mucus layer (Peppas *et al.*, 1985 & Snyman, 2000). Each of these characteristics favours the formation of bonds that are either chemical or mechanical in origin.

From a molecular point of view, several mechanisms have been proposed to explain the interaction of a bioadhesive polymer and a biological surface, such as mucus, in order to create a mucoadhesive bond (Junginger, 1990 & Snyman, 2000). The following are possible mechanisms to explain mucoadhesion:

- The Electronic theory suggests that electron transfer upon contact of the polymer with the mucus glycoprotein network between the two electronic structures of the surfaces can contribute to the formation of a double layer of electrical charge at the mucoadhesive interface.
- The Adsorption theory analyses the phenomenon in terms of the forces manifesting themselves during mucoadhesion. The Adsorption theory states that the bioadhesive bond formed is due to Van der Waals interactions, hydrogen bonds and related forces.
- The Wetting theory is based on the ability of mucoadhesives to spread and develop intimate contact with the mucus surface. Thus expressions of the interfacial tension are obtained which can be used to screen various polymers for their ability to adhere to tissues.
- The Fracture theory examines the force necessary to separate the two surfaces after the mucoadhesive bond has been established.
- The Diffusion or interpenetration theory has the interpenetration of the macromolecular chains at the polymer-polymer interface as its basis. This is schematically presented in figure 3.1. The bond strength increases with the degree of penetration of the polymer chains into the mucus (Junginger, 1990 & Snyman, 2000).

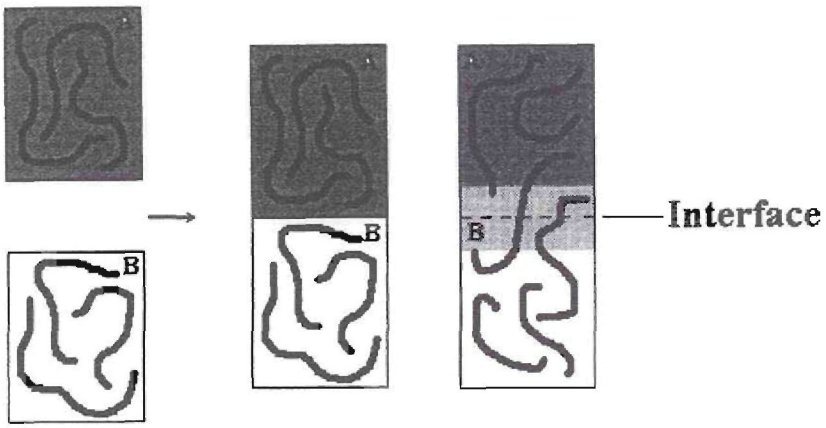

Figure 3.1: Schematic presentation of the chain adsorption and chain interpenetration during mucoadhesion of a polymer (A) with glycoprotein structure of mucus (B) and the subsequent forming of an interface between the two entities (Junginger, 1990: 113).

3.2.2 Factors influencing mucoadhesion

There is a wide range of factors, which could influence the strength of the observed mucoadhesive bond (Tobyn *et al.*, 1995 & Snyman, 2000). Numerous studies have indicated that there is a certain molecular weight at which bioadhesion reaches a maximum. It has been shown that low molecular weight polymers have a higher degree of interpenetration, whereas high molecular weight polymers have a higher degree of entanglement. According to Gurny *et al.* (1984) it seems that the bioadhesive force increase with the molecular weight of the bioadhesive polymer up to 100 000 dalton. Beyond this level bioadhesive forces do not change noticeably. Size and configuration of the mucoadhesive polymer molecules are also important factors (Ahuja *et al.*, 1997 & Snyman, 2000).

The effect of molecular weight of TMC on its mucoadhesive properties will be evaluated. Other factors must be also kept constant during the measurement of the mucoadhesive properties of TMC to determine the effect of molecular weight. These factors include (Snyman, 2000):

- Initial contact and prehydration time – Ponchel *et al.* (1987) found that the observed mucoadhesive force developed according to time, which showed that interpenetration

between polymer and mucus chains could be a major factor in determining the strength of the observed mucoadhesive force.

- Selection of the model substrate surface – In a study done by Rossi *et al.* (1995) the type of mucus used in mucoadhesion studies were investigated. It was found that commercial mucus is suitable for the comparison of mucoadhesive properties of the tested mucoadhesive polymer if they showed the same mechanisms of interaction with mucus and have the same sensitivities to medium characteristics such as pH and ion content.
- Applied strength – The adhesion strength increase with an increase in the applied strength or with the duration of its application, up to an optimum. A possible reason maybe that the pressure initially applied to the mucoadhesive tissue contact may affect the depth of interpenetration. It is even possible that when high pressure is applied for a sufficiently long period of time, that the polymers may become mucoadhesive even though they do not have mucoadhesive interactions with mucus (Ahuja *et al.*, 1997).
- pH of the medium – Mucus will have a different charge density depending on the pH because of differences in dissociation of functional groups on the carbohydrate moiety and amino acids of the polypeptide backbones (Ahuja *et al.*, 1997).
- Concentration – According to Ponchel *et al.* (1987) the concentration of the mucoadhesive polymer in the test tablet (or solution) has an effect on the measured mucoadhesion.
- Flexibility of polymer chains – As water-soluble polymers become cross-linked, the mobility of the individual densities of the polymers increases. The effective length of the chain, which can penetrate into the mucus layer, decreases and mucoadhesive strength is reduced (Ahuja *et al.*, 1997).
- Spatial conformation – A helical conformation may shield many adhesively active groups and thus negatively influence mucoadhesion (Ahuja *et al.*, 1997).

3.3 EXPERIMENTAL

There are several methods to measure the mucoadhesion of different substances. These methods (Snyman, 2000) include the method of Kellaway (Junginger, 1990), the method of Robinson (Junginger, 1990), the method of Leung and Robinson (Leung, 1991) and many more. It has been

noted that the wide variation in published results for *in vitro* mucoadhesion may be due to lack of universal test methods. According to Tobyn *et al.* (1995) the parameters of Ponchel *et al.* (1989) can be applied across different instrumentation set-ups with acceptable reproducibility. To determine the effect of molecular weight on the mucoadhesive properties of the synthesised TMC polymers, an adaptation of the tensile separation testing system used by Ponchel *et al.* (1987), was used on the three different molecular weights TMC polymer and the data obtained was used to determine the intrinsic mucoadhesivity. This adaptation was used because of the cost of production and the amount of polymer required to make a mucoadhesive tablet for the classic tensile separation test. For this adaptation a film of mucoadhesive polymer, which was dried from solution onto aluminium plates, was used.

A problem experienced with the tensile separation test is the interface that is formed between the polymer film and the mucus. The separation of the polymer and the mucus usually occurs inside the interface and this may result in high deviations for the experiments. The inconsistency caused by this interface, in different experimental set-ups, may be solved by testing a mixture of the polymer and the mucus for any synergistic effects on the surface tension (Snyman, 2000). A surface tension analysis was also done on the TMC polymers.

3.3.1 Tensile separation test

The mucoadhesive properties of the selected mucoadhesive polymers were measured with the use of a tensile separation test in which the polymer was brought into contact with mucus for a period of time during which interpenetration of the polymer into the mucus and hydration of the polymer film resulted in mucoadhesive bonding with the mucus chains. The tensile separation apparatus was based on an adaptation of the Wilhelmy plate method in which the mucoadhesion strength of the bond between mucus and the polymer was measured (Snyman, 2000). The experimental set-up for the tensile testing procedure is shown in figure 3.2. The basis for construction of the apparatus was vibration free, and the water bath was able to keep the temperature at a consistent 25 °C (Snyman, 2000).

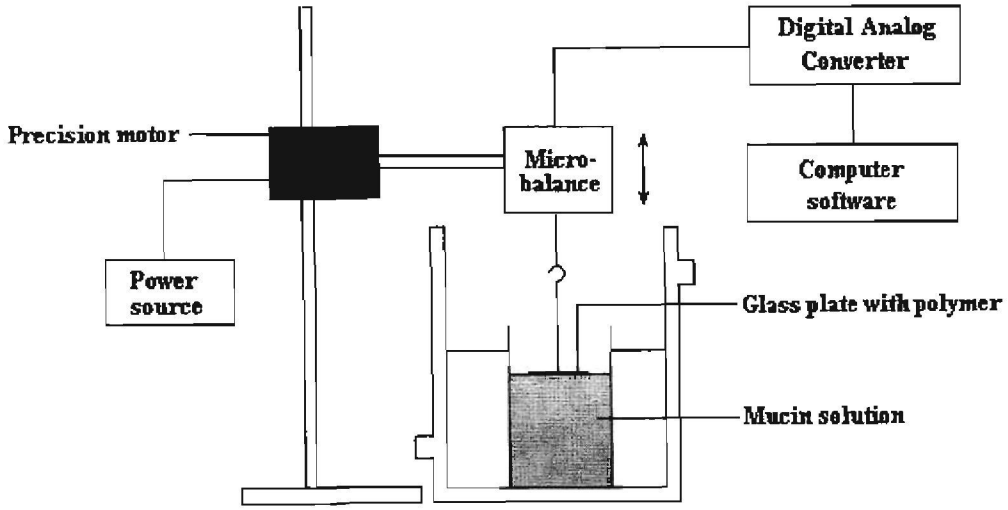

Figure 3.2: Experimental setup for the tensile separation testing.

3.3.1.1 Control

A clean aluminium plate is used as the control experiment for the tensile separation test.

3.3.1.2 Reference standards

Pectin was used as the reference standard in the tensile separation test. Pectin is a polysaccharide substance present in the cell walls of all plant tissues. Pectin functions as an intercellular cementing material. It consists mainly of partially methoxylated polygalacturonic acids. The molecular weight of pectin is between 20 000 and 400 000 Dalton (Merck Index, 1989). Pectin exhibits relative poor mucoadhesive properties but it is frequently used as a reference in mucoadhesion testing (Smart *et al.*, 1984; Junginger, 1991 & Snyman, 2000).

3.3.1.3 Method

Solutions of the TMC polymers were made by dissolving 0.1 g of each TMC polymer in 10 ml distilled water (1 % w/v solution). The aluminium plates were prepared by adding 0.5 g of the solution on each plate to produce 0.05 g of polymer film after drying. The mucus (partially

purified porcine gastric mucin type III, Sigma) was prepared by adding 1.5 g to 5 ml of distilled water. This solution was stirred for 2 minutes until the consistency of the mucus was uniform. The beaker with mucus was placed in a waterbath at 25 °C and left to reach the appropriate temperature. The aluminium plate was suspended from the microbalance (Force Transducer F30 Type 372, Hugo Sachs Elektronik) using a fine metallic thread that was free from elasticity. The plate was lowered until contact with the mucus was achieved and the tension between the plate and the microbalance declined, ensuring a 2 g downwards pressure on the mucus. The plate was left in this position for hydration of the polymer to occur after which it was again lifted at a tempo of 0.25 mm/s. The separation was registered by software (Chart for Windows v3.4, Powerlab System) and the maximum detachment force was noted in Newton. The detection system was calibrated using standard calibration weights (Hugo Sachs Elektronik, 1 g). The experiments were done at different hydration time intervals to measure the effect of time on the mucoadhesive properties. The time intervals were 20, 40, 60, 80, 100 and 120 seconds and each experiment was done in triplicate (Snyman, 2000).

3.3.2 Surface tension analysis

The interpenetration theory states that an interface forms with interpenetration of the mucus and mucoadhesive polymer. During tensile separation testing, the separation of the mucoadhesive polymer does occur in the interface, but on a level nearer to the mucus. The variation of results obtained between laboratories may be due to this variable. A possible solution to this problem was proposed by Tamburic and Craig (1997) who suggested that the synergistic increase in the viscosity of a mixture of mucus and polymer was the result of mucoadhesion and this could be measured by a probe connected to a microbalance. The work done is measured in Joule as the total area under the curve of the penetration/extraction experiment and could be used as an indicator of relative mucoadhesion.

Information on the effect described above could be obtained by measuring the surface tension of a mixture of mucoadhesive polymer and mucus. For these experiments the synergistic effect on the surface tension of a mixture of TMC and mucus was analysed with a Du Noüy tensiometer as a function of time (Snyman, 2000).

3.3.2.1 Method

A 2.5 % w/v polymer solution was prepared by adding 0.125 g of the polymer to 5 ml of distilled water and stirred for at least 4 hours at a temperature of 25 °C before tests were performed. The surface tensions of the polymer solutions were tested as a control value at a temperature of 25 °C. The surface tension of a mixture was measured by adding 0.5 g of mucus to 5 ml of the polymer solution to provide 10 % w/v mucus and 2.5 % w/v polymer mixture. The mixture was stirred for short intervals during which hydration of the matrix occurred. The surface tension was measured in 10 minute intervals over a one hour period. The mixtures were occasionally stirred to ensure that consistency of the mixture was uniform. Surfaces tension measurements were made in dynes/cm. Each experiment was done in triplicate (Snyman, 2000).

3.4 RESULTS

3.4.1 Mucoadhesion profiles obtained with tensile separate testing

Pectin was used as the reference standard and the clean aluminum plate was used as control. The relationship between time and mucoadhesion can be seen in figure 3.3, where with contact of the mucoadhesive polymer with the mucus, a mucoadhesive bond is form that strengthens with an increase in time. All the mucoadhesive polymers (TMC and Pectin) show higher mucoadhesive strength that the clean plate. They also begin at higher mucoadhesive strength than the clean plate. It is clear that the high molecular weight TMC exhibited the highest mucoadhesive strength and that the order decreased to the low molecular weight TMC with lowest mucoadhesivity. The error bars were omitted for reasons of clarity. In Appendix C the error bars are included.

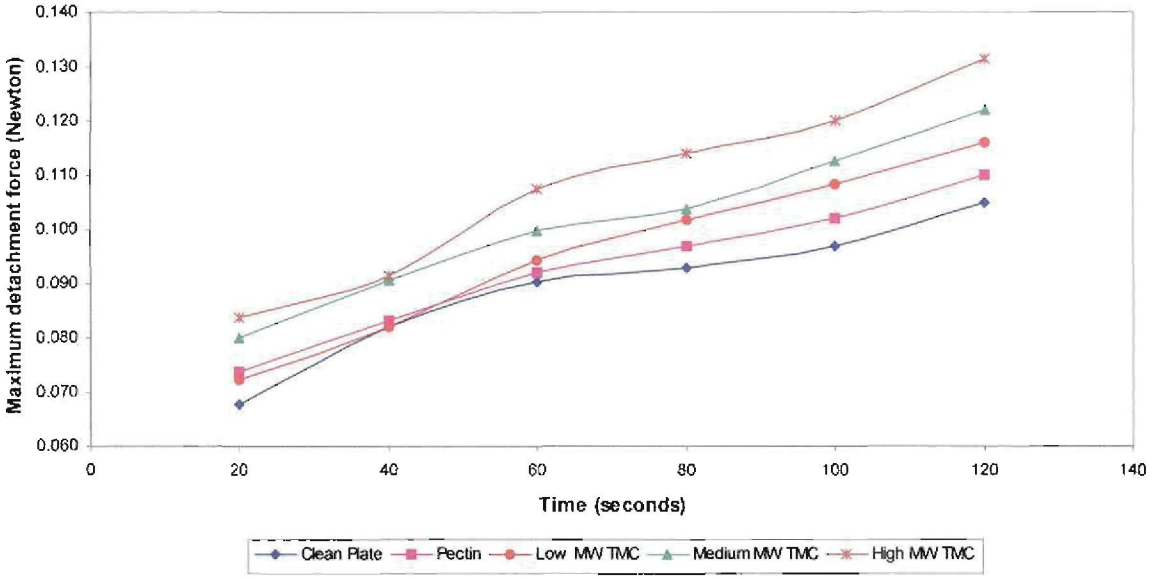

Figure 3.3: Mucoadhesion as a function of time.

3.4.2 Surface tension analysis

The results of the surface tension analysis of the different TMC polymers are given in figure 3.4. The data at time zero (t = 0 minutes) is an indication of the surface tension prior to mixing of the individual polymers and mucus. All the TMC polymers show a marked decrease in surface tension immediately after mixing. After 10 minutes the surface tension showed a marked increase, with the high molecular weight TMC exhibiting the highest increase

After 20 minutes the surface tension decreased, with high molecular weight TMC having the lowest decrease rate. The error bars were omitted for reasons of clarity. In Appendix C the error bars are included.

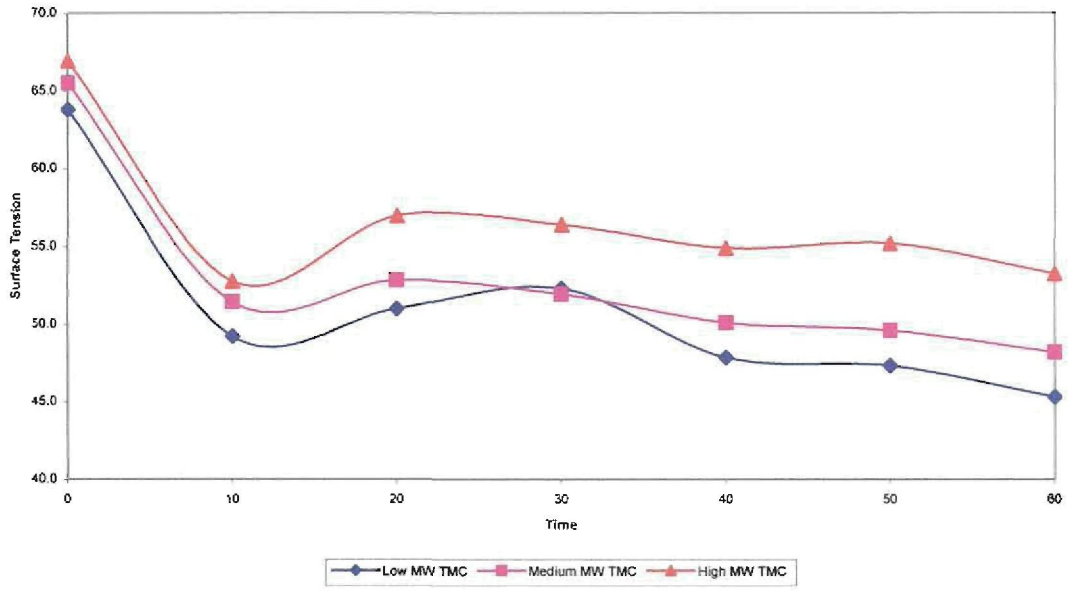

Figure 3.4: Surface tension analysis of a mixture of TMC polymer with mucus.

3.5 CONCLUSION

Both the pectin and the TMC exhibited higher mucoadhesive strength than the clean plate sample. Clear differences in the mucoadhesive strength of the different polymers can be seen. High molecular weight TMC has the highest mucoadhesive strength. This is due to the fact that with an increase in the molecular weight of the polymer, the polymer size increases and therefore the polymer has a bigger contact area to bind with the mucus. Peppas *et al.*, 1985 also noted that high molecular weight was a required polymer characteristic to obtain adhesion.

The marked decrease in surface tension immediately after mixing of the polymer with mucus is due to the formation of a gel between the mucus and the polymer (Snyman, 2000). Low molecular weight TMC had the highest decrease and this corresponds well with literature where low molecular weight polymers had a higher degree of interpenetration. Thus it has the fastest rate of decrease in surface tension. The high molecular weight TMC had the highest initial surface tension because it has the highest viscosity of all the polymers tested. The increase in

surface tension after 10 minutes is an indication of the formation of adhesive bond between the mucus and polymer and this correspondences well with literature (Snyman, 2000). High molecular weight TMC showed the highest increase and this is due to the fact that the high molecular weight TMC has more contact area to form stronger adhesive bonds with the mucus. After 20 minutes the surface tension decreased, which indicates that excessive hydration of the polymer mucus mixture causes the mucoadhesive properties to decrease.

From the data obtained, it can be concluded that high molecular weight TMC had the best mucoadhesive properties, which means that the high molecular weight TMC will bond best to epithelial surfaces and have a longer contact period, thus improving its absorption enhancing effect.

The effect of molecular weight on the mucoadhesive strength and surface tension can clearly be seen. An increase in molecular weight had an increase in both mucoadhesive strength and surface tension.

CHAPTER 4

The effect of molecular weight on the absorption enhancing properties of *n*-Trimethyl chitosan chloride

4.1 INTRODUCTION

Studies done by Kotzé *et al.* (1999), Hamman *et al.* (2003) and Van der Merwe *et al.* (2004) established that TMC could be used as an absorption enhancer for large hydrophilic compounds (peptides) across mucosal surfaces. TMC at neutral and basic conditions caused a decrease in the transepithelial electrical resistance (TEER) and an increase the permeability of human intestinal epthelial cells (Caco-2) (Kotzé *et al.*, 1999).

Schipper *et al.* (1996) studied the influence of molecular weight and degree of acetylation (DA) of chitosan on drug transport across Caco-2 cell monolayers. They concluded that at high degrees of deacetylation (99 %) the low molecular weight chitosan (31 x 10^3 Dalton) caused higher permeability of mannitol across the monolayer than the high molecular weight chitosan (170 x 10^3 Dalton). At a 85 % degree of deacetylation the situation changed. The high molecular weight chitosan (190 x 10^3 Dalton) caused higher permeability of mannitol across the monolayer than the low molecular weight chitosan (4.7 x 10^3 Dalton).

In this chapter, the effect of molecular weight of TMC on the permeability of Caco-2 cell monolayers will be discussed and a transport model will be proposed in order to determine the diffusion coefficient of mannitol through the epithelial membrane.

4.2 THEORETICAL BACKGROUND

4.2.1 Transepithelial electrical resistance

Transepithelial electrical resistance (TEER) measurements have been used to study the paracellular transport properties of epithelia grown on permeable filters, especially the barrier function of the tight junctions (Lo *et al.*, 1999). TEER is also an indication of the integrity of the cell monolayer (Artursson, 1990 & Karlsson *et al.*, 1991). The movement of ions between the

apical and basolateral sides of epithelial cells through intercellular spaces depends on the integrity of the tight junctions, therefore a decrease in the TEER value is associated with the opening of the tight junctions (decrease in integrity) (Schipper *et al.*, 1997 & Van der Merwe *et al.*, 2004). Electrical resistance is closely related to tightness of the tight junctions (Collett *et* al., 1996). The schematical set-up for the TEER measurements across epithelial membrane is shown in the figure 4.1:

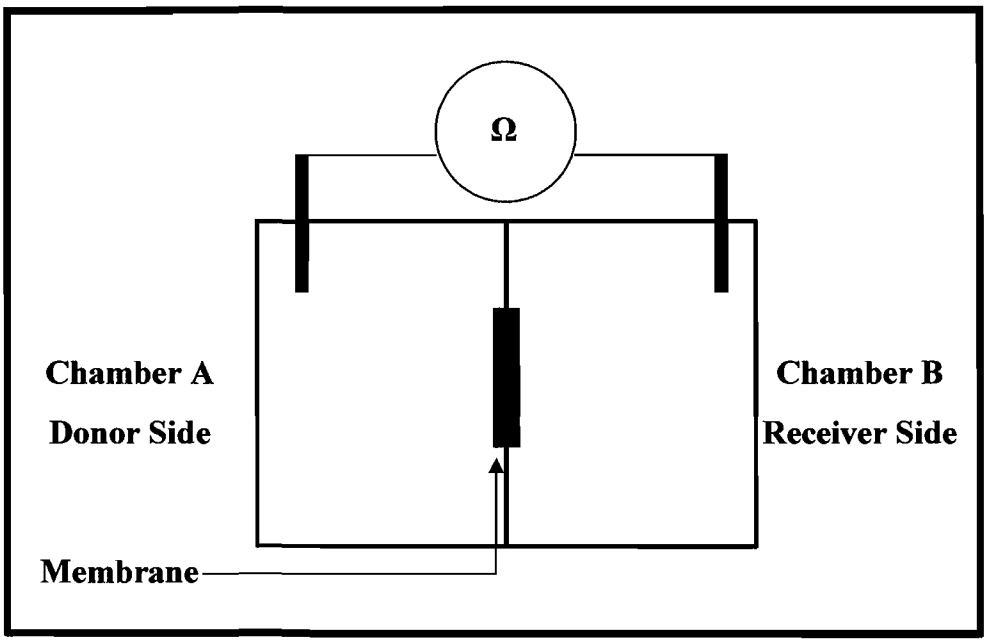

Figure 4.1: Schematic presentation of TEER experimental set-up

TEER is calculated from the measured electrical potential between the apical and the basolateral sides of the cell monolayer and is inversely related to the ion flow across the cell monolayer. The passive ion flow through the tight junction and the active ion transport in the cell membrane both contribute to the measured electrical potential difference and consequently to TEER (Powel, 1987). For this study, the TEER was measured before and after the administration of the TMC solutions.

4.2.2 Transport

The human adenocarcinoma cell line Caco-2 has been used widely as a model to predict human oral drug absorption (Collett *et al.*, 1996). The reason for Caco-2's usage is due to the fact that it spontaneously differentiates into polarized, columnar cells, which are more representative of the small intestine despite its colonic origin. Specifically, it exhibits well-developed microvilli and a polarized distribution of brush border enzymes and when grown on plastic it forms domes typical of normal, transporting epithelium (Hilgers *et al.*, 1990).

Caco-2 cell monolayers were used to determine the transport of the hydrophilic model compound ([^{14}C]-mannitol) when administered together with TMC. [^{14}C]-mannitol (MW 182 g/mol, specific radioactivity 56 mCi/mmol, 200 mCi/ml, obtained from Amersham Life Science) was selected as the hydrophilic model compound of choice for this study. [^{14}C]-mannitol is a metabolically inert and a highly hydrophilic molecule that has been used previously to follow changes in the epithelial integrity of the intestinal mucosa (Artursson *et al.*, 1994). Borchard *et al.* (1996) concluded that the transport pathway for [^{14}C]-mannitol is by means of paracellular transport. Duizer *et al.* (1997), Knipp *et al.* (1997), Hamman *et al.*, 2003 and Van der Merwe *et al.*, 2004 verified this conclusion.

4.2.3 Transport Model

The schematical set-up for the transport of [^{14}C]-Mannitol across epithelial membrane is shown in the figure 4.2 and which consist of the following:

1. The diffusion unit consists of two equal chambers separated by an epithelial membrane.
2. Donor side (apical side) and receiver side (basolateral side) are filled with transport buffer solution.
3. The transport drug [^{14}C]-Mannitol with TMC is placed in the donor side and samples are taken in the receiver side over a certain time period.
4. A gas mixture (95% O_2, 5% CO_2) at a constant flow rate is added by means of a gas manifold to each diffusion cell, to insure adequate mixing and oxygenation.
5. Samples are analysed by means of a scintillation counter and the concentration of [^{14}C]-Mannitol is measured.

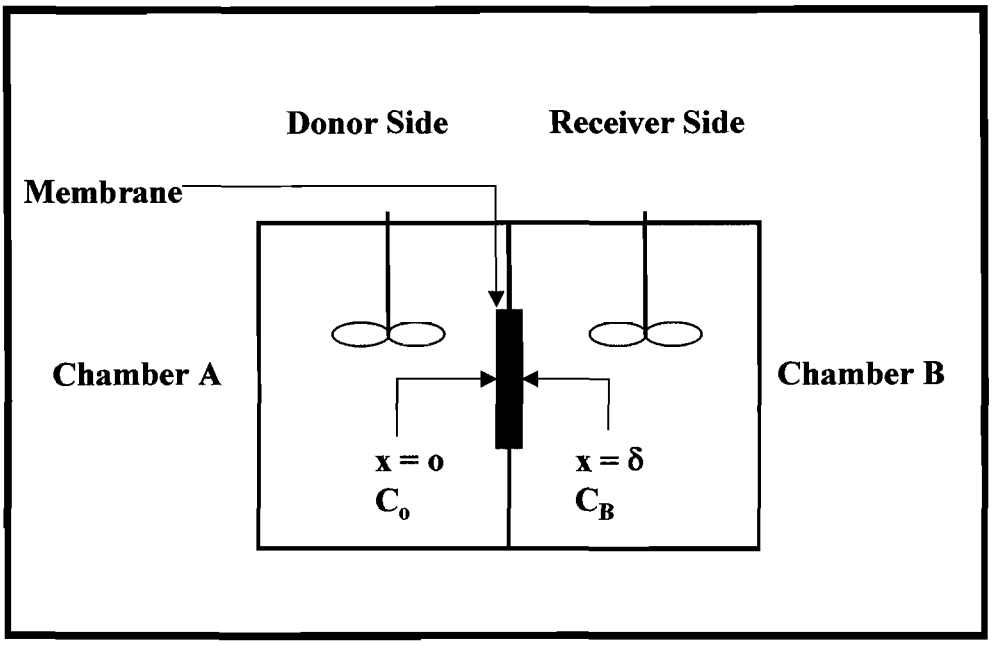

Figure 4.2: Schematic presentation of experimental set-up

To model the transport of [^{14}C]-Mannitol across epithelial membrane, the following assumptions are made:

1. Diffusion through the tight junction of the membrane is rate determining.
2. Constant diffusion coefficient (D).
3. Ideal mixing conditions in both chambers.
4. The membrane has no capacity.
5. No reactions take place.
6. The volumes in the chambers remain constant (V_A and V_B are constant).

A non-steady state mass balance over chamber B results in

$$\frac{d(V_B C_B)}{dt} = A\,J \qquad (4.1\text{-}1)$$

in which the flux (J) through the membrane can be described with Fick's law, resulting in

$$\frac{d(V_B C_B)}{dt} = D\,A\frac{dC}{dx} \qquad (4.1\text{-}2)$$

Taken into account that V_B is constant and assuming a linear concentration gradient in the membrane, the following equation is obtained.

$$V_B \frac{dC_B}{dt} = D\,A\frac{(C_A - C_B)}{\delta} \tag{4.1-3}$$

where C_A is the concentration in chamber A and C_B is the concentration in chamber B.

An overall macro balance over the system gives:

$$V_A(C_O - C_A) = V_B C_B \tag{4.1-4}$$

Combining equation 4.1-3 and 4.1-4, gives the following equation

$$\frac{dC_B}{dt} = \frac{A\,D}{\delta}\left[\frac{C_O}{V_B} - \frac{C_B}{V_A} - \frac{C_B}{V_B}\right] \tag{4.1-5}$$

Since $V = V_A = V_B$, this reduces to the following:

$$\frac{dC_B}{dt} = \frac{A\,D}{V\,\delta}[C_O - 2C_B] \tag{4.1-6}$$

After integration of the following equation

$$\int \frac{dC_B}{[C_O - 2\,C_B]} = \frac{A\,D}{V\,\delta}\int t\,dt \tag{4.1-7}$$

It results in

$$-\frac{1}{2}\ln[C_O - 2\,C_B(t)] = \frac{A\,D}{V\,\delta}t + K \tag{4.1-8}$$

Using the initial condition $C_B\,(t = 0) = 0$

The constant K is determined

$$K = -\frac{1}{2}\ln C_O \tag{4.1-9}$$

Substituting equation 4.1-9 in to equation 4.1–8, the following is obtained

$$-\ln\left[1 - \frac{2\,C_B(t)}{C_O}\right] = 2\frac{A\,D}{V\,\delta}t \tag{4.1-10}$$

And rearranging the result, will give the concentration in B as function of time:

$$C_B(t) = \frac{C_O}{2}\left(1 - e^{-2\frac{A\,D}{V\,\delta}t}\right) \tag{4.1-11}$$

Assumption 5 (no capacity) of the model is only valid when transport is relatively fast compared to the thickness of the membrane. This however is not the case for the experiments carried out in this study. Due to the relative slow transport and thick membrane, the capacity of the membrane does play a role especially at the beginning of the experiment. Thus, the proposed model is only valid after a certain time. This time is characterised by the penetration time (t_δ) (Bird *et al.*, 1960):

$$t_\delta = \frac{\delta_i^2}{4\,D} \qquad (4.1\text{-}12)$$

and was verified to be in the order of 120 minutes depending on the experimental conditions. After an in depth inspection of the experimental results, it could be concluded that after a period of 120 min the capacity effect of the membrane was absent, and therefore only the experimental values after 120 minutes were used for modelling purposes. This can also be visualised in figure 4.3, where a distinct break between the experiments before and after 120 minutes can be seen.

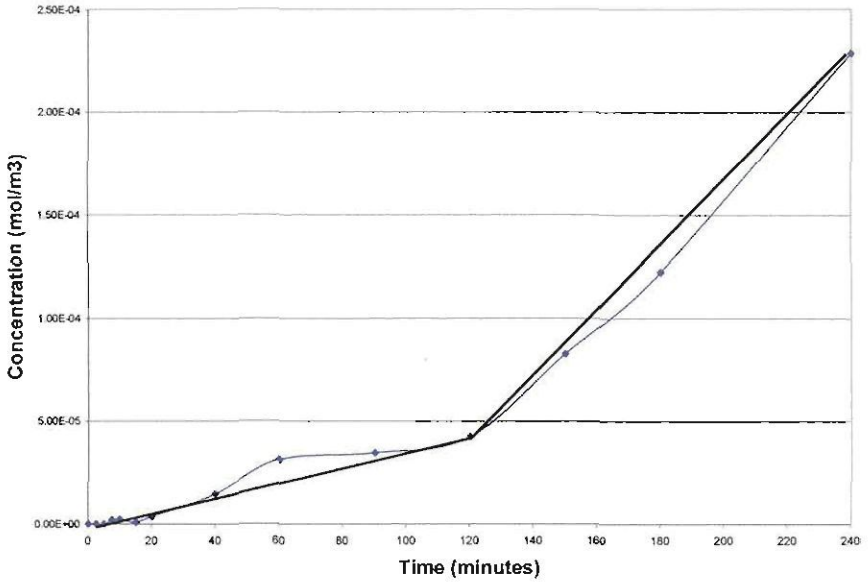

Figure 4.3: Penetration and transport of [^{14}C]-Mannitol (High MW TMC)

4.3 EXPERIMENTAL

All the transepithelial electrical resistance and transport experiments were performed at Amsterdam Centre for Drug Research at Leiden University, Nederland.

4.3.1 Culturing and seeding of Caco-2 monolayers

Caco-2 cells (passage 91) were used for the transport and TEER experiments with different molecular weight TMC. The cells were seeded on tissue culture treated polycarbonate filters (area 4.7 cm^2) in Costar Transwell 6-well plates at a seeding density of 1 x 10^4 cells/cm^2. Dulbecco's Modified Eagle Medium [DMEM, pH 7.4], supplemented with 1 % non-essential amino acids, 10 % foetal bovine serum, benzylpenicillin G (160 U/ml) and streptomycin sulphate (100 µg/ml), were used as culture medium, and added to both the donor and acceptor compartments. The medium was changed every second day and cell cultures were kept at a temperature of 37 °C in an atmosphere of 95 % air and 5 % CO_2. Transwell plates were used for transepithelial electrical resistance and transport studies 21 – 23 days after seeding (Kotzé *et al.*, 1997).

4.3.2 Transepithelial electrical resistance (TEER) measurements

The transport buffer used was DMEM containing HEPES at pH 7.4. Solutions of TMC polymers at concentrations of 0.1 and 0.5% (w/v) for all three different molecular weights were used. TEER measurements were taken at time intervals of 5 minutes starting 1 hour prior to incubation with the different TMC solutions on the apical side of the cells and continued for 2 hour after incubation. All the experiments were done in triplicate. The TEER values were plotted as a function of time and expressed as a percentage using the following equation (Duizer *et al.*, 1997).

$$\%TEER = \left(\frac{R(t)}{R_{t=0}} \right) \times 100 \qquad (4.2\text{-}1)$$

4.3.3 Transport of a hydrophilic model compound

The transport buffer used was DMEM containing HEPES at pH 7.4. Control values were obtained from mannitol solutions in DMEM containing HEPES in the absence of TMC polymers.

Caco-2 cells were incubated with a [^{14}C]-mannitol (specific activity 56 mCi/mmol) solution of an activity of 0.2 µCi/ml with TMC polymers at concentrations of 0.1 and 0.5 % (w/v) for all three different molecular weights. In these studies [^{14}C]-mannitol together with TMC is administered to the apical side of the monolayers. For determination of mannitol transport, 200 µl samples were taken from the basolateral compartment at given times, and substituted with fresh buffer. Samples were then mixed with scintillation counter, and the radioactivity in the samples measured in a betacounter. The data obtained from scintillation counter was converted from counters per minute (cpm) to Ci by plotting an activity (Ci) versus cpm standard curve with a range of mannitol concentrations. See Appendix D for more details. The conversion from Ci to mol was done using specific activity supplied by supplier. All the experiments were done in triplicate (Appendix D). The following constant variables were used in the calculation of the transport model.

Table 4.1: Constant variables for transport model

Constant variable	Value	Reference
C_0	3.6×10^{-3} mol/m^3	Experimental
A	4.5×10^{-4} m^2	Corning Life Science Website
V	2.5×10^{-6} m^3	Experimental setup
δ	3.5×10^{-5} m	Hilgers *et al.*, 1990

4.4 RESULTS

4.4.1 Transepithelial electrical resistance experiments

The effect of TMC on the TEER is presented graphically for 0.1 and 0.5% w/v respectively (see figures 4.4 and 4.5). For more details see Appendix. TEER measurements were taken 1 hour prior to incubation with the different TMC solutions on the apical side of the cells and continued for 2 hour after incubation. This was done to ensure that identical experimental conditions for the membranes were used.

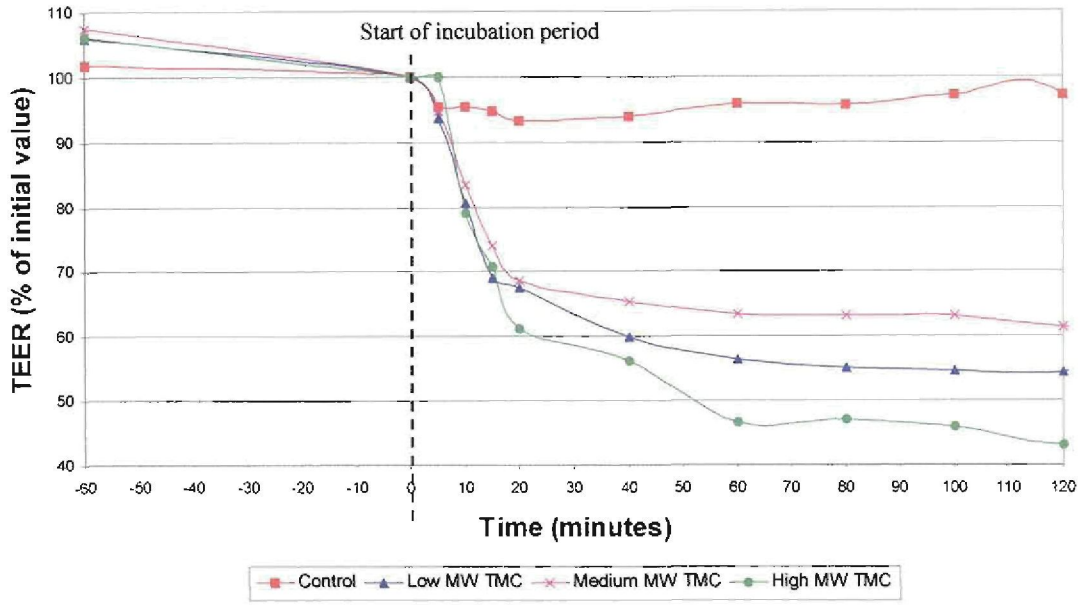

Figure 4.4: Effect of different molecular weight TMC polymers (concentration of TMC = 0.1 % w/v) on the TEER of Caco-2 cell monolayer at pH 7.4.

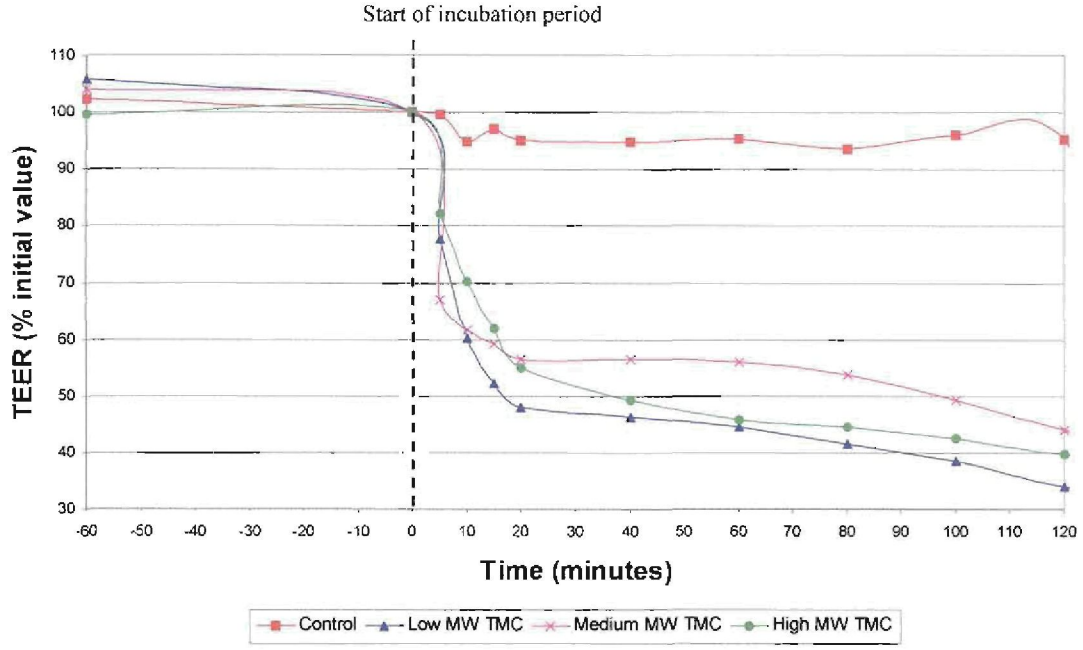

Figure 4.5: Effect of different molecular weight TMC polymers (concentration of TMC = 0.5 % w/v) on the TEER of Caco-2 cell monolayer at pH 7.4.

All three different molecular weight TMC showed an immediate and pronounced decrease in TEER values with the low molecular weight TMC showing the largest influence at 0.5% concentration and high molecular weight TMC at 0.1% concentration. The concentration of 0.5% (w/v) had the bigger influence of the two concentrations on the TEER. All the experiments show high levels of reproducibility as shown in Appendix D.

4.4.2 Transport of [^{14}C]-mannitol

The effect of TMC and the use of different molecular weight TMC on the transport of [^{14}C]-mannitol are shown in the following graphs (see figures 4.6, 4.7 and 4.8).

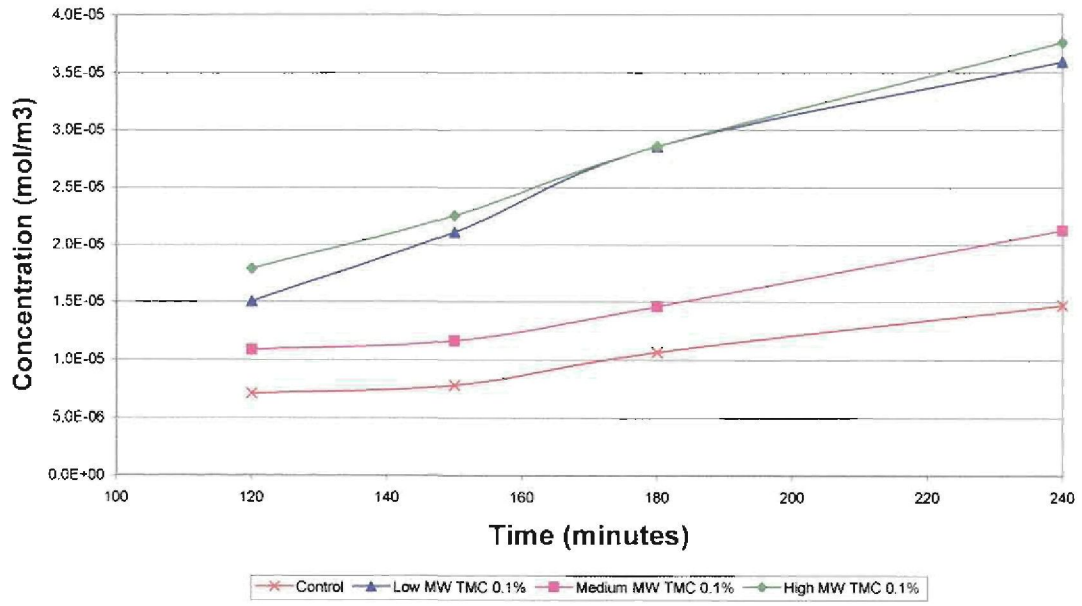

Figure 4.6: Effect of molecular weight on the transport of [^{14}C]-mannitol (concentration of TMC = 0.1% w/v)

All three molecular weight showed an increase in transport of [^{14}C]-mannitol with the high molecular weight TMC giving the highest improvement at 0.1% concentration while low molecular weight TMC showed the highest improvement at the 0.5% concentration. The 0.5% (w/v) concentration showed the largest influence. All the experiments show high levels of reproducibility. For more detail see Appendix D.

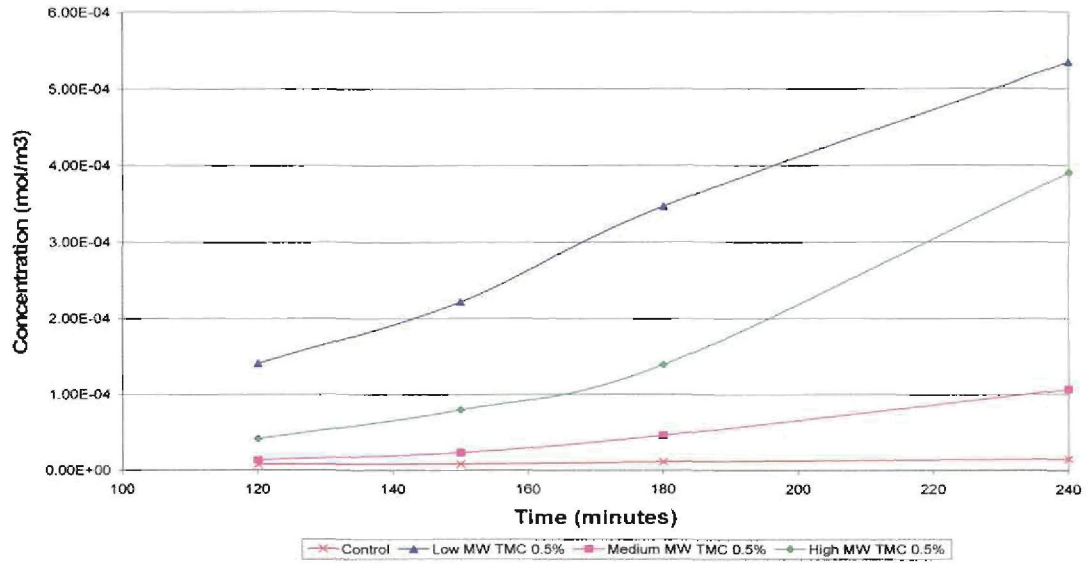

Figure 4.7: Effect of molecular weight on the transport of [^{14}C]-mannitol (concentration of TMC = 0.5% w/v)

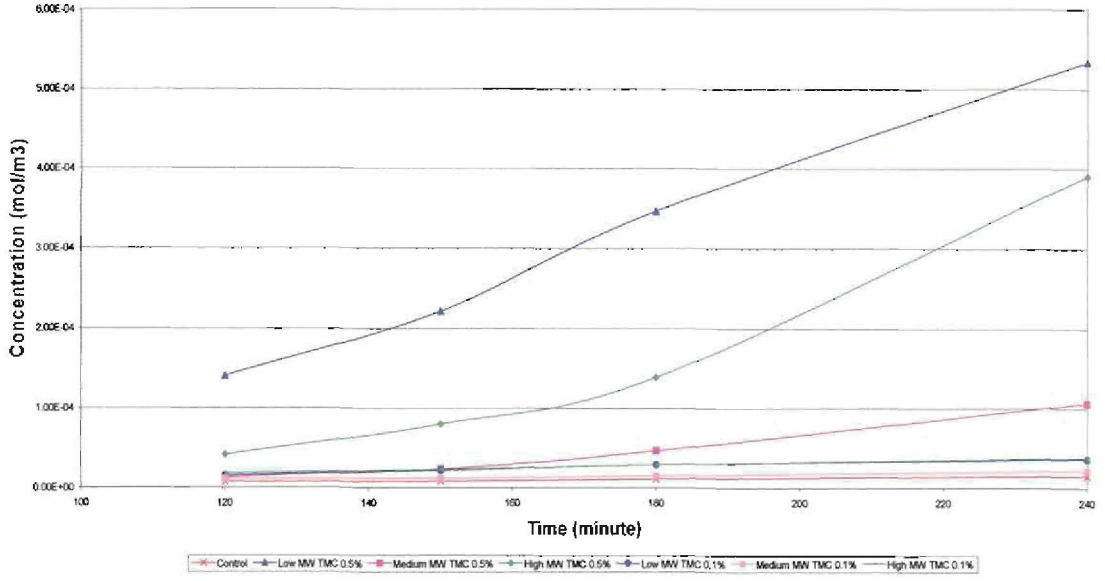

Figure 4.8: Effect of concentration of different molecular weight TMC on the transport of [^{14}C]-mannitol

4.4.3 Modeling of the transport of [^{14}C]-mannitol across epithelial membrane

From the transport data obtained, it was concluded that the assumption made that the membrane has no capacity was incorrect and that there was a period of penetration of the [^{14}C]-mannitol into the membrane before the actual transport of the mannitol across the membrane took place. For the calculations of the diffusion coefficient, only transport data from 120 minutes and onwards were used.

Using equation 4.1-10, the diffusion coefficient can be calculated from the slope of the left hand side of the equation versus time, which is given in figure 4.9, which was obtained for high molecular weight TMC at concentration of 0.5% (w/v).

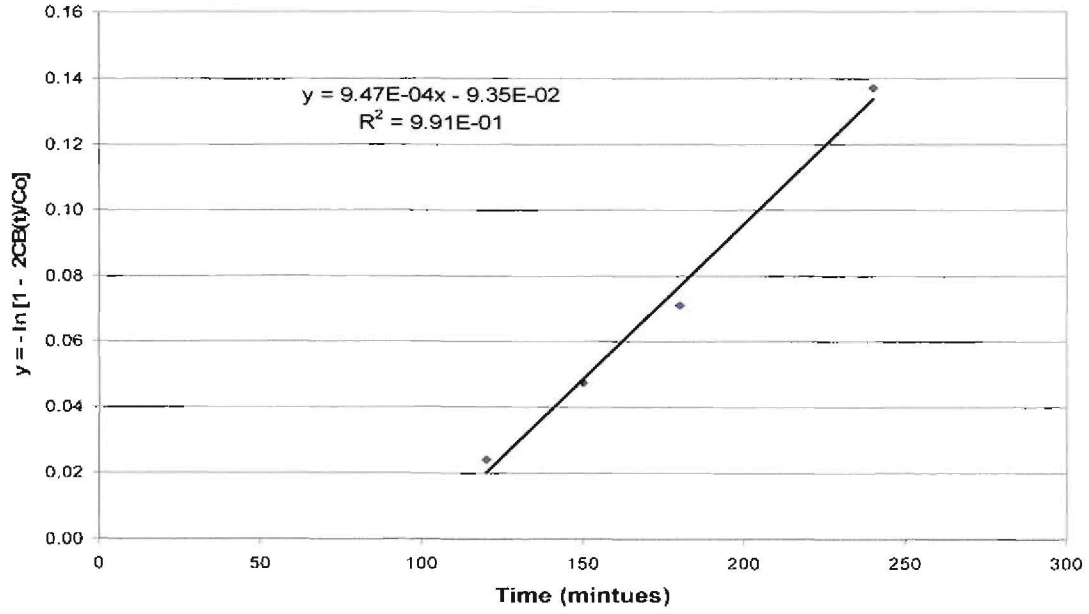

Figure 4.9: $y = -\ln\left[1 - \frac{2\,C_B(t)}{C_O}\right]$ **as a function of time for experiment 1 of high molecular weight TMC (0.5 % w/v)**

A gradient of 9.47 x 10^{-4} min^{-1} was obtained for experiment 1. This was repeated for the two other experiments done with high molecular weight (0.5% w/v). The diffusion coefficients (D) were calculated using equation 4.1-10 where

$$slope = 2\frac{A\,D}{V\,\delta} \qquad (4.3\text{-}1)$$

The average of the three experiments was taken for each different molecular weight at different weight percentages and is given in table 4.2.

Table 4.2: Diffusion coefficient obtained by means of transport model

TMC (w/v)		Average Gradient	Average Diffusion Coefficient (m^2/min)
0.1 %			
	Low MW	1.15×10^{-4}	1.12×10^{-11}
	Med MW	5.12×10^{-5}	4.98×10^{-12}
	High MW	1.24×10^{-4}	1.21×10^{-11}
0.5 %			
	Low MW	2.38×10^{-3}	2.31×10^{-10}
	Med MW	4.66×10^{-4}	4.53×10^{-11}
	High MW	1.93×10^{-3}	1.88×10^{-10}
	Control	3.76×10^{-5}	3.65×10^{-12}

4.5 CONCLUSION

TEER data showed an immediate and pronounced decrease in TEER values due to the administration of TMC to the transport solution. An increase in concentration caused an increase in the effect of TMC on the TEER. The decrease in the TEER value is associated with the opening of the tight junctions (decrease in integrity) (Schipper *et al.*, 1997 & Van der Merwe *et al.*, 2004) and electrical resistance is closely related to tightness of the tight junction (Collett *et* al., 1996). This can be seen in the increase in transport rates of [^{14}C]-mannitol across the epithelial membrane. All three different molecular weights of TMC caused an increase in the transport rate. There was also an increase in transport rates with an increase in concentrations of TMC. Was also report by Kotzé *et al.* (1997).

Low molecular weight TMC had the most pronounced effect on TEER and transport rate at higher concentrations (0.5% w/v) of TMC polymer. Due to the short chain length (lowest molecular weight) and low viscosity of low molecular weight TMC, the compound could "move" closer to the tight junctions and have the largest influence on the tight junction. This can be seen in the decrease in TEER and the increase in transport rates. But at the low concentrations (0.1% w/v) however, the high molecular weight TMC had the highest transport rate and biggest decrease in TEER values. At higher concentrations (0.5% w/v) the high molecular weight TMC could be clogging the tight junctions. But because of its high mucoadhesive property and contact sites (due to large chain), at lower concentrations the high molecular weight TMC has a bigger effect than the low molecular weight TMC. The discrepancy in TEER and transport results of the medium molecular weight can possible be attributed to the degree of quaternization (DQ) which the medium molecular weight TMC has the highest value (see chapter 2). DQ is a relationship of the amount of tri-methyl amino groups present on the TMC molecule. The medium molecular weight TMC has thus more of the tri-methyl amino groups and these might also be clogging the tight junction openings and restricting the transport of [^{14}C]-mannitol despite causing the tight junction to open up as seen by drop in TEER values.

The mathematical model (equation 4.1-8) showed the effect of using an absorption enhancer. There was an increase in the diffusion coefficient with the administration of TMC. A period of penetration of [^{14}C]-mannitol into the membrane was observed and this influenced the calculation of the diffusion coefficients. When the effect of penetration depth was included, better data fitting was obtained. For all the different molecular weights and concentrations of TMC, the effect of penetration depth was incorporated into the calculation of diffusion coefficients by assuming that "true" transport of [^{14}C]-mannitol was only taking place after 120 minutes. The choice of 120 minutes was based on the fact that there was a comprehensive increase in the transport rate of [^{14}C]-mannitol. This implies that [^{14}C]-mannitol has to over come the membrane barrier and then only can the transport of [^{14}C]-mannitol take place.

CHAPTER 5

A final summary of the main conclusions

The aim of this study was to determine the effect of the molecular weight of TMC on its absorption enhancing properties. This would be done by:

- Characterising three different molecular weights of chitosans by determining their molecular weight, viscosity and degree of acetylation and deacetylation.
- Synthesising three different molecular weights of TMC from three different molecular weights of chitosan.
- Characterising the TMC polymers by determining their molecular weight, viscosity and degree of quaternization.
- Determining the effect of the molecular weight of TMC on its mucoadhesive properties by tensile separation testing and surface tension analysis.
- Determining the effect of the molecular weight of TMC on its absorption enhancing properties by measurement of the transepithelial electrical resistance of Caco-2 cell monolayer and by permeability studies on Caco-2 cell monolayers.
- Describing mathematically the transport of [^{14}C]-mannitol in the presence of TMC polymers.

From the data presented in chapter 2, it could be concluded that three different molecular weights chitosan was used to synthesis three different molecular weights of TMC and that the degree of acetylation and degree of deacetylation of the chitosan are relative constant. Except for the low molecular weight TMC, the degree of quaternization for the medium and high molecular weight TMC were relatively close to each other. The lower degree of quaternization of the low molecular weight TMC could be caused by the low value of the molecular weight of the chitosan polymer that was used to synthesis TMC. A lower molecular weight points to smaller molecular chain which means that the methyl groups that had bonded to the chain during the reductive methylation process would hinder other methyl groups from binding even if there are sites available to bind. The increase in degree of quaternization with the increase in molecular weight was also noted. The intrinsic viscosity increased with an increase in molecular weight and there was also a pronounce decrease in the intrinsic viscosity of TMC, compared with the original

chitosan, and this was consistent with what is found in literature (Snyman *et al.*, 2002 and Kotzé *et al.*, 1999).

The analysis of mucoadhesive properties in chapter 3 concluded clear differences in the mucoadhesive strength of the different polymers. High molecular weight TMC had the highest mucoadhesive strength. This was due to the fact that with an increase in the molecular weight of the polymer, the polymer size increased and therefore the polymer had a bigger contact area to bind with the mucus. Low molecular weight TMC had the highest decrease in surface tension and this corresponds well with literature where low molecular weight polymers had a higher degree of interpenetration. The high molecular weight TMC had the highest initial surface tension because it has the highest viscosity of all the polymers tested. The increase in surface tension after 10 minutes was an indication of the formation of adhesive bond between the mucus and polymer and this correspondences well with literature (Snyman, 2000). High molecular weight TMC showed the highest increase and this was due to the fact that the high molecular weight TMC has more contact area to form stronger adhesive bonds with the mucus. After 20 minutes the surface tension decreased, which indicated that excessive hydration of the polymer mucus mixture caused the mucoadhesive properties to decrease. From the data obtained, it could be concluded that high molecular weight TMC had the best mucoadhesive properties, which meant that the high molecular weight TMC would bond best to epithelial surfaces and have a longer contact period, thus improving its absorption enhancing effect.

In chapter 4, TEER data showed an immediate and pronounced decrease in TEER values due to the administration of TMC to the transport solution. An increase in concentration caused an increase in the effect of TMC on the TEER. The decrease in the TEER value was associated with the opening of the tight junctions (decrease in integrity) (Schipper *et al.*, 1997 & Van der Merwe *et al.*, 2004) and electrical resistance is closely related to tightness of the tight junction (Collett *et* al., 1996). This can be seen in the increase in transport rates of [^{14}C]-mannitol across the epithelial membrane. All three different molecular weights of TMC caused an increase in the transport rate. There was also an increase in transport rates with an increase in concentrations of TMC. Low molecular weight TMC had the most pronounced effect on TEER and transport rate at higher concentrations (0.5% w/v) of TMC polymer. This was due to the short chain length

(lowest molecular weight) and low viscosity of low molecular weight TMC, the compound could "move" closer to the tight junctions and have the largest influence on the tight junction. But at the low concentrations (0.1% w/v) however, the high molecular weight TMC had the highest transport rate and biggest decrease in TEER values. At higher concentrations (0.5% w/v) the high molecular weight TMC could be clogging the tight junctions. But because of its high mucoadhesive property and contact sites (due to large chain), at lower concentrations the high molecular weight TMC has a bigger effect than the low molecular weight TMC. The discrepancy in TEER and transport results of the medium molecular weight could possible be attributed to the degree of quaternization (DQ) where the medium molecular weight TMC has the highest value as seen in chapter 2. DQ is a relationship of the amount of tri-methyl amino groups present on the TMC molecule. The medium molecular weight TMC has thus more of the tri-methyl amino groups and these might also be clogging the tight junction openings and restricting the transport of [^{14}C]-mannitol despite causing the tight junction to open up as seen by drop in TEER values.

The mathematical model (equation 4.1-8) showed the effect of using an absorption enhancer. There was an increase in the diffusion coefficient with the administration of TMC. A period of penetration of [^{14}C]-mannitol into the membrane was observed and this influenced the calculation of the diffusion coefficients. When the effect of penetration depth was included, better data fitting was obtained. For all the different molecular weights and concentrations of TMC, the effect of penetration depth was incorporated into the calculation of diffusion coefficients by assuming that "true" transport of [^{14}C]-mannitol was only taking place after 120 minutes. The choice of 120 minutes was based on the fact that there was a comprehensive increase in the transport rate of [^{14}C]-mannitol. This implies that [^{14}C]-mannitol has to over come the membrane barrier and then only can the transport of [^{14}C]-mannitol take place.

REFERENCES

1. AHUJA, A., KHAR, R.K. & ALI, J., 1997, *Mucoadhesive drug delivery systems*, Drug Development and Industrial Pharmaceutics, 23 (5): 489 – 515.
2. ANON. 1965. (*In Encyclopaedia of Polymer Science and Technology.* New York: John Wiley & Sons, Inc. 717p.)
3. ARTURSSON, P, 1990, *Epithelial transport of drugs in cell culture. 1: A model for studying the passive diffusion of drugs over intestinal absorbtive (Caco-2) cells*, Journal of Pharmaceutical Sciences, 79 (6): 476-482.
4. ARTURSSON, P., LINDMARK, T., DAVIS, S.S., & ILLUM, L., 1994, *Effect of chitosan on the permeability of monolayers of intestinal epithelial cells (Caco-2)*, Pharmaceutical Research, 11 (9): 1358-1361.
5. BIRD, R.B., STEWART, W.E. & LIGHTFOOT, E.N., *Transport phenomena*, John Wiley & Sons, New York, 1960.
6. BORCHARD, G., LUEßEN, H.L., DE BOER, A.G., VERHOEF, J.C., LEHR, C-M. & JUNGINGER, H.E., 1996 *The potential of mucoadhesive polymers in enhancing intestinal peptide drug absorption. III: Effects of chitosan-glutamate and carbomer on epithelial tight junctions in vitro*, Journal of controlled release, 39: 131-138.
7. BURTON, P.S., CONRADI, R.A., HO, N.F.H., HILGERS, A.R., & BORCHARDT, R.T., 1996, *How structural features influence the biomembranes permeability of peptides*, Journal of Pharmaceutical Sciences, 85 (12): 1336 – 1340.
8. CHICKERING III, D.E. & MATHIOWITZ, E., 1999, *Definitions, mechanisms and theories of bioadhesion*, (In Mathiowithz et al., ed. Bioadhesive drug delivery systems New York: Marcel Dekker 1 – 10.)
9. COLLETT,A., SIMS, E., WALKER, D., HE, Y-L., AYRTON, J., ROWLAND, M. & WARHURST, G., 1996, *Comparison of HT29-18-C_1 and Caco-2 cell lines as models for studying intestinal paracellular absorption*, Pharmaceutical Research, 13 (2): 216 – 221.
10. COLLINS, E.A., BARES, J., BILLMEYER jr., F.W., *Experiments in Polymer Science*, John Wiley & Sons. Inc., 1973.

11. CONRADI, R.A., HILGERS, A.R., HO, N.F.H. & BURTON, P.S., 1991, *The influence of peptide structure on transport across Caco-2 cells*, Pharmaceutical Research, 8 (12): 1453 – 1460.
12. Corning Life Science Website, http://www.corning.com/Lifesciences/technical_information/faqs/cell_culture.asp.
13. DUCHENE, D., TOUCHARD, F. & PEPPAS, N.A., 1988, *Pharmaceutical and medical aspects of bioadhesive systems for drug administration*, Drug Development and Industrial Pharmacy, 14: 283.
14. DUIZER, E., PENNINKS, A.H., STENHUIS, W.H. & GROTEN, J.P., 1997, *Comparison of permeability characteristics of the human colonic Caco-2 and rat small intestinal IEC-18 cell lines*, Journal of Controlled Release, 49: 39-49.
15. GRAMAIN, P. & LIBEYERE, R., 1970, *Journal of Applied. Polymer Science,* 14: 383.
16. GU, J.M., ROBINSON, J.R. & LEUNG, S.H.S, 1988, *Binding of acrylic polymers to mucin-epithelial surface: Structure – property relationship*, Critical Reviews of Therapeutic Drug Carrier Systems, 5: 21 – 67.
17. GURNY, R., MEYER, J. & PEPPAS, N.A., 1984, *Bioadhesive intraoral release systems: design, testing and analysis*, Biomaterials, 5(6):336-340.
18. HAMMAN, J.H., 2000, *Enhancement of paracellular drug transport in neutral environments with quaternized chitosan: In vitro evaluation in intestinal epithelial cells (Caco-2)*. Potchefstroom: PU vir CHO. (Dissertation – Ph.D.)139p.
19. HAMMAN, J.H., SCHULTZ, C.M. & KOTZE, A.F., 2003, *N-trimethyl chitosan chloride: optimum degree of quaternization for drug absorption enhancement across epithelial cells*, Drug Dev Ind Pharm., 29(2): 161 -172.
20. HIDALGO, I.J, HILLGREN, K.M., GRASS, G.M. & BORCHARDT, R.T., 1991, *Characterization of the unstirred water layer in Caco-2 cell monolayers using a novel diffusion apparatus*, Pharmaceutical Research, 8(2): 222 – 227.
21. HILGERS, A.R., CONRADI, R.A. & BURTON, P.S., 1990, *Caco-2 cell monolayers as a model for drug transport across the intestinal mucosa*, Pharmaceutical Research, 7 (9): 902 – 910.
22. JUNGINGER, H.E., 1990, *Bioadhesive polymer systems for peptide delivery*, Acta Pharm. Technol., 36 (3): 110 – 126.

23. JUNGINGER, H.E., 1991, *Mucoadhesive hydrogels*, Pharmaceutical Industry, 53 (11): 1056 – 1065.
24. JUNGINGER, H.E., THANOU, M., KOTZE, A.F., LUESSEN, H.L. & VERHOEF, J.C., 1998, *Safe mucosal penetration enhancers – a fiction?* Proceeding at the 26th international symposium of controlled release and bioactive materials, 194 –195.
25. KARLSSON, J. & ARTURSSON, P., 1991, *A method for the determination of cellular permeability coefficients and aqueous boundary layer thickness in monolayers of intestinal epithelial (Caco-2) cells grown in permeable filter chambers*, Industrial Journal of Pharmaceutics, 71: 55 – 64.
26. KNIPP, G.T., HO, N.F.H., BARSUHN, C.L. & BORCHARDT, R.T., 1997, *Paracellular diffusion in Caco-2 cell monolayers: Effect of perturbation on the transport of hydrophilic compounds that vary in charge and size*, Journal of Pharmaceutical Sciences, 86 (10): 1105 – 1110.
27. KOTZE, A.F., LUEßEN, H.L., DE LEEUW, B.J., DE BOER, A.G., VERHOEF, J.C. and JUNGINGER, H.E., 1997, *N-trimethyl chitosan chloride as a potential absorption enhancer across mucosal surfaces: In vitro evaluation in intestinal epithelial cells (Caco-2)*, Pharmaceutical research, 14 (9): 1197 – 1202.
28. KOTZE, A.F., LUEßEN, H.L., DE BOER, A.G., VERHOEF, J.C. and JUNGINGER, H.E., 1998, *Chitosan for enhanced intestinal permeability: prospects for derivatives soluble in neutral and basic environments*, European Journal of pharmaceutical Sciences, 7: 145 – 151.
29. KOTZE, A.F., THANOU, M.M., LUEßEN, H.L., DE BOER, A.G., VERHOEF, J.C. & JUNGINGER, H.E., 1999, *Enhancement of paracellular drug transport in neutral and basic environments by highly quaternized N-trimethyl chitosan chloride: in vitro evaluation in intestinal epithelial cells (Caco-2)*, Journal of Pharmaceutical Sciences, 88 (2): 253 – 257.
30. KOTZE, A.F., THANOU, M.M., LUEßEN, H.L., DE BOER, A.G., VERHOEF, J.C. and JUNGINGER, H.E., 1999, *Effect of the degree of quaternization of N-trimethyl chitosan chloride on the permeability of intestinal epithelial cells (Caco-2)*, European Journal of Pharmaceutics and Biopharmacy.

31. LEE, V.H.L., YAMAMOTO, A. & KOMPELLA, U.B., 1991, *Mucosal penetration enhancers for facilitation of peptide and protein drug absorption*, Critical reviews in therapeutic drug carriers systems, 8(2): 91 – 192.
32. LEHR, C.M., BOUWSTRA, J.A., SCHACHT, E.H., & JUNGINGER, H.E., 1992, *In vitro evaluation of mucoadhesive properties of chitosan and some other natural polymers*, International Journal of Pharmaceutica, 78: 43-48.
33. LEUNG, S.H.S., 1991, *Mucoadhesive dosage forms for peptide and protein drug delivery*, In. Lee, V.H.L., Peptide and protein drug delivery, New York, Marcel Dekker Inc., 17: 741-767.
34. LO, C-H., KEESE, C.R. & GIAEVER, I., 1999, *Cell-substrate contact: Another factor may influence transepithelial electrical resistance of cell layers cultured on permeable filters*, Experimental Cell Research, 250: 576 – 580.
35. NEUTRA, M.R. & FORSTNER, J.F., 1987, *Gastrointestinal mucus: Synthesis, secretion and function*, (In Johnson, L.R., ed., Physiology of the gastrointestinal tract. Second edition. Raven Press. New York. 975 – 1109).
36. PARK, K., 1989, *A new approach to study mucoadhesion: colloidal gold staining*, International Journal of Pharmaceutics, 53: 209-217.
37. PEPPAS, N.A. & BURI, P.A., 1985, *Surface, interfacial and molecular aspects of polymer bioadhesion on soft tissues*, Journal of Controlled Release, 2: 257 – 275.
38. PONCHEL, G., TOUCHARD, F., DUNCHENE, D. & PEPPAS, N.A., 1987, *Bioadhesive analysis of controlled-release systems I: Facture and interpenetration analysis in poly(acrylic-acid)-containing systems*, Journal of Controlled Release, 5 (9): 129 – 141.
39. POWELL, D.W., 1987, *Intestinal water and electrolyte transport.* (In Johnson, L.R. ed., Physiology of the gastrointestinal tract. 2nd edition. New York: Raven Press. 1780)
40. ROSSI, S., BONFERONI, M.C., LIPPOLI, G., FERRARI, F., CARAMELLA, C. & CONTE, 1995, *Influence of mucin type on polymer-mucin rheological interactions*, Biomaterials, 16 (14): 1073-1079.
41. SATO, H., MIZUTANI, S., TSUGE, S., OHTANI, H., AOI, K., TAKASU, A., OKADA, M., KOBAYASHI, S., KIYOSADA, T., and SHODA, S., 1998, *Determination of the degree of acetylation of chitin/chitosan by pyrolysis-gas chromatography in the presence of oxalic acid,* Analytical Chemistry, 70 (1): 7 –12.

42. SCHIPPER, N.G.M., VÅRUM, K.M. & ARTURSSON, P., 1996, *Chitosans as absorption enhancers for poorly absorbable drugs 1: Influence of molecular weight and degree of acetylation on drug transport across human intestinal epithelial (Caco-2) cells*, Pharmaceutical Research, 13 (11): 1686-1691.
43. SCHIPPER, N.G.M, OLSSON, S., HOOGSTRAATE, J.A., DE BOER, A.G., VÅRUM, K.M. & ARTURSSON, P., 1997, *Chitosans as absorption enhancers for poorly absorbable drugs 2: Mechanism of adsorption enhancement*, Pharmaceutical Research, 14 (7): 923-929.
44. SIEVAL, A.B., THANOU, M., KOTZE, A.F., VERHOEF, J.C., BRUSSEE, J. & JUNGINGER, H.E., 1998, *Preparation and NMR characterization of highly substituted N-trimethyl chitosan chloride*, Carbohydrate Polymers, 36: 157 – 165.
45. SKOOG, D.A. & LEARY, J.J., *Principles of Instrumental Analysis (4th Ed.)*, Saunders College Publishing, New York, 1992.
46. SMART, J.D., 1999, *The role of water movement and polymer hydration in mucoadhesion*, (In Mathiowithz et al., ed. Bioadhesive drug delivery systems New York Marcel Dekker 11 – 23.)
47. SMART, J.D., KELLAWAY, I.W. & WORTHINGTON, 1984, *An in-vitro investigation of mucosa-adhesive materials for use on controlled drug delivery*, Journal of Pharmaceutics and Pharmacology, 36: 295.
48. SNYMAN, D. 2000. *Evaluation of the mucoadhesive properties of n-trimethyl chitosan chloride*. Potchefstroom: PU vir CHO. (Dissertation – M.Sc.) 83p.
49. SNYMAN, D., HAMMAN, J.H., KOTZE, J.S., ROLLINGS, J.E. & KOTZE, A.F., 2002, *The relationship between absolute molecular weight and the degree of quaternisation of N-trimethyl chitosan chlorideI*, Carbohydrate Polymers, 50(2): 145 – 150.
50. TAMBURIC, S. AND CRAIG, D.Q., 1997, *Comparison of different in-vitro methods for measuring mucoadhesive performance*, European Journal of Pharmaceutics and Biopharmaceutics, 44 (2): 159 – 167.
51. THANOU, M.M., KOTZE, A.F., SCHARRINGHAUSEN, T., LUEßEN, H.L., DE BOER, A.G., VERHOEF, J.C., JUNGINGER, H.E., 2000, *Effect of degree of quaternization of N-trimethyl chitosan chloride for enhanced transport of hydrophilic*

compounds across intestinal Caco-2 cell monolayers, Journal of Control Release, 64: 15 – 25.

52. THANOU, M., VERHOEF, J.C. & JUNGINGER, H.E., 2001, *Oral drug absorption enhancement by chitosan and its derivatives*, Advanced Drug Delivery Reviews, 52(2): 117 –126.
53. TOBYN, M.J., JOHNSON, J.R. & DETTMAR, P.W., 1995, *Factors affecting in-vitro gastric mucoadhesion I: Test conditions and instrument parameters*, European Journal of Pharmaceutics and Biopharmaceutics, 41: 235 – 241.
54. TUIJMAN, C.A.F. & HERMANS, J.J., 1957, *Journal of Polymer Science,* 25: 385.
55. VAN DER MERWE, S.M., VERHOEF, J.C., VERHEIJDEN, J.H.M., KOTZE, A.F. & JUNGINGER, H.E., 2004, *Trimethylated chitosan as polymeric absorption enhancer for improved peroral delivery of peptide drugs*, European Journal of Pharmaceutics and Biopharmaceutics, 58(2): 225 – 235.
56. VAN HOOGDALEM, E.J., DE BOER, A.G. & BREIMER, D.D., 1989, *Intestinal drug absorption enhancement: an overview*, Pharmaceutical therapeutics, 44: 407 – 443.
57. WILSON, C.G. & WASHINGTON, N. 1989. Physiological pharmaceutics: biological barriers to drug absorption. Chichester : Horwood Ellis. 186p.

APPENDIX A

A) CALCULATION OF THE INTRINSIC VISCOSITY

The relative viscosity is defined as the quotient of the viscosity of the solution, η_s, and the viscosity of the solvent, η_o,

$$\eta_r = \frac{\eta_S}{\eta_0} \qquad (A.1)$$

or

$$\eta_r = \frac{t_S}{t_0} \qquad (A.2)$$

Where t_s is the efflux for the solution and t_o is the efflux time for the solvent (Collins *et al.*, 1973). Plotting the inherent viscosity against concentration and fitting a straight light fit at zero concentration, the intrinsic viscosity is calculated.

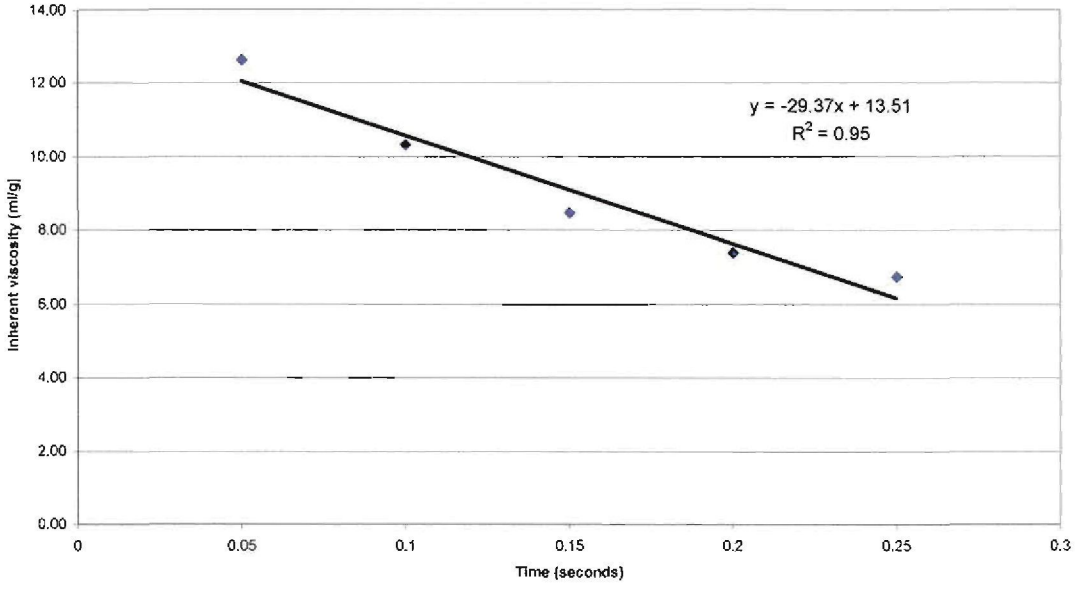

Figure A.1: Inherent viscosity versus concentration for low molecular weight chitosan

The straight line fit through the data points gave the following fit: y = -29.37x + 13.51 from figure A.1, where the intrinsic viscosity is the intercept of the line. So the intrinsic viscosity of the low molecular weight chitosan was determined as $[\eta]$ = 13.5 dl/g. These calculations were repeated for all different molecular weight chitosan and TMC polymers.

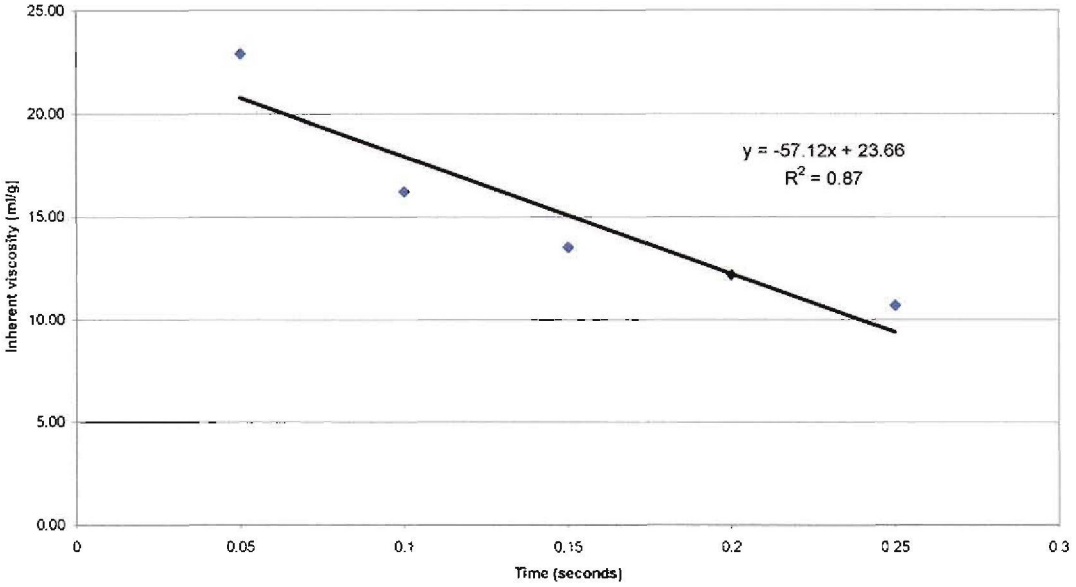

Figure A.2: Inherent viscosity versus concentration for medium molecular weight chitosan

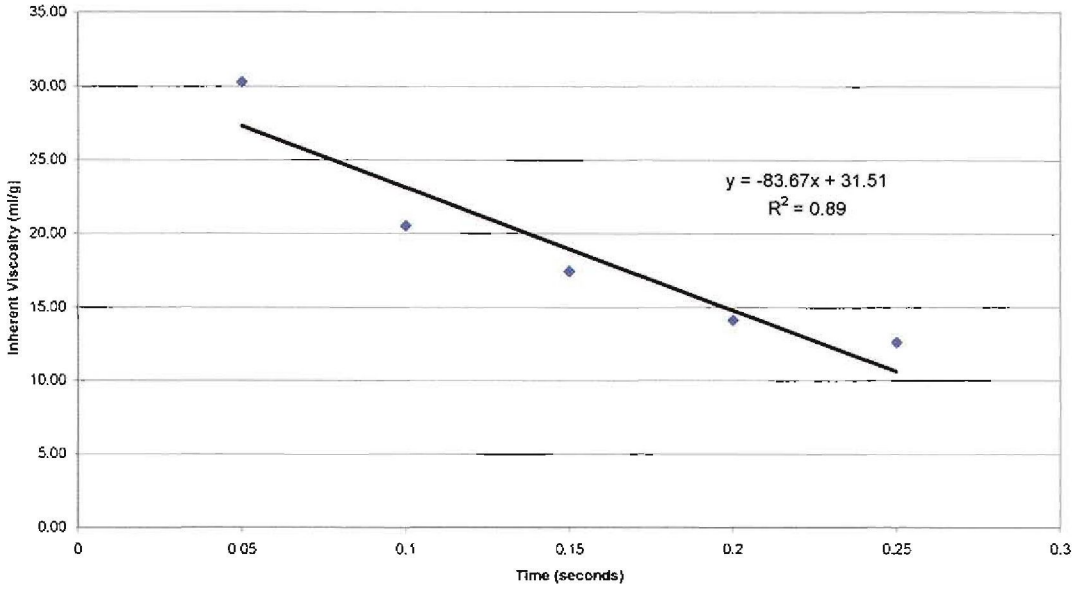

Figure A.3: Inherent viscosity versus concentration for high molecular weight chitosan

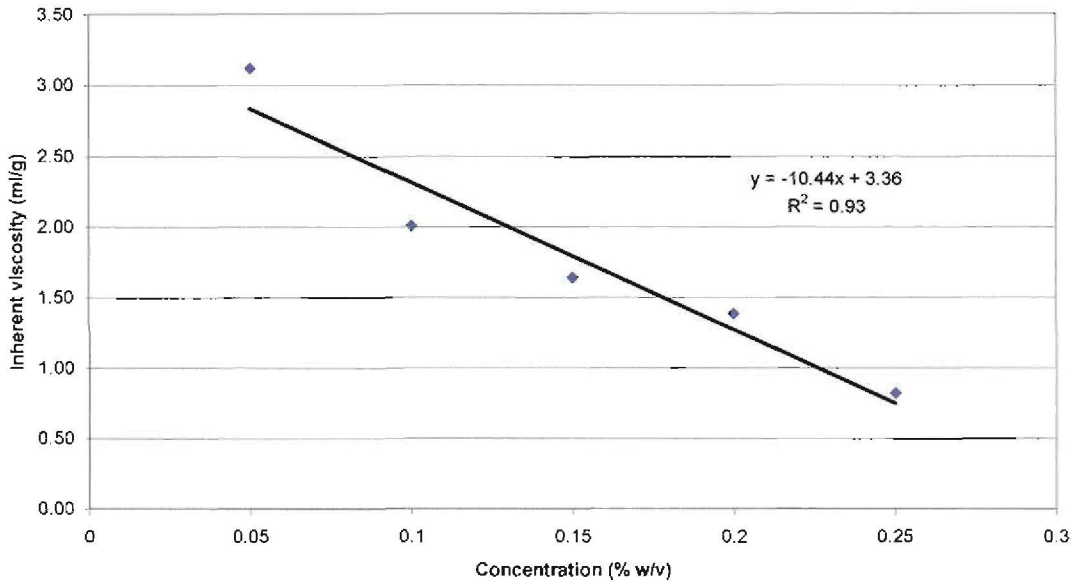

Figure A.4: Inherent viscosity versus concentration for low molecular weight TMC

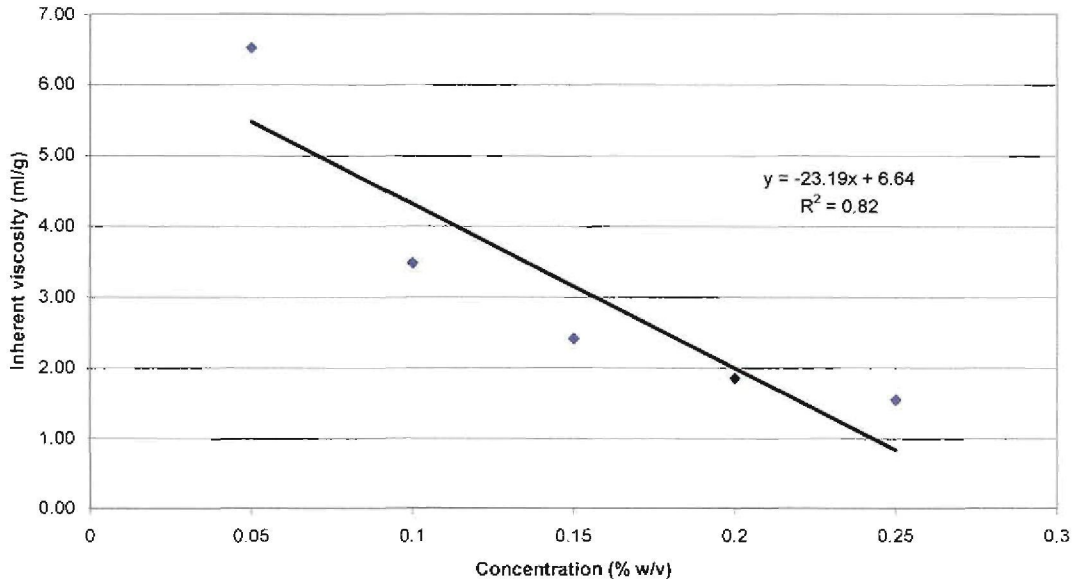

Figure A.5: Inherent viscosity versus concentration for medium molecular weight TMC

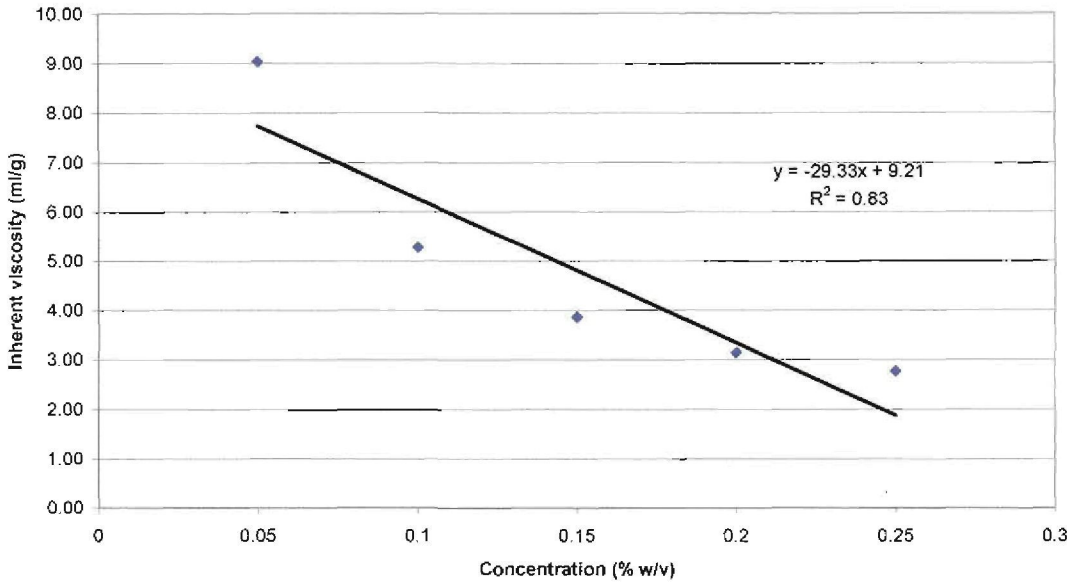

Figure A.6: Inherent viscosity versus concentration for high molecular weight TMC

From viscosity data obtained, the following table could be constructed:

Table A.1: Intrinsic viscosity of chitosan and TMC polymers

Polymer	Intrinsic Viscosity (dl/g)
Chitosan	
Low MW Chitosan	13.5
Medium MW Chitosan	23.7
High MW Chitosan	31.5
TMC	
Low MW TMC	3.4
Medium MW TMC	6.6
High MW TMC	9.2

APPENDIX B

A) CALCULATION OF DEGREE OF ACETYLATION AND DEGREE OF DEACTYLATION

Using the NMR data obtained and the following equation, the degree of acetylation (DA) for chitosan can be determined:

$$DA(\%) = \frac{I_{H1'} + \frac{I_{AC}}{3}}{I_{H1} + I_{H2} + I_{H1'} + \frac{I_{AC}}{3}} \times 100 \qquad \text{(B.1)}$$

where $I_{H1'}$, I_{H1}, I_{H2} and I_{AC} are peak intensities for H-1 or D-glucosamine (GlcN) unit at 4.60 ppm, for H-1 of N-acetyl-D-glucosamine (GlcNAc) unit at 4.86 – 4.88 ppm, for H-2 of GlcN at 3.17 ppm, and for the acetyl group of the GlcNAc unit at 2.05 ppm, respectively. The dividing factor of 3 for I_{AC} is associated with the proton number for the acetyl group (Sato *et al.*, 1998).

The degree of deacetylation (DDA) can then be determined as follows:

$$DDA\,(\%) = 100 - DA\,(\%) \qquad \text{(B.2)}$$

Table B.1: Degrees of acetylation and deacetylation of chitosan

Chitosan	DA (%)	DDA (%)
Low MW	19.7	80.3
Medium MW	18.6	81.4
High MW	22.4	77.6

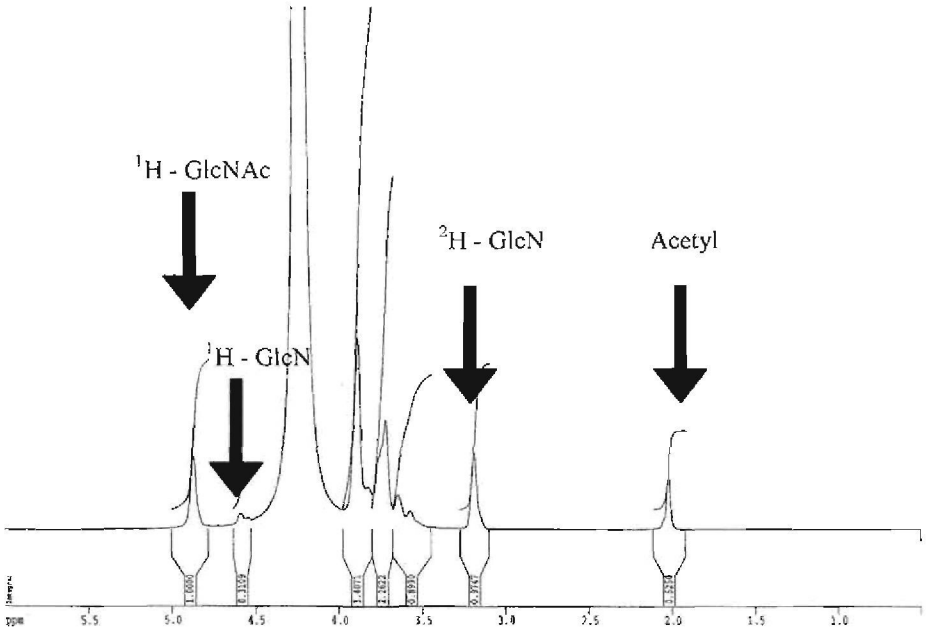

Figure B.1: ^{1}H-NMR spectrum of low molecular weight chitosan

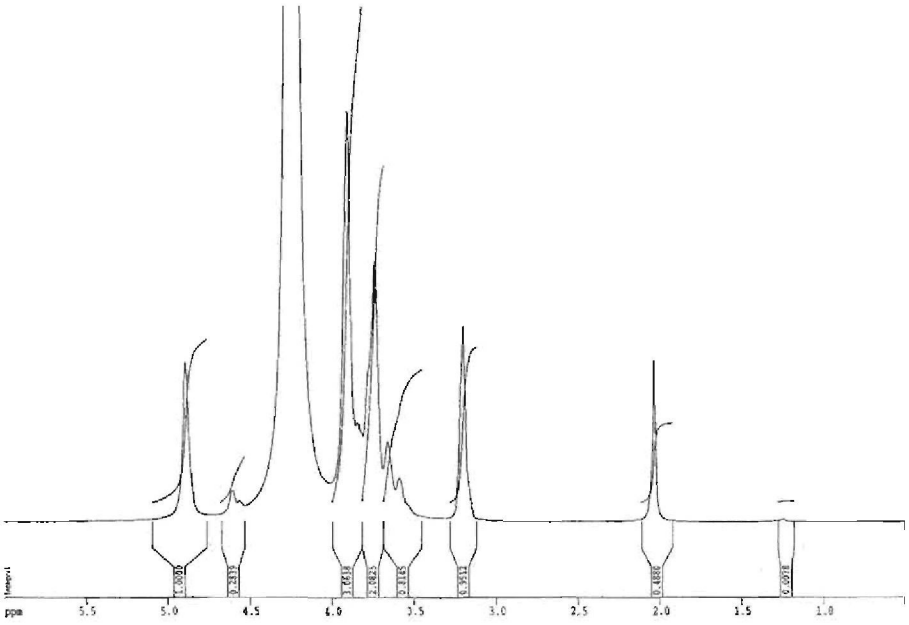

Figure B.2: ^{1}H-NMR spectrum of medium molecular weight chitosan

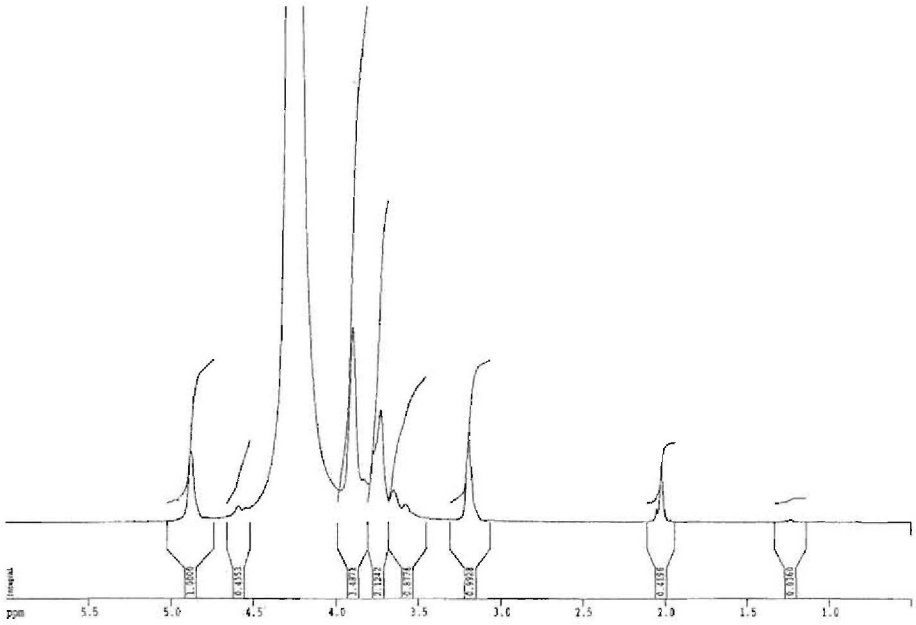

Figure B.3: ^{1}H-NMR spectrum of high molecular weight chitosan

B) CALCULATION OF THE DEGREE OF QUATERNIZATION

The degree of quaternization (DQ) of TMC can be determined by using the following equation (Thanou *et al.*, 2000):

$$DQ\,(\%) = \frac{\int peak\ at\ 3.4\ ppm}{\left(\int peak\ at\ 4.7\ ppm + \int peak\ at\ 5.4\ ppm\right)} \times \frac{1}{9} \times 100 \qquad \text{(B.3)}$$

where

$\int$ peak at 3.4 ppm = integral of the tri-methyl amino group peak at 3.4 ppm

$\int$ peak at 4.7 ppm and $\int$ peak at 5.4 ppm = integral of the ^{1}H peaks at 4.7 and 5.4 ppm

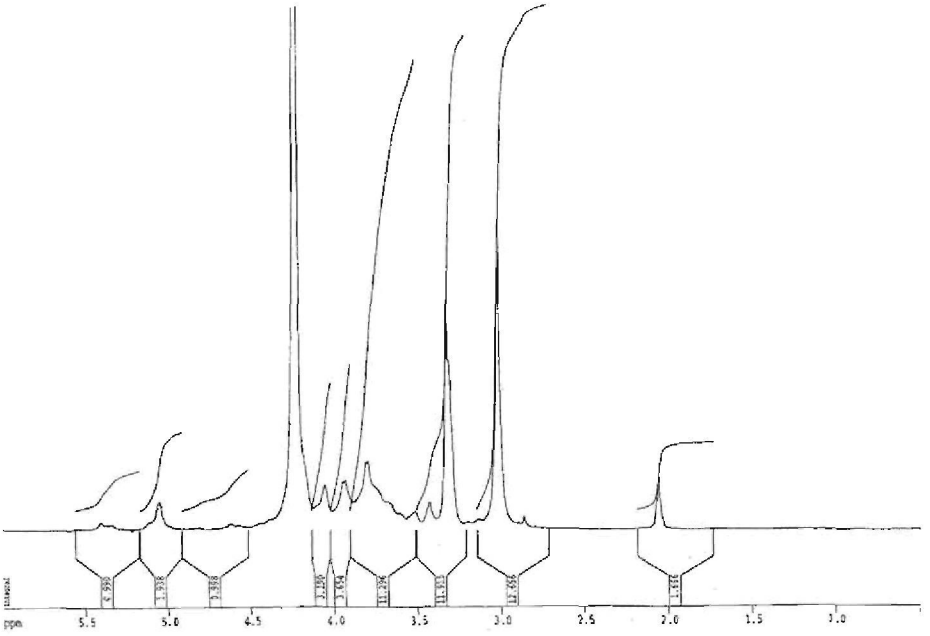

Figure B.4: ^{1}H-NMR spectrum of low molecular weight TMC

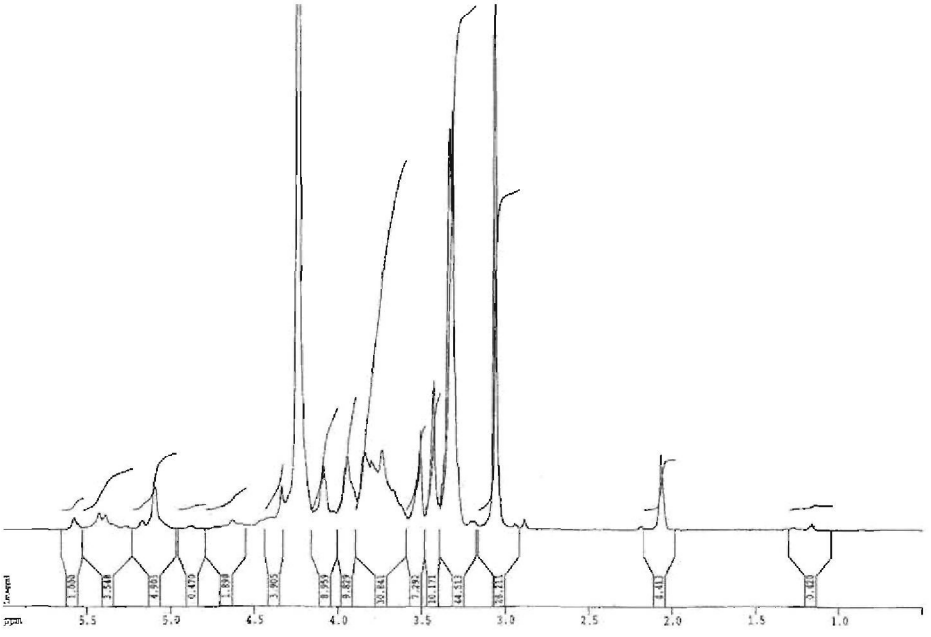

Figure B.5: ^{1}H-NMR spectrum of medium molecular weight TMC

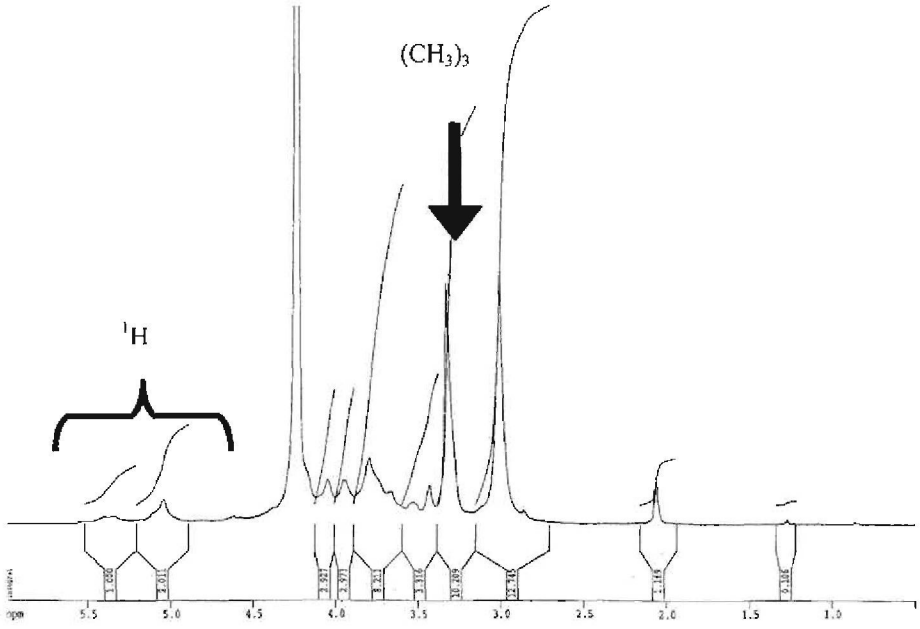

Figure B.6: ^{1}H-NMR spectrum of high molecular weight TMC

Thanou *et al.*, (2000) has assigned the peak at 3.4 ppm to trimethyl amino groups and the peaks between 4.7 and 5.4 ppm were assigned to the ^{1}H-protons for the ^{1}H-NMR spectra of TMC (see figure B.6). Using the NMR data of TMC (figures B.4 – B.6) and equation B.3, the following degrees of quaternization (DQ) were calculated.

Table B.2: Degrees of quaternization of TMC

TMC Polymer	DQ (%)
Low MW	33.7
Medium MW	41.9
High MW	37.7

APPENDIX C

A) DETERMINING THE REPRODUCIBILITY OF THE TENSILE SEPARATION TEST

The separation test (as described in chapter 3) was done for the clean plate (control), pectin (reference) and the three different TMC molecular weights and this was done in triplicate. All the experiments show high levels of reproducibility (See figures C.1 to C.5).

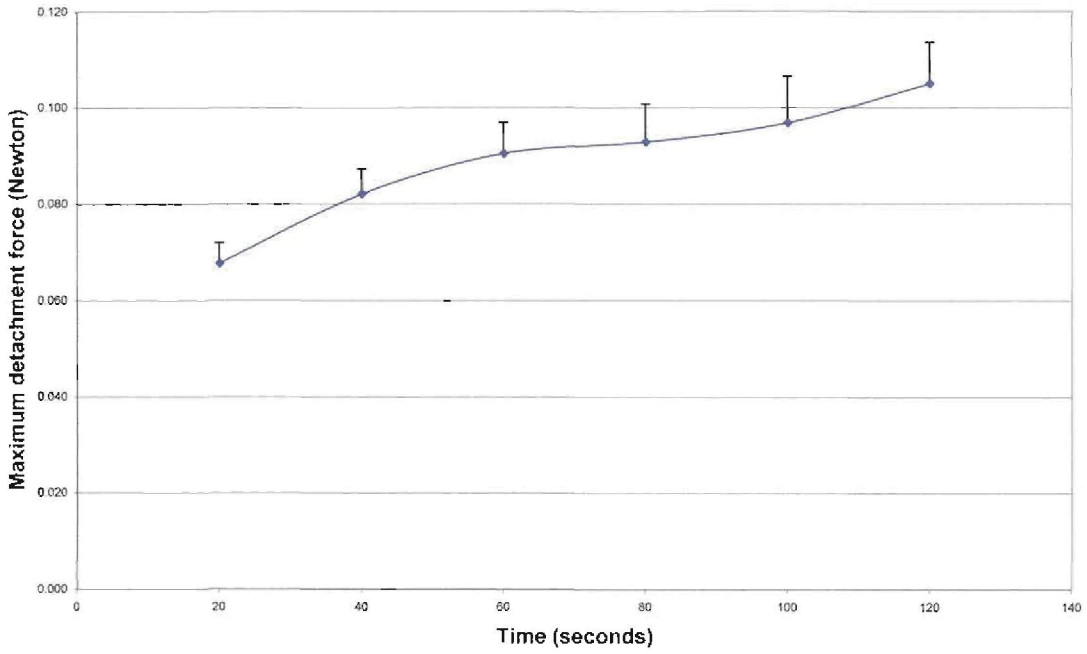

Figure C.1: Mucoadhesion profile for clean plate

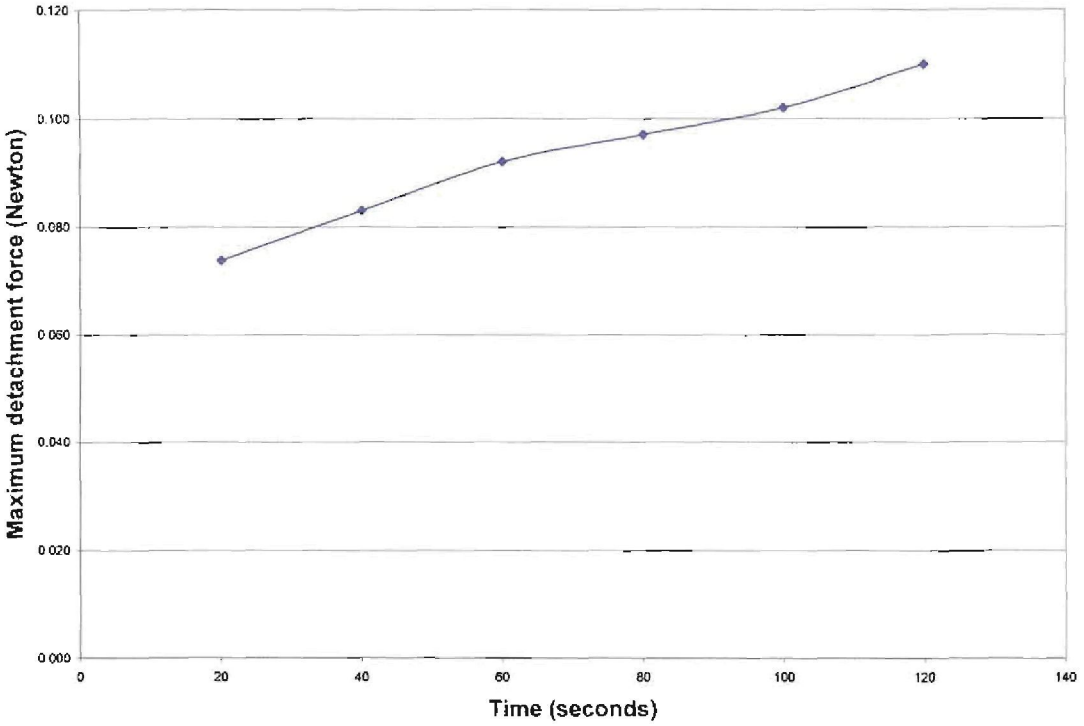

Figure C.2: Mucoadhesion profile for pectin

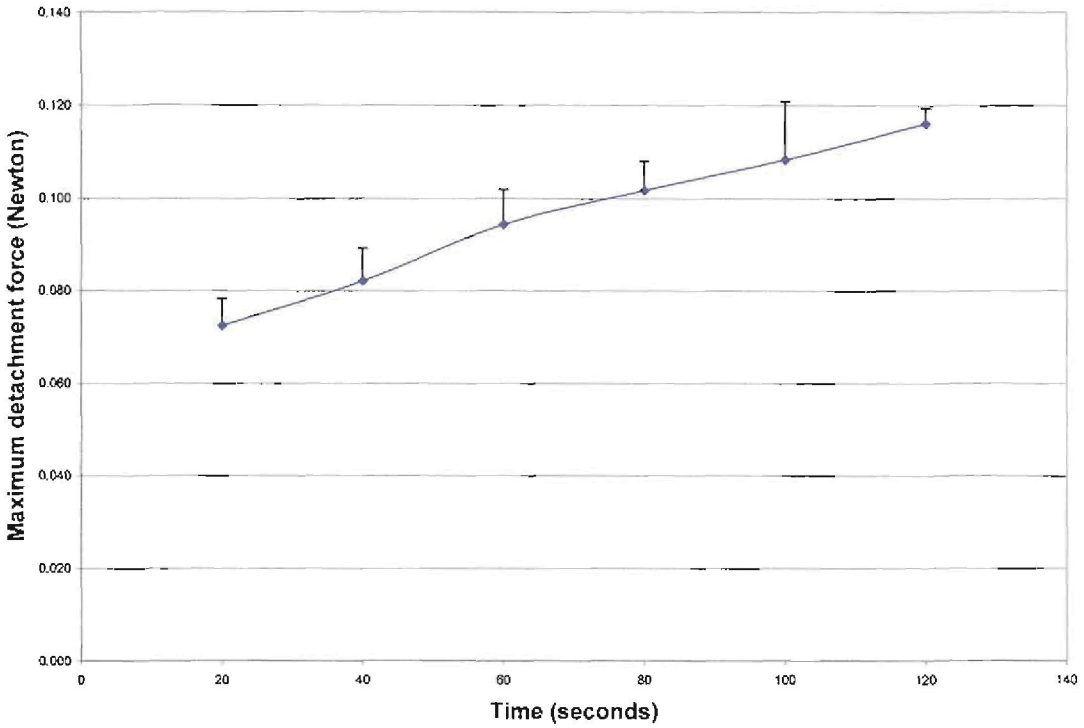

Figure C.3: Mucoadhesion profile for low molecular weight TMC

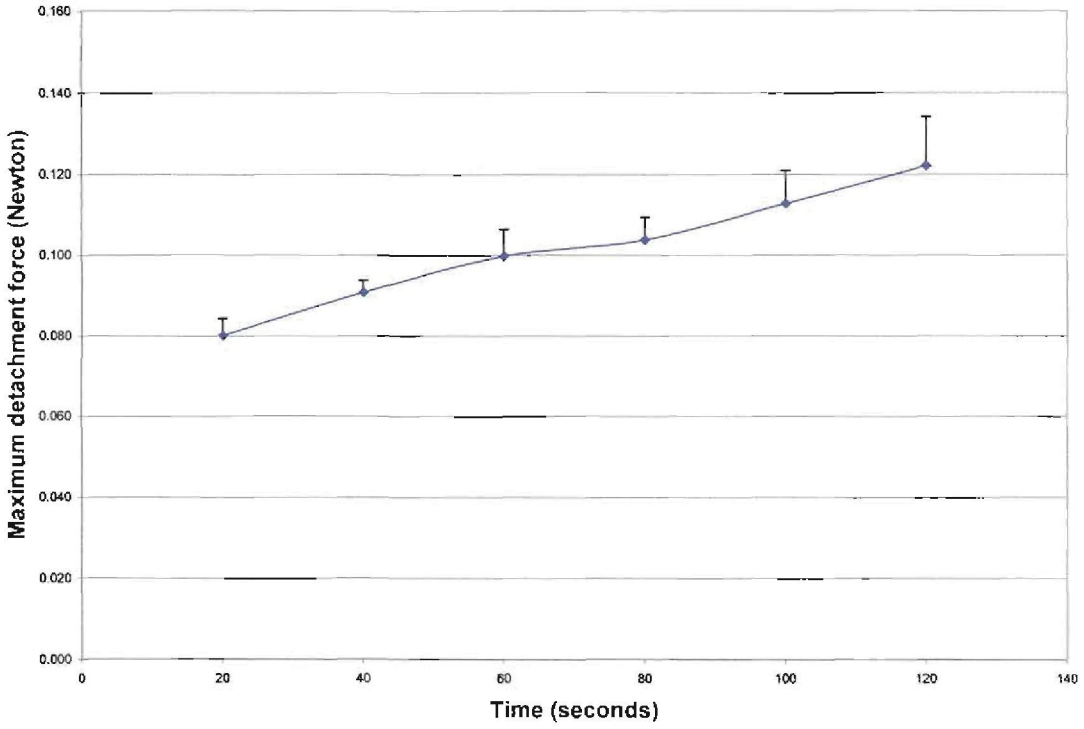

Figure C.4: Mucoadhesion profile for medium molecular weight TMC

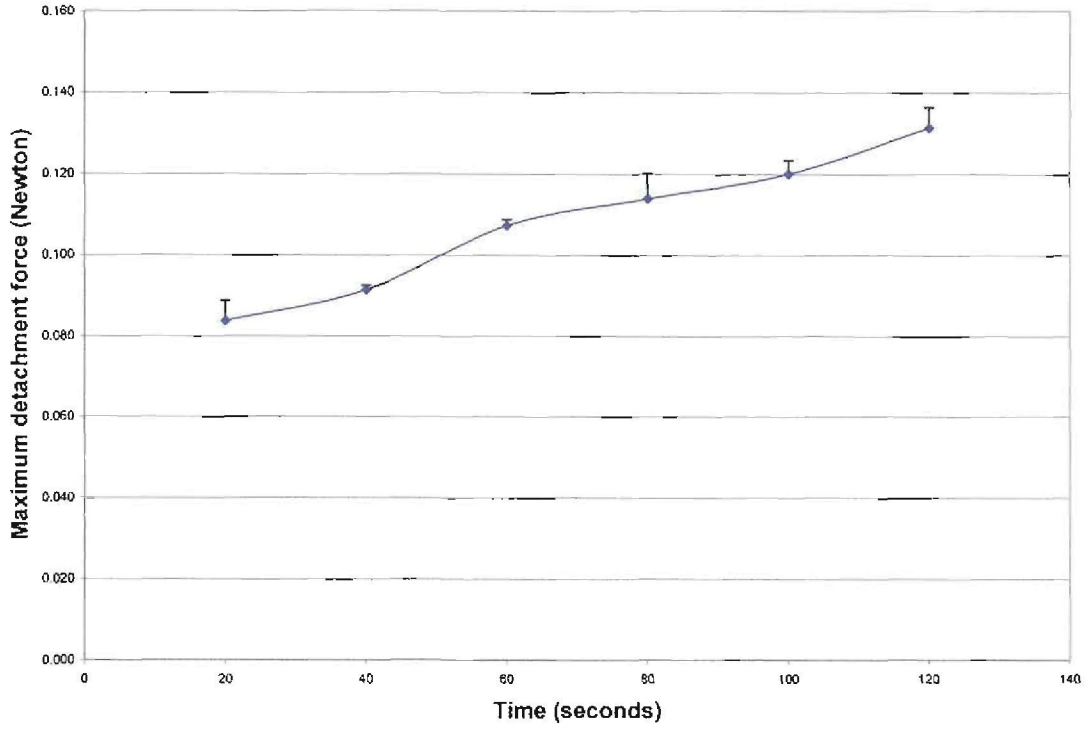

Figure C.5: Mucoadhesion profile for high molecular weight TMC

APPENDIX D

A) REPRODUCIBILTY OF THE TEER EXPERIMENTS

All experiments were done in triplicate and repeated for each different molecular weight of TMC at two different concentrations of TMC. The standard deviation was calculated by means of Microsoft's Excel. All the experiments show high levels of reproducibility (see figures D.1 to D.6).

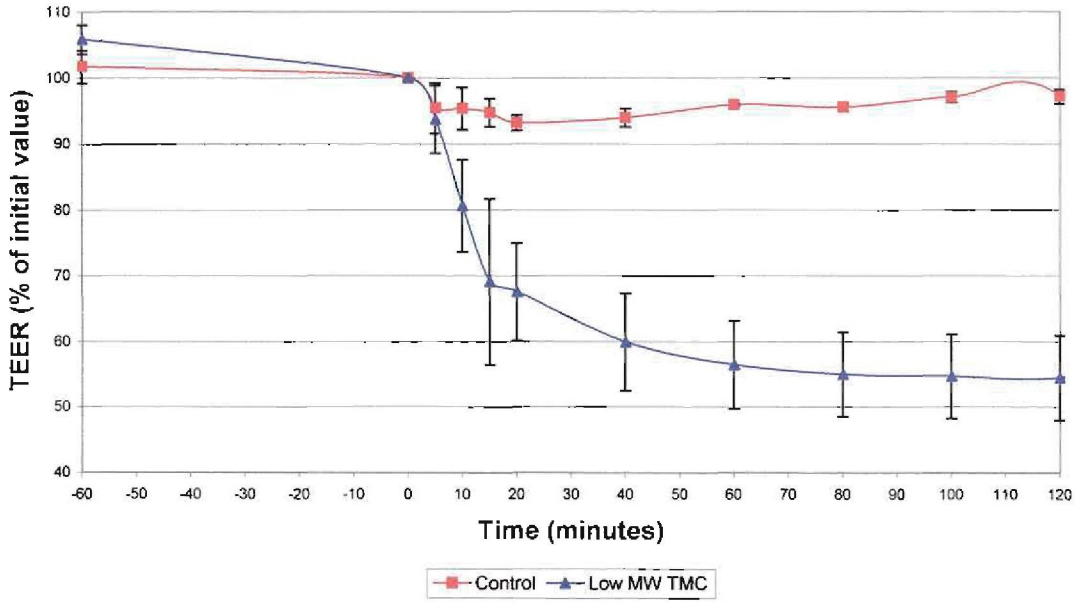

Figure D.1: TEER experiments with 0.1 % low molecular weight TMC

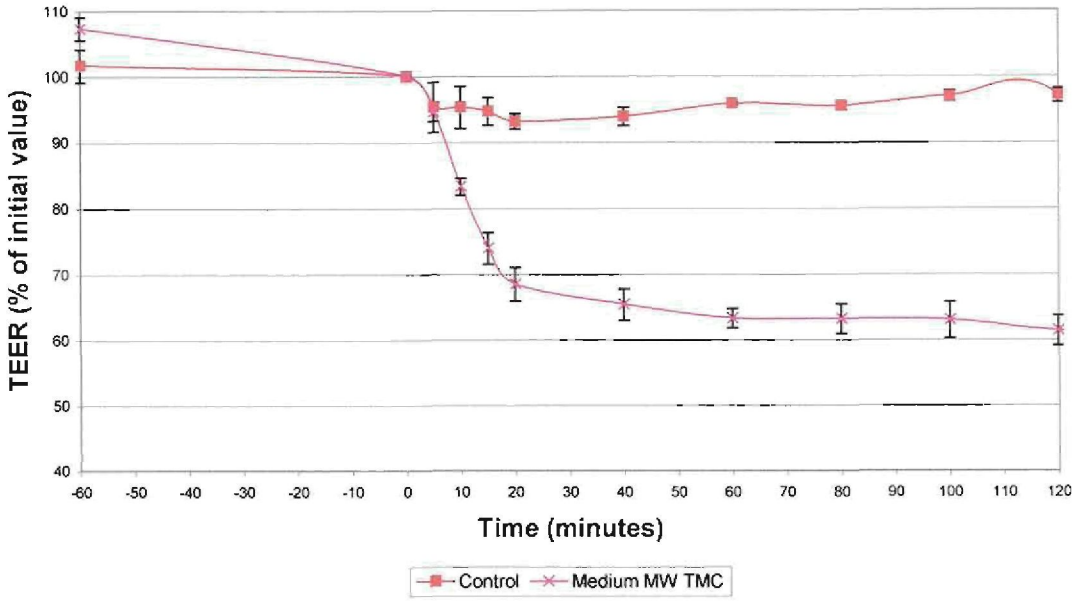

Figure D.2: TEER experiments with 0.1 % medium molecular weight TMC

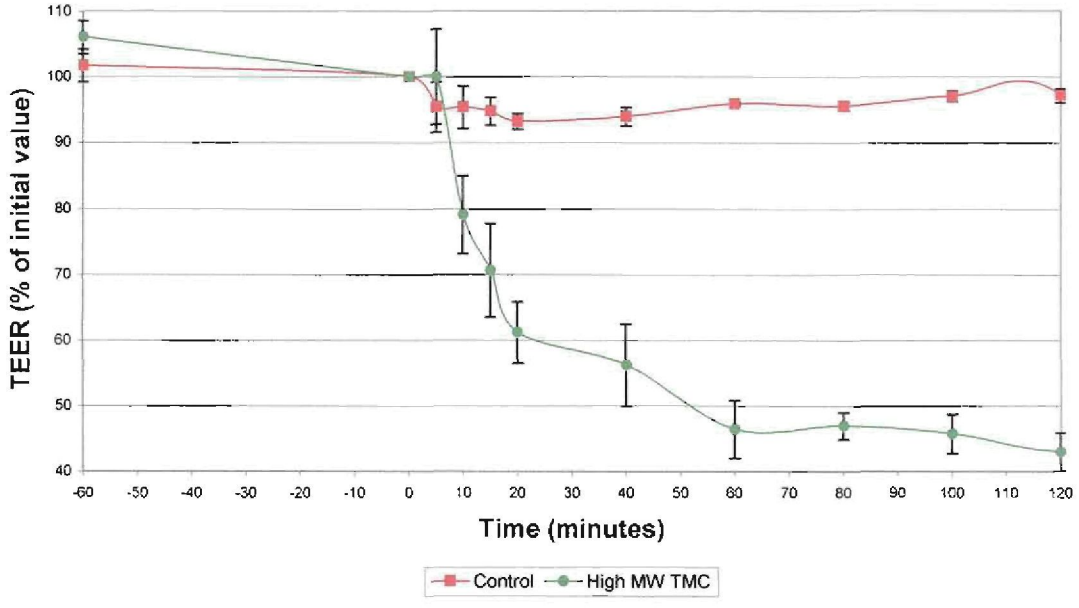

Figure D.3: TEER experiments with 0.1 % high molecular weight TMC

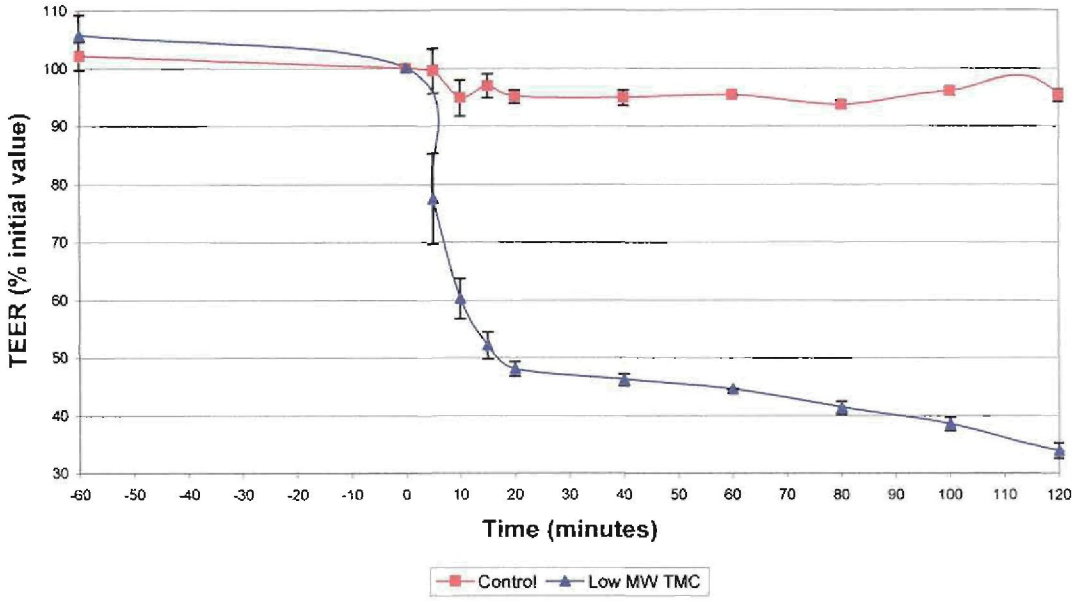

Figure D.4: TEER experiments with 0.5 % low molecular weight TMC

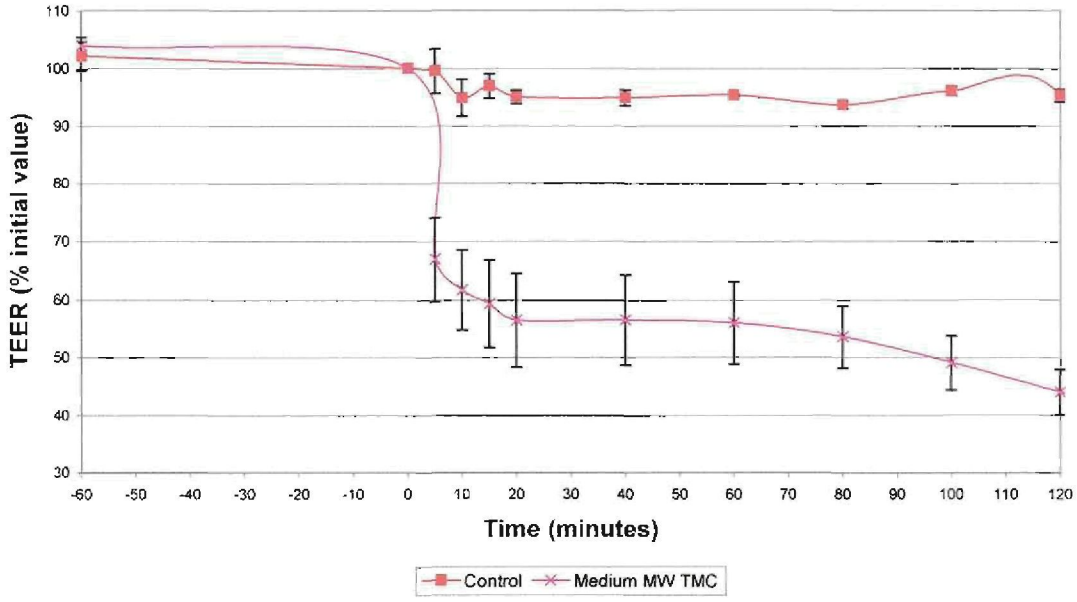

Figure D.5: TEER experiments with 0.5 % medium molecular weight TMC

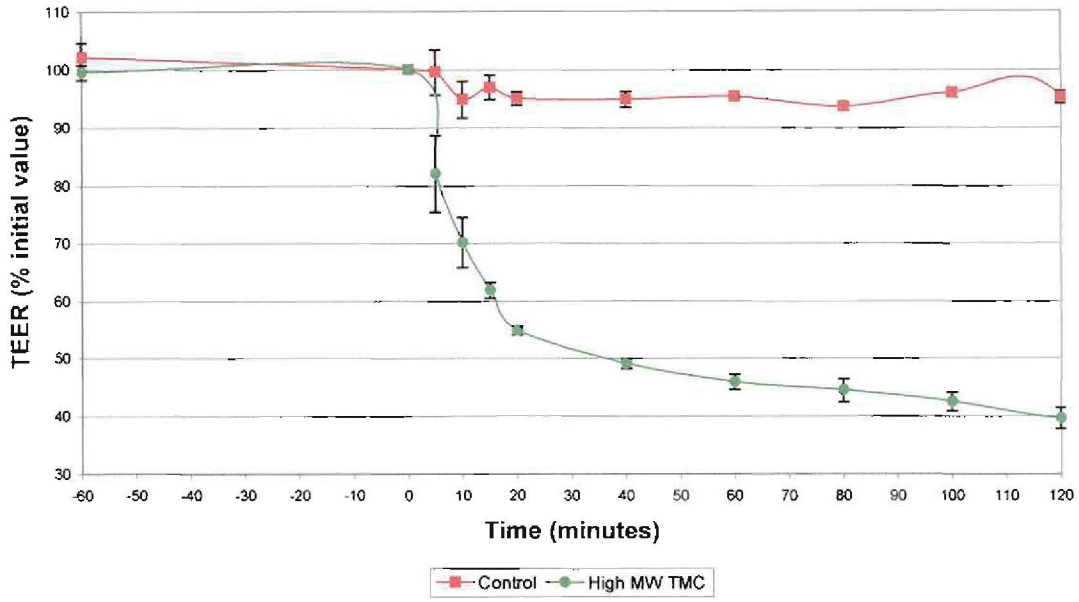

Figure D.6: TEER experiments with 0.5 % high molecular weight TMC

B) CORRELATION BETWEEN CPM AND ACTIVITY IN CI

Different concentrations of [^{14}C]-mannitol (specific activity 56 mCi/mmol) samples were then mixed with scintillation counter, and the radioactivity in the samples measured in a betacounter. The data obtained from scintillation counter was plotted on an activity (Ci) versus cpm standard curve (figure D.7) and straight line (y = mc) was fitted. The equation obtained was used to convert cpm measurements to activity measurements (Ci).

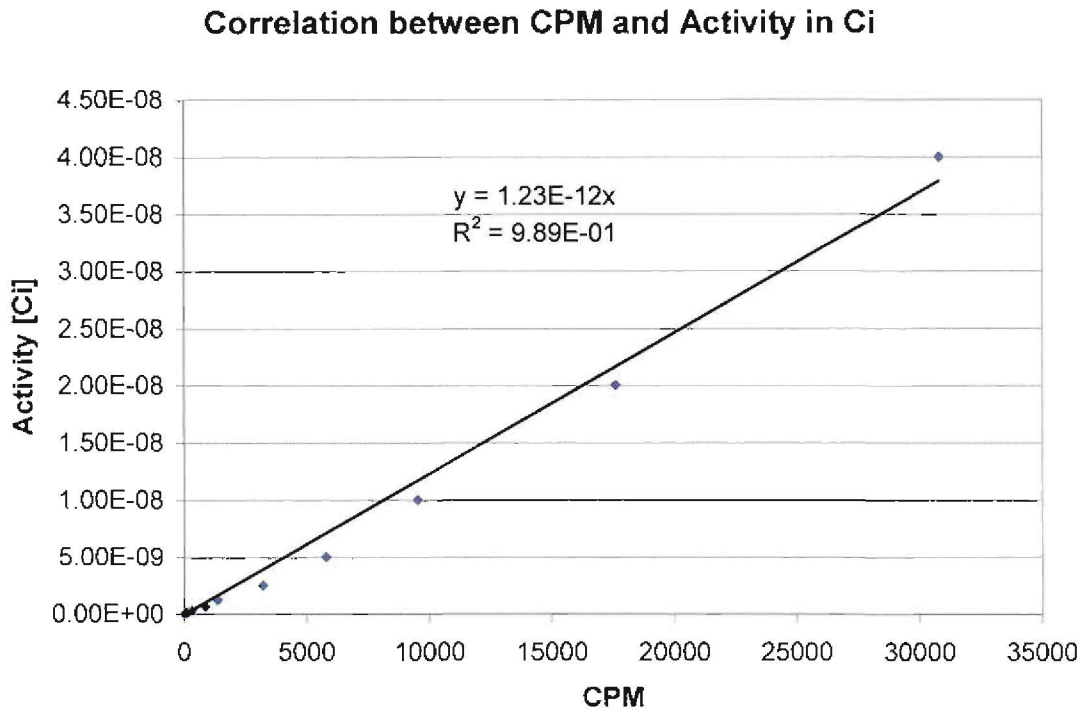

Figure D.7: Activity (Ci) as function of counts per minute (cpm)

C) REPRODUCIBILTY OF THE TRANSPORT EXPERIMENTS

All experiments were done in triplicate and repeated for each different molecular weight of TMC at two different concentrations of TMC. The standard deviation was calculated by means of Microsoft's Excel. Most of the experiments show high levels of reproducibility (see figures D.8 to D.14).

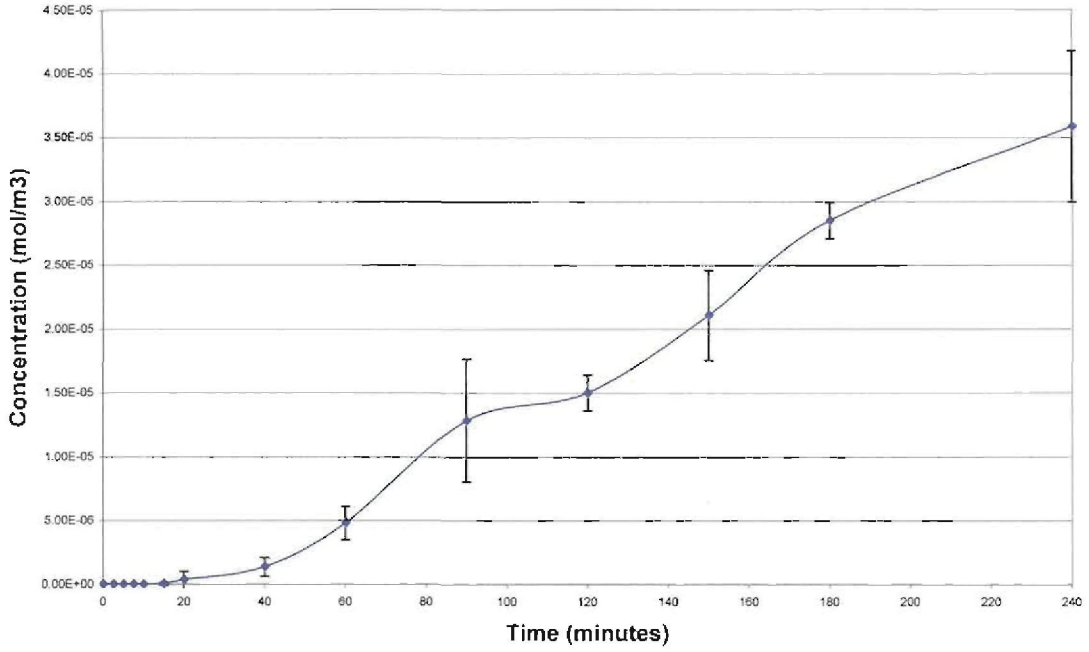

Figure D.8: Transport experiments with 0.1 % low molecular weight TMC

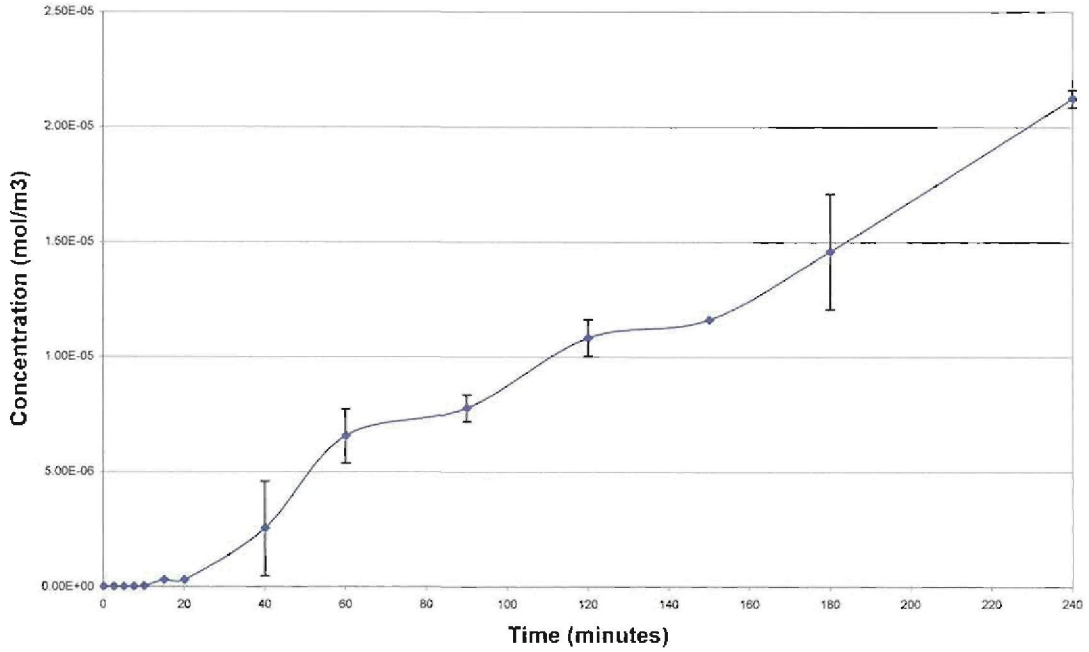

Figure D.9: Transport experiments with 0.1 % medium molecular weight TMC

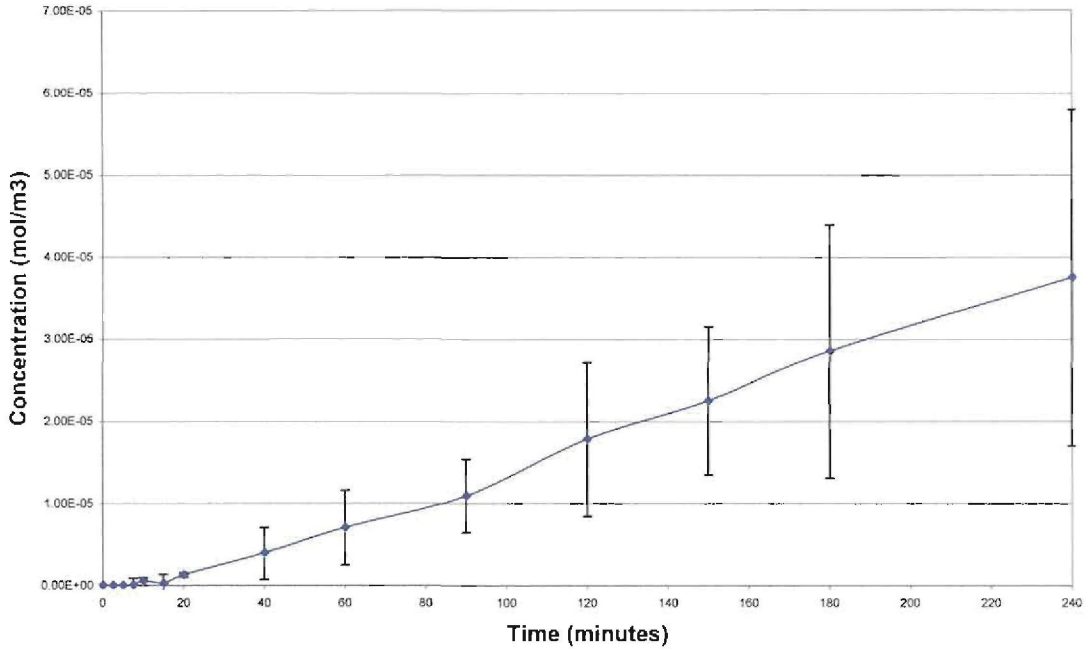

Figure D.10: Transport experiments with 0.1 % high molecular weight TMC

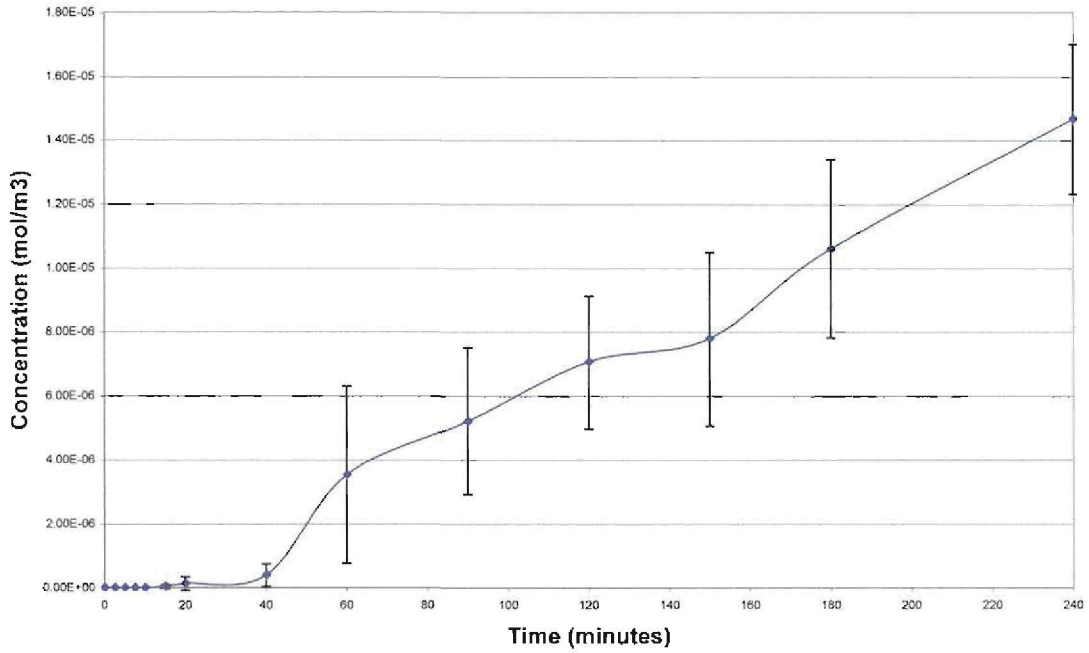

Figure D.11: Transport experiments with no TMC (Control)

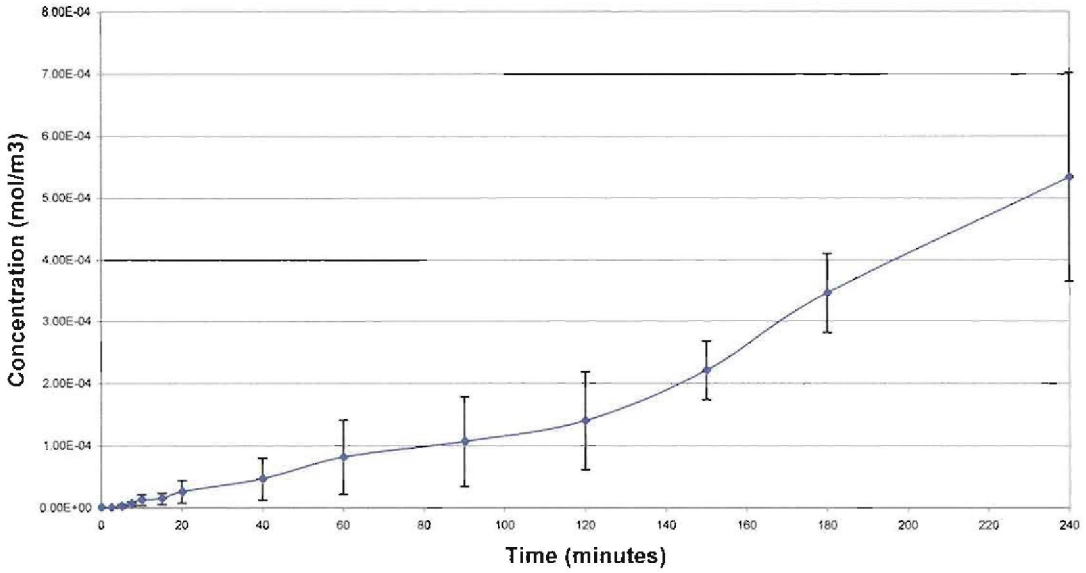

Figure D.12: Transport experiments with 0.5 % low molecular weight TMC

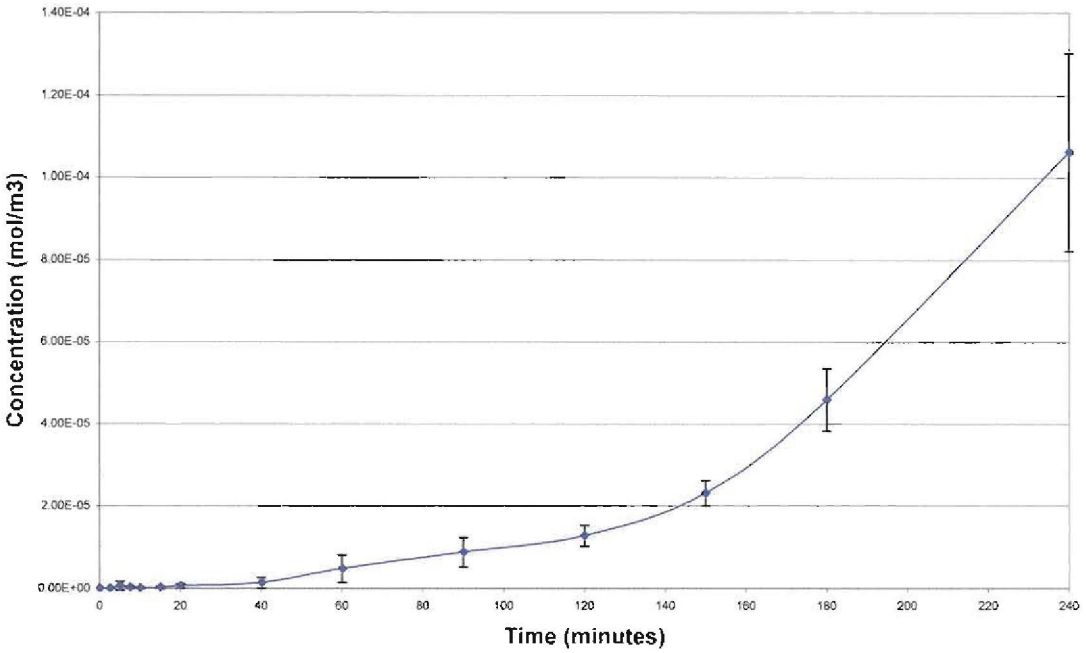

Figure D.13: Transport experiments with 0.5 % medium molecular weight TMC

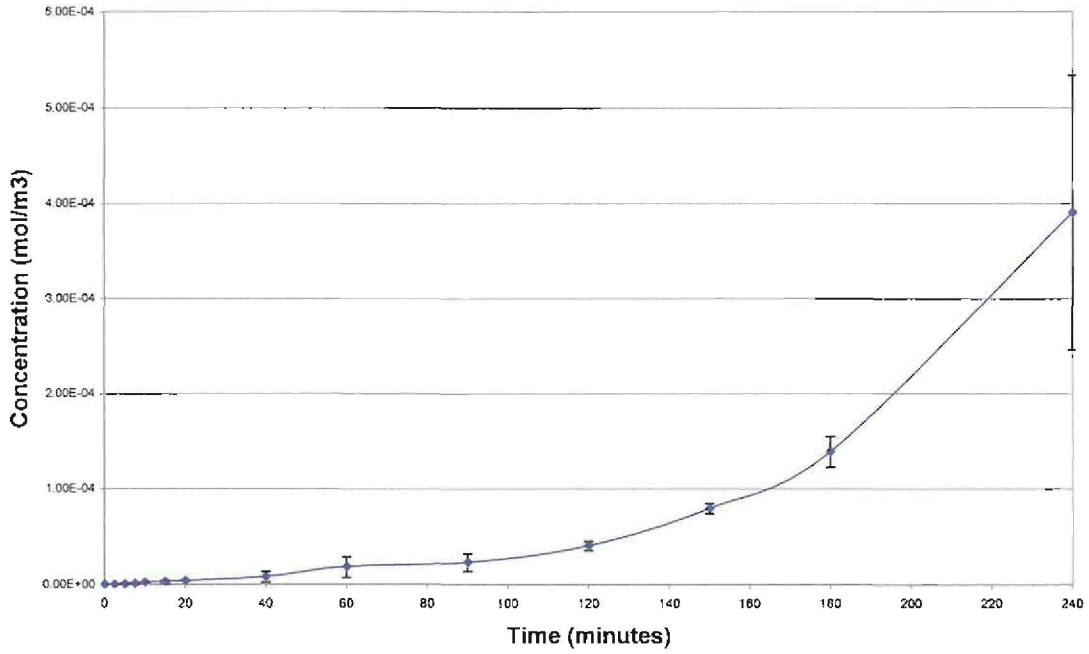

Figure D.14: Transport experiments with 0.5 % high molecular weight TMC

APPENDIX E

A) MODELING OF TRANSPORT OF [^{14}C]-MANNITOL

As discussed in chapter 4, only transport data from 120 minutes and onwards was used in the calculation of the diffusion coefficients. Using equation E-1 and the transport data obtained, diffusion coefficients were determined for the all molecular weights as well as the control values.

$$-\frac{1}{2}\ln[C_O - 2\,C_B(t)] = \frac{A\,D}{V\,\delta}t + K \qquad \text{(E-1)}$$

Using equation (E-1) and the transport data obtained, diffusion coefficients were determined for the all molecular weights as well as the control values. The straight line equation, y = m x + c, was fitted through the data with following equations

$$y = -\ln\left[1 - \frac{2\,C_B(t)}{C_O}\right] \qquad \text{(E-2)}$$

$$x = t \qquad \text{(E-3)}$$

and

$$m = 2\frac{A\,D}{V\,\delta} \qquad \text{(E-4)}$$

Time (t) was plotted against y, and the gradient (m) was determined using the following values (table E.1):

Table E.1: Constant variables for transport model

Constant variable	Value	Reference
C_0	3.6 x 10^{-3} mol/m^3	Experimental
A	4.5 x 10^{-4} m^2	Corning Life Science Website
V	2.5 x 10^{-6} m^3	Experimental setup
δ	3.5 x 10^{-5} m	Hilgers *et al.*, 1990

The following graphs were obtained for all molecular weights at different concentrations (w/v) and the gradient of the straight line fit was determined.

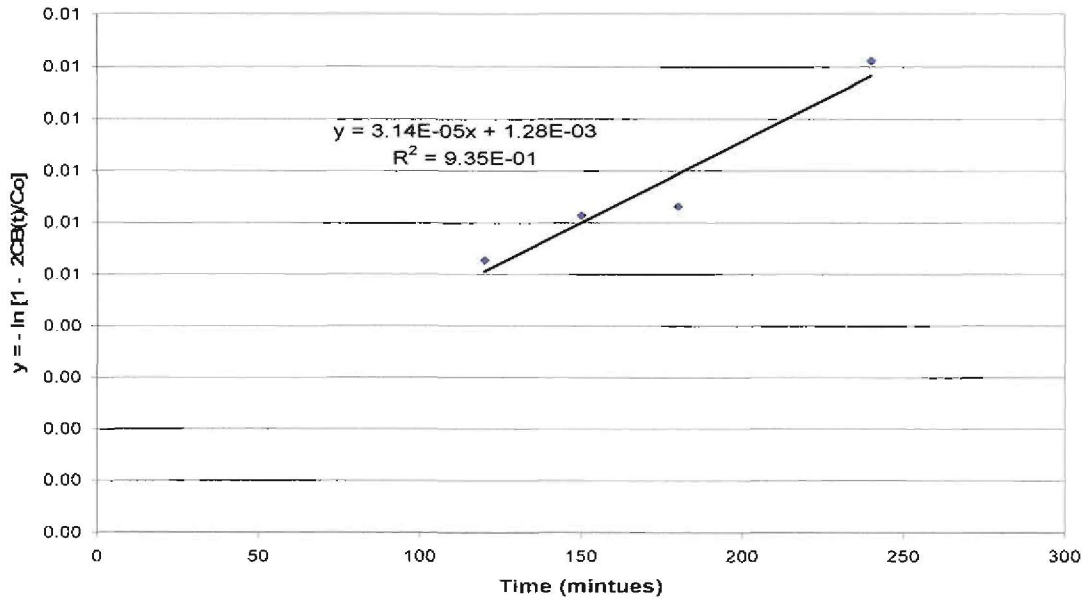

Figure E.1: $y = -\ln\left[1 - \frac{2\,C_B(t)}{C_O}\right]$ **as function of time for control experiment 1.**

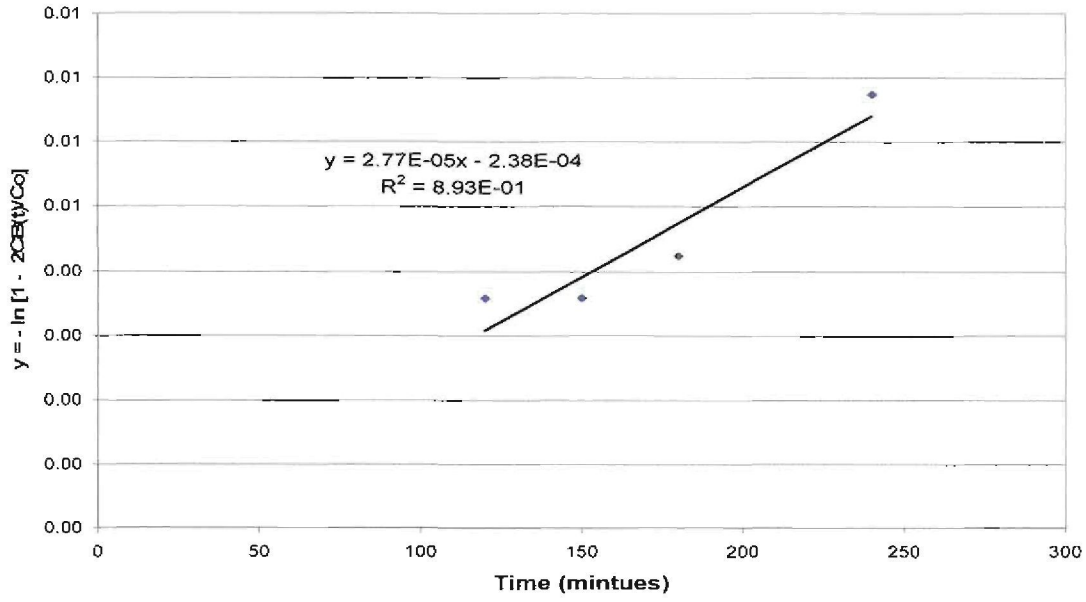

Figure E.2: $y = -\ln\left[1 - \frac{2\,C_B(t)}{C_O}\right]$ **as function of time for control experiment 2.**

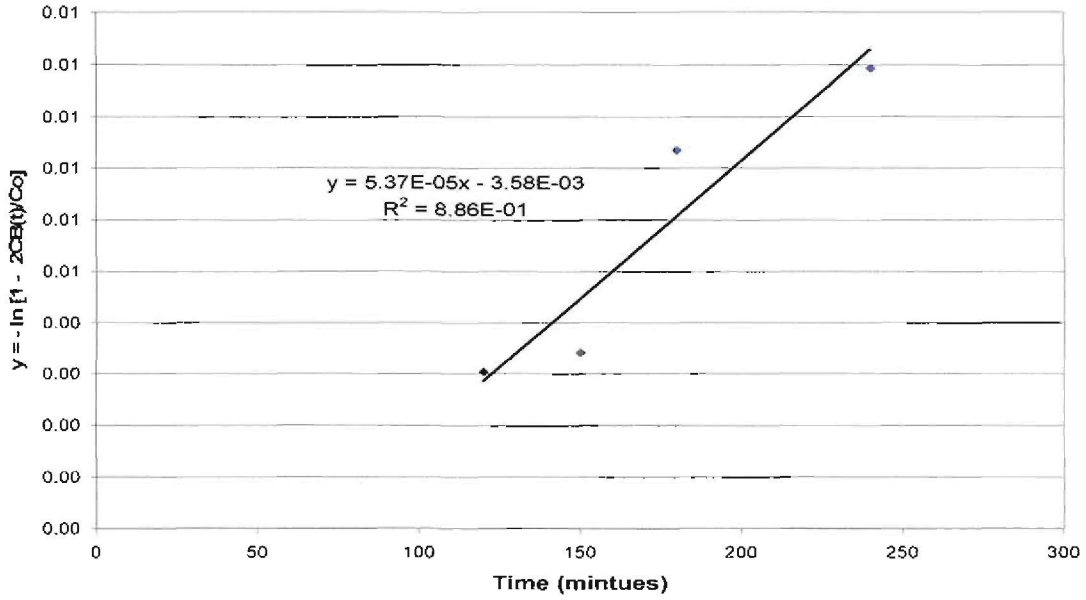

Figure E.3: $y = -\ln\left[1 - \frac{2\,C_B(t)}{C_O}\right]$ **as function of time for control experiment 3.**

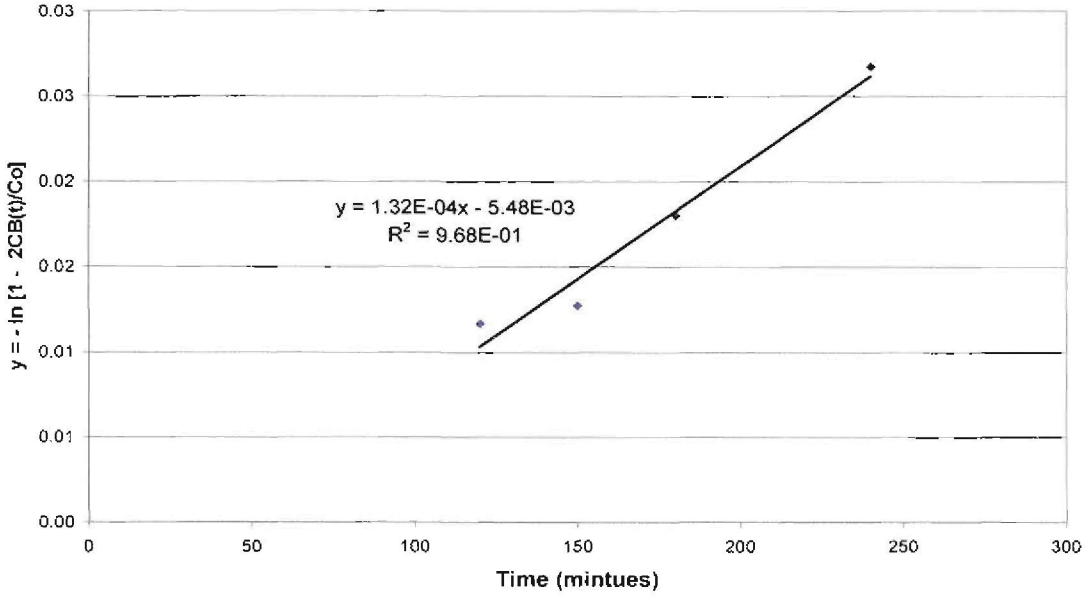

Figure E.4: $y = -\ln\left[1 - \frac{2\,C_B(t)}{C_O}\right]$ **as function of time for low molecular weight TMC (0.1 % w/v) experiment 1.**

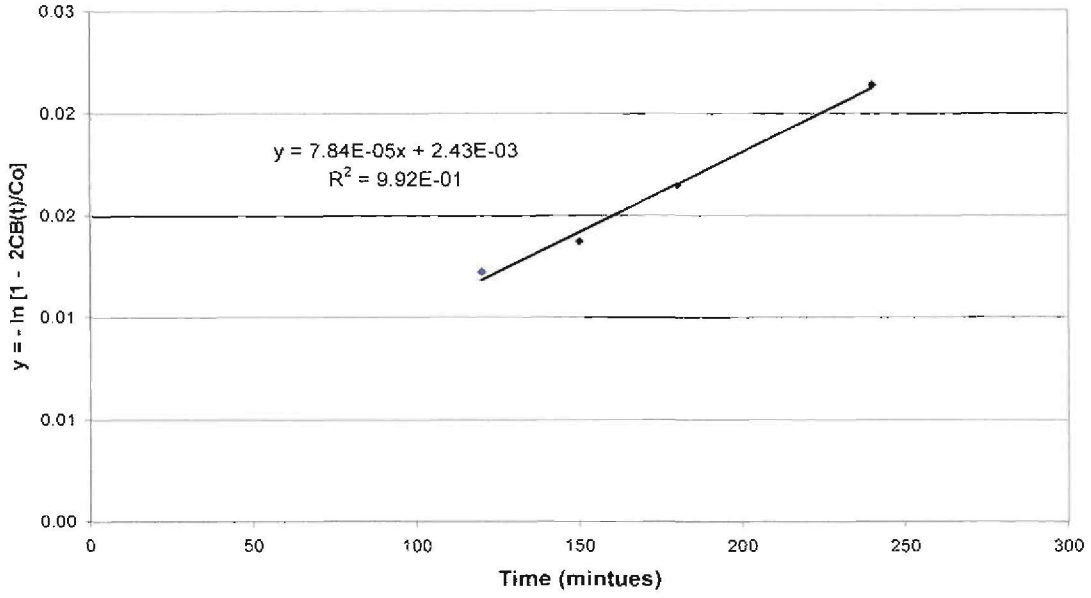

Figure E.5: $y = -\ln\left[1 - \frac{2\,C_B(t)}{C_O}\right]$ **as function of time for low molecular weight TMC (0.1 % w/v) experiment 2.**

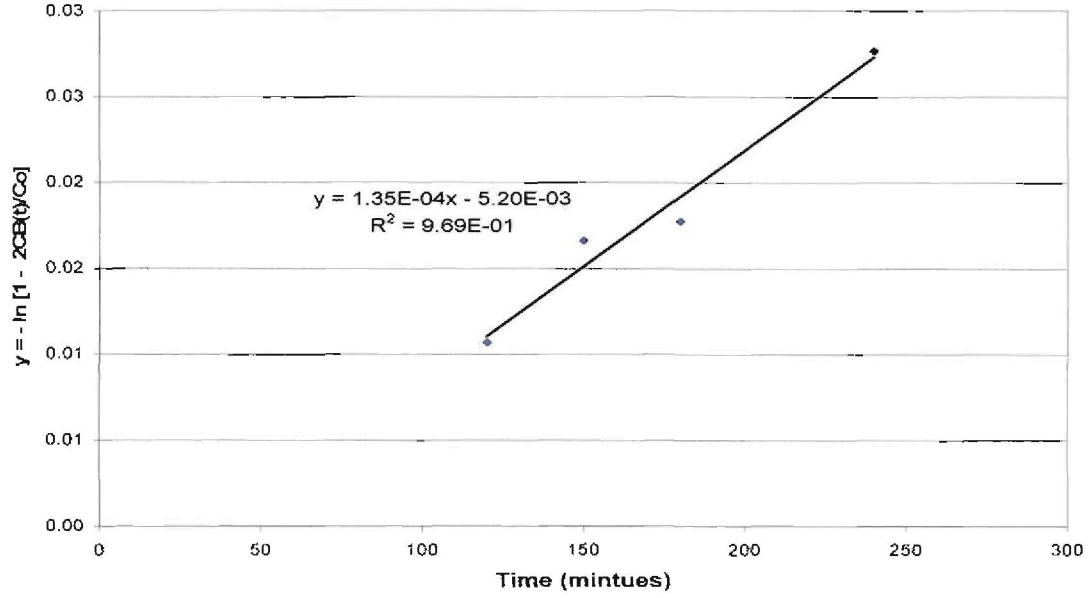

Figure E.6: $y = -\ln\left[1 - \frac{2\,C_B(t)}{C_O}\right]$ **as function of time for low molecular weight TMC (0.1 % w/v) experiment 3.**

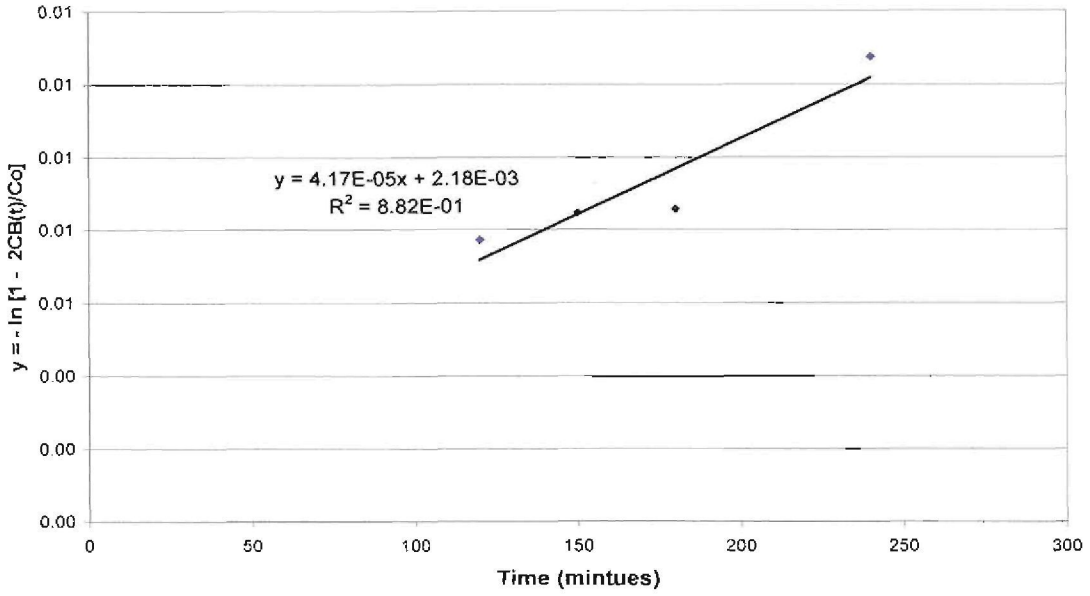

Figure E.7: $y = -\ln\left[1 - \frac{2\,C_B(t)}{C_O}\right]$ **as function of time for medium molecular weight TMC (0.1 % w/v) experiment 1.**

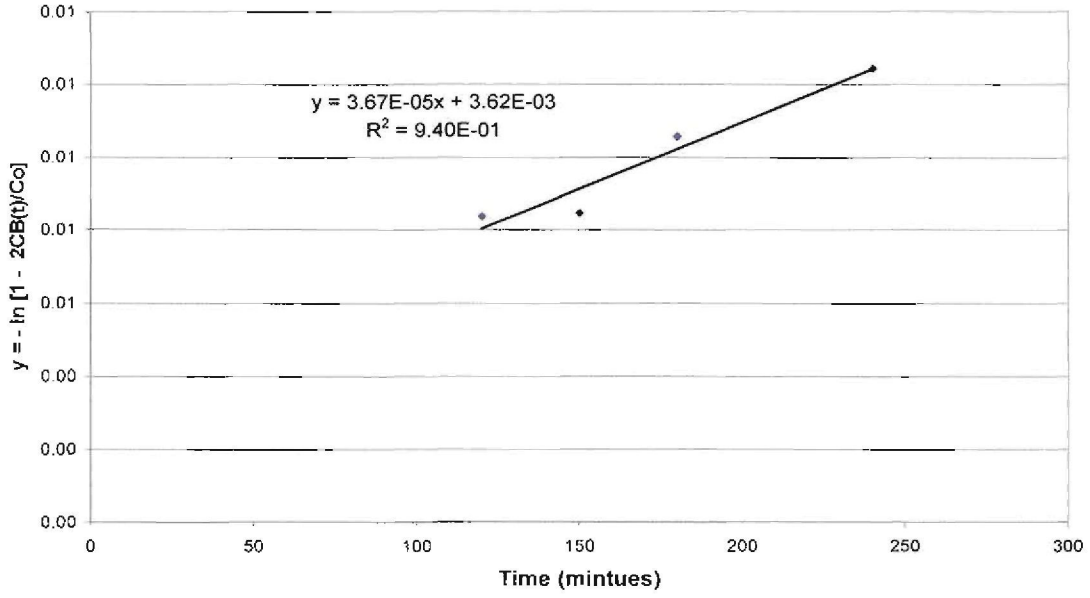

Figure E.8: $y = -\ln\left[1 - \frac{2\,C_B(t)}{C_O}\right]$ **as function of time for medium molecular weight TMC (0.1 % w/v) experiment 2.**

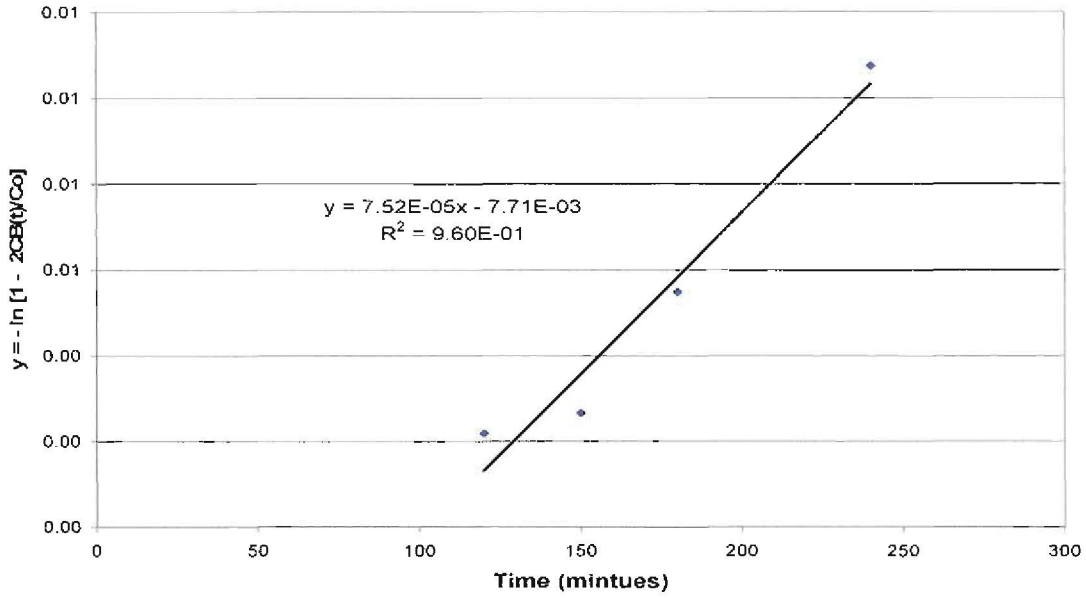

Figure E.9: $y = -\ln\left[1 - \frac{2\,C_B(t)}{C_O}\right]$ **as function of time for medium molecular weight TMC (0.1 % w/v) experiment 3.**

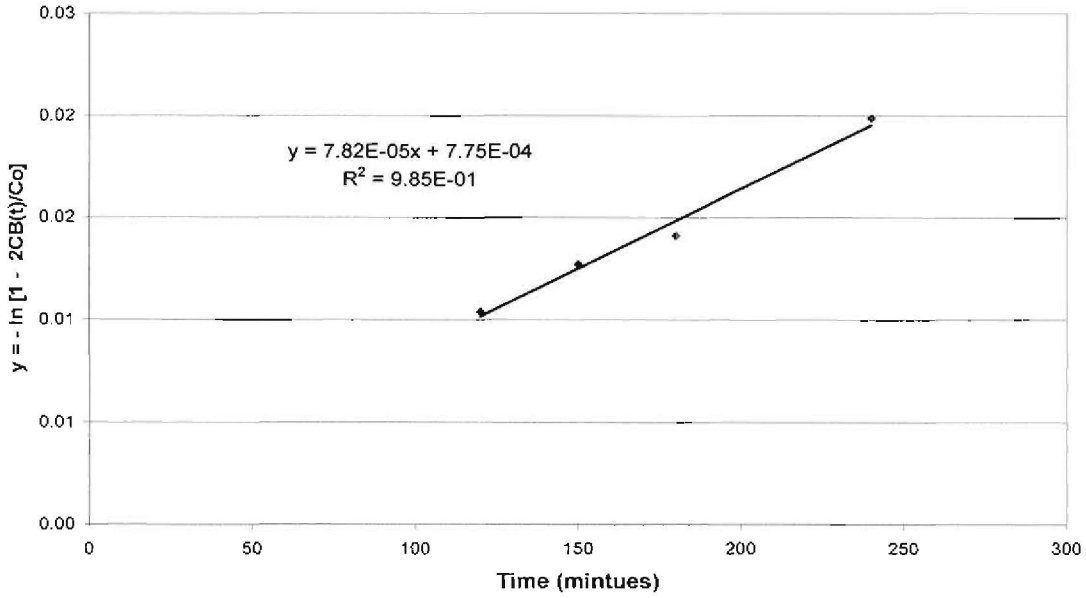

Figure E.10: $y = -\ln\left[1 - \frac{2\,C_B(t)}{C_O}\right]$ **as function of time for high molecular weight TMC (0.1 % w/v) experiment 1.**

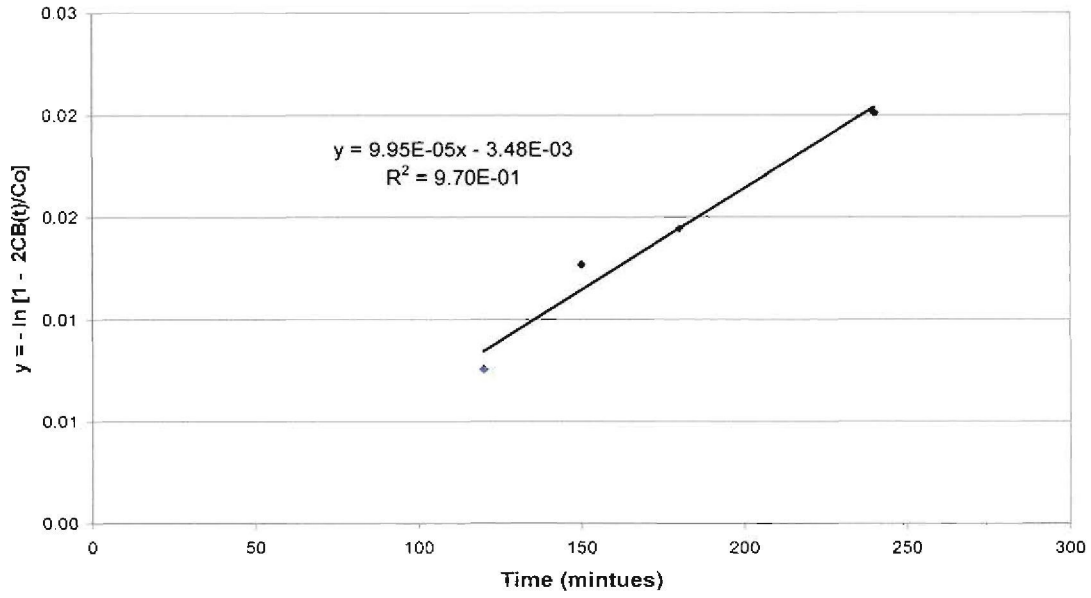

Figure E.11: $y = -\ln\left[1 - \frac{2\,C_B(t)}{C_O}\right]$ **as function of time for high molecular weight TMC (0.1 % w/v) experiment 2.**

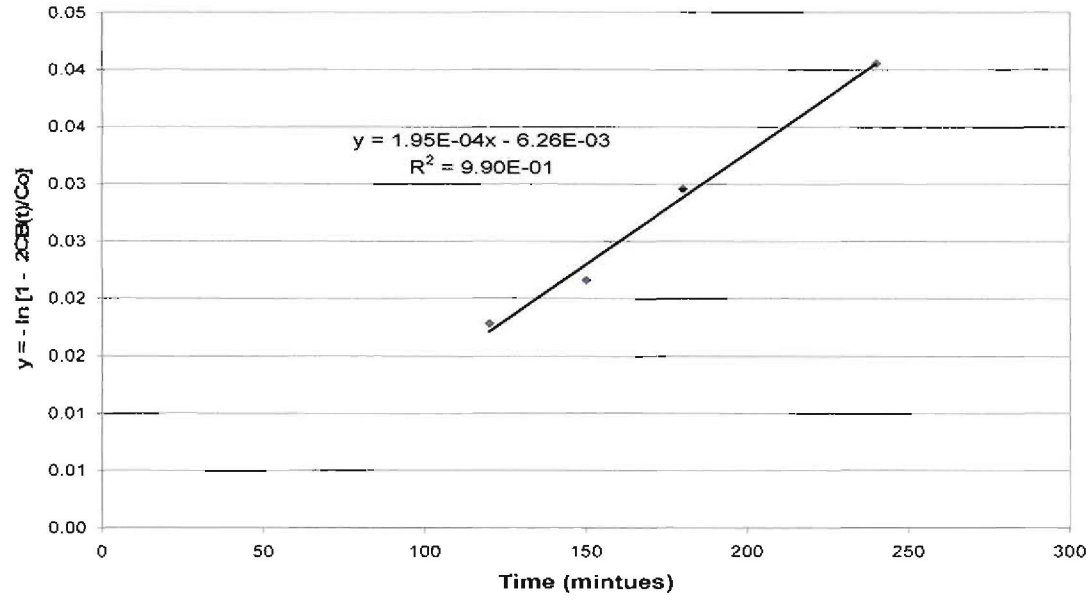

Figure E.12: $y = -\ln\left[1 - \frac{2\,C_B(t)}{C_O}\right]$ **as function of time for high molecular weight TMC (0.1 % w/v) experiment 3.**

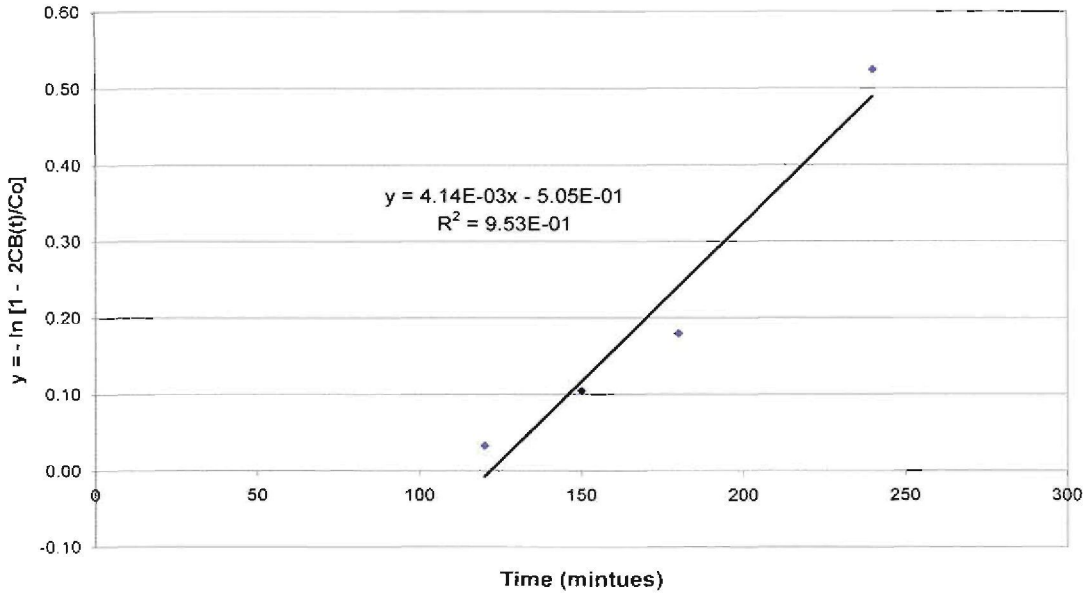

Figure E.13: $y = -\ln\left[1 - \frac{2\,C_B(t)}{C_O}\right]$ **as function of time for low molecular weight TMC (0.5 % w/v) experiment 1.**

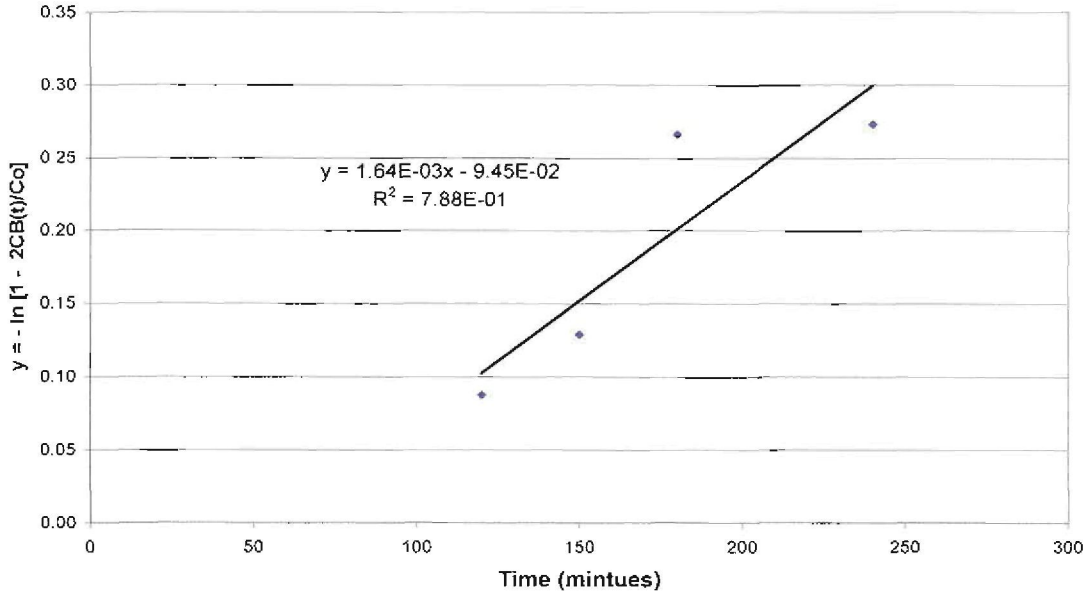

Figure E.14: $y = -\ln\left[1 - \frac{2\,C_B(t)}{C_O}\right]$ **as function of time for low molecular weight TMC (0.5 % w/v) experiment 2.**

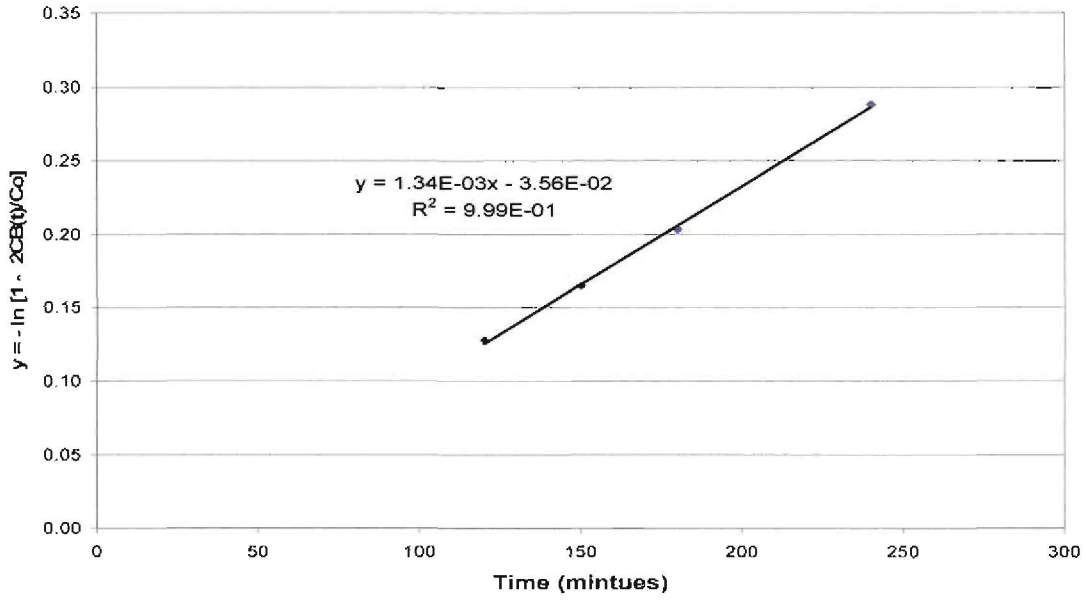

Figure E.15: $y = -\ln\left[1 - \frac{2\,C_B(t)}{C_O}\right]$ **as function of time for low molecular weight TMC (0.5 % w/v) experiment 3.**

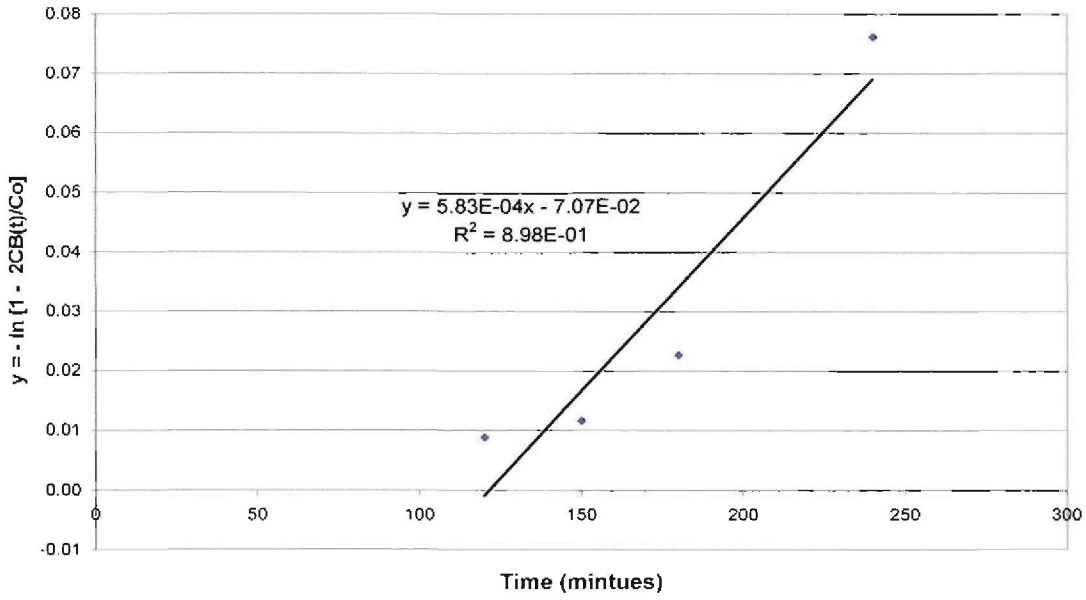

Figure E.16: $y = -\ln\left[1 - \frac{2\,C_B(t)}{C_O}\right]$ **as function of time for medium molecular weight TMC (0.5 % w/v) experiment 1.**

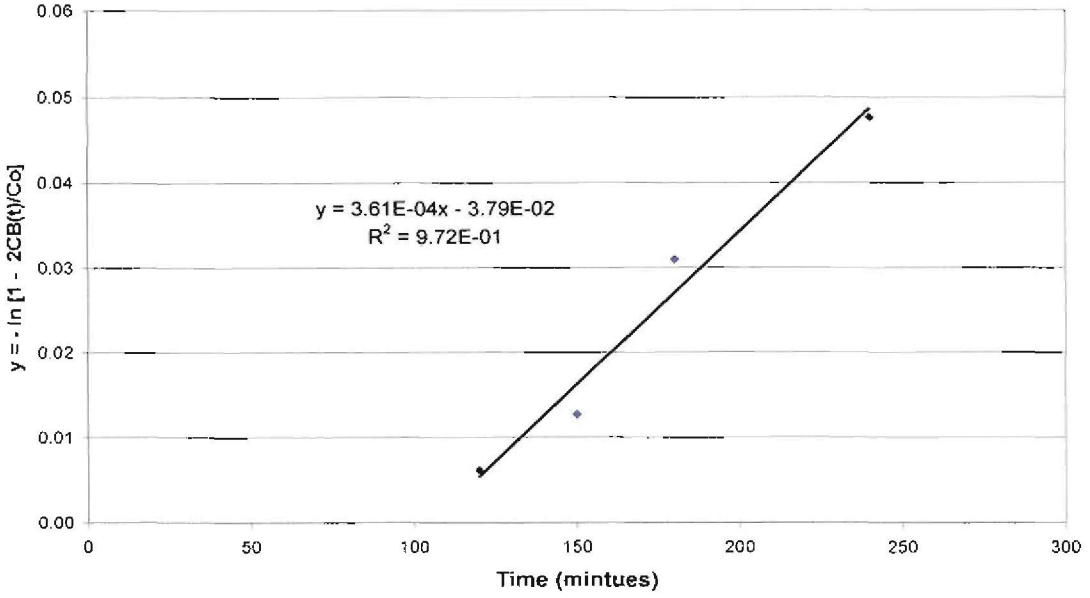

Figure E.17: $y = -\ln\left[1 - \frac{2\,C_B(t)}{C_O}\right]$ **as function of time for medium molecular weight TMC (0.5 % w/v) experiment 2.**

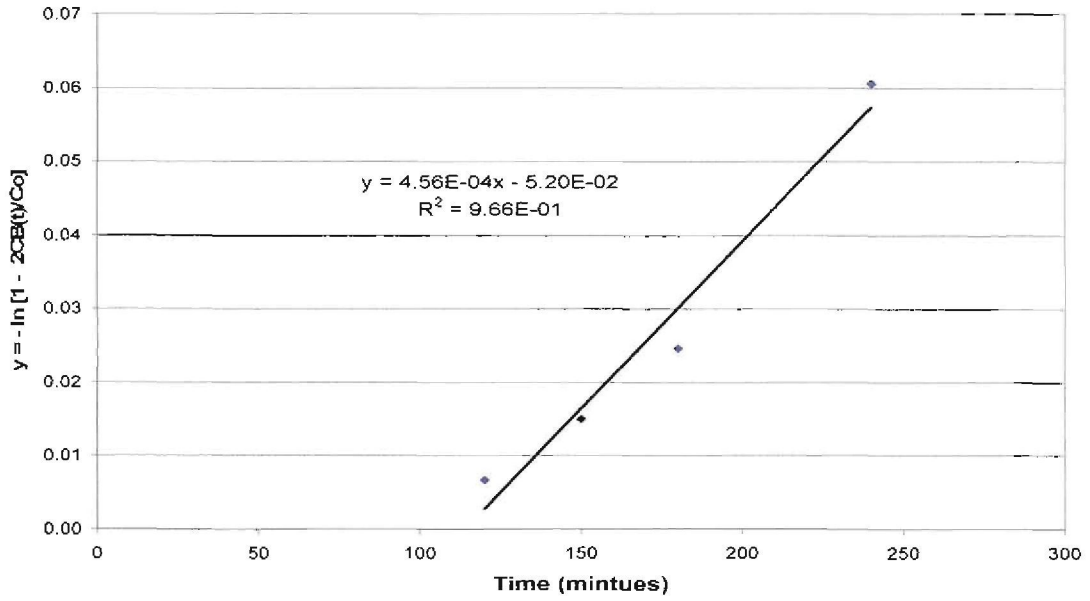

Figure E.18: $y = -\ln\left[1 - \frac{2\,C_B(t)}{C_O}\right]$ **as function of time for medium molecular weight TMC (0.5 % w/v) experiment 3.**

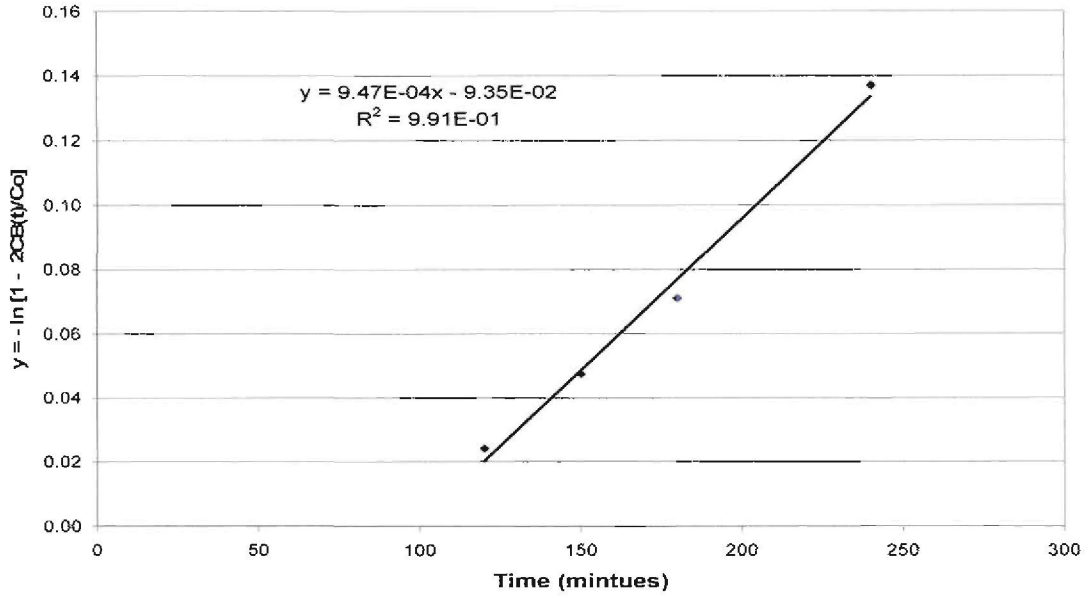

Figure E.19: $y = -\ln\left[1 - \frac{2\,C_B(t)}{C_O}\right]$ **as function of time for high molecular weight TMC (0.5 % w/v) experiment 1.**

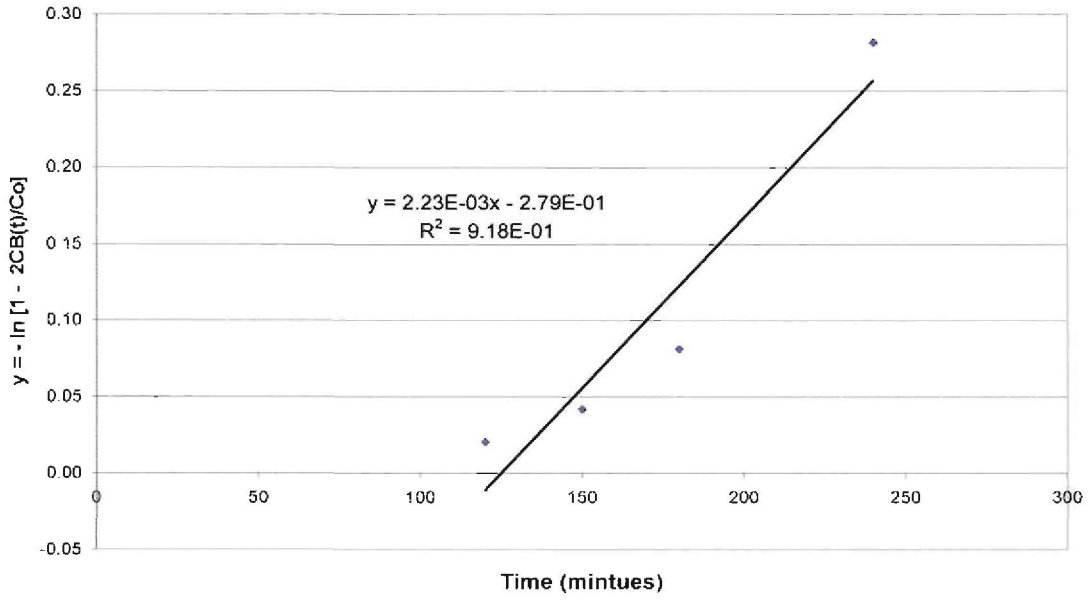

Figure E.20: $y = -\ln\left[1 - \frac{2\,C_B(t)}{C_O}\right]$ **as function of time for high molecular weight TMC (0.5 % w/v) experiment 2.**

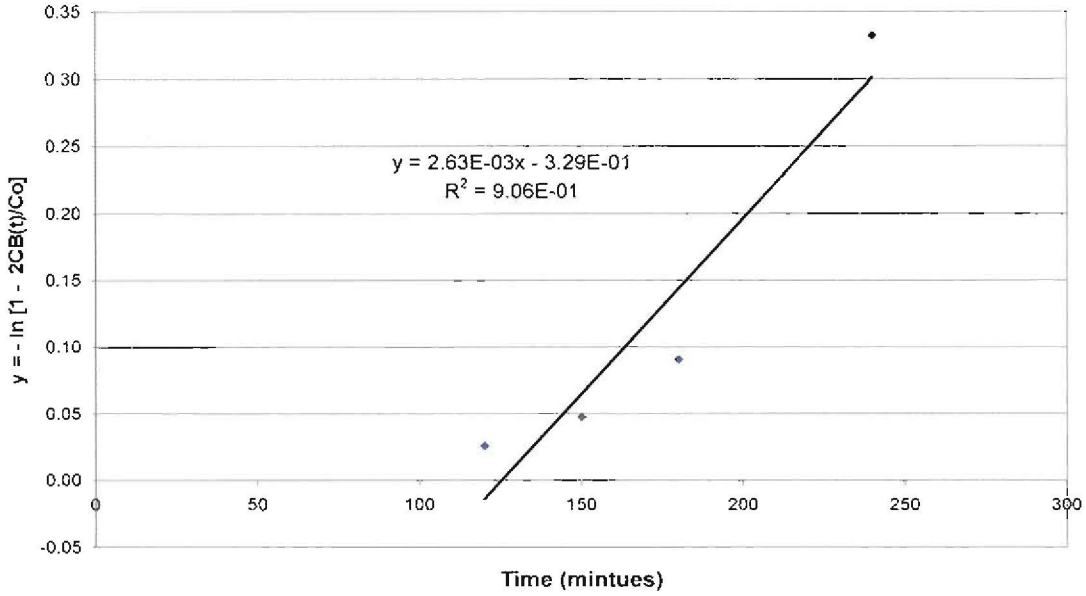

Figure E.21: $y = -\ln\left[1 - \frac{2\,C_B(t)}{C_O}\right]$ **as function of time for high molecular weight TMC (0.5 % w/v) experiment 3.**

The diffusion coefficient (D) was calculated using equation E-4 and the average values are given in table E.2.

Table E.2: Diffusion coefficient obtained by means of transport Model

TMC (w/v)		Average Gradient	Gradient Standard deviation	Average Diffusion Coefficient (m^2/min)	Diffusion coefficient standard deviation
0.1 %					
	Low MW	1.15E-04	3.20E-05	1.12E-11	3.11E-12
	Med MW	5.12E-05	2.09E-05	4.98E-12	2.03E-12
	High MW	1.24E-04	6.21E-05	1.21E-11	6.04E-12
0.5 %					
	Low MW	2.38E-03	1.54E-03	2.31E-10	1.50E-10
	Med MW	4.66E-04	1.11E-04	4.53E-11	1.08E-11
	High MW	1.93E-03	8.78E-04	1.88E-10	8.54E-11